Max-Planck-Institut für Meteorologie
Max Planck Institute for Meteorology

On biogeophysical interactions between vegetation phenology and climate simulated over Europe

Diana Rechid


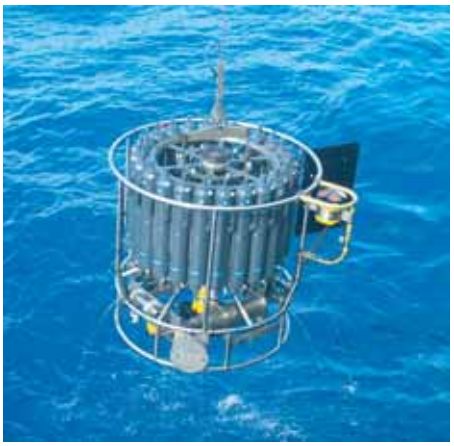


Berichte zur Erdsystemforschung 61/2009

Reports on Earth System Science

Hinweis

Die Berichte zur Erdsystemforschung werden vom Max-Planck-Institut für Meteorologie in Hamburg in unregelmäßiger Abfolge herausgegeben.

Sie enthalten wissenschaftliche und technische Beiträge, inklusive Dissertationen.

Die Beiträge geben nicht notwendigerweise die Auffassung des Instituts wieder.

Die "Berichte zur Erdsystemforschung" führen die vorherigen Reihen "Reports" und "Examensarbeiten" weiter.

Notice

The Reports on Earth System Science are published by the Max Planck Institute for Meteorology in Hamburg. They appear in irregular intervals.

They contain scientific and technical contributions, including Ph. D. theses.

The Reports do not necessarily reflect the opinion of the Institute.

The "Reports on Earth System Science" continue the former "Reports" and "Examensarbeiten" of the Max Planck Institute.

Anschrift / Address

Max-Planck-Institut für Meteorologie
Bundesstrasse 53
20146 Hamburg
Deutschland

Tel.: +49-(0)40-4 11 73-0
Fax: +49-(0)40-4 11 73-298
Web: www.mpimet.mpg.de

Layout:

Bettina Diallo, PR & Grafik

Titelfotos:
vorne:
Christian Klepp - Jochem Marotzke - Christian Klepp
hinten:
Clotilde Dubois - Christian Klepp - Katsumasa Tanaka

Berichte zur Erdsystemforschung 61/2009

On biogeophysical interactions between vegetation phenology and climate simulated over Europe

Dissertation zur Erlangung des Doktorgrades der Naturwissenschaften
im Departement Geowissenschaften der Universität Hamburg
vorgelegt von

Diana Rechid

aus Leipzig

Hamburg 2008

Reports on Earth System Science 61/2009

ISSN 1614-1199

Diana Rechid
Max-Planck-Institut für Meteorologie
Bundesstrasse 53
20146 Hamburg
Germany

Als Dissertation angenommen
vom Departement Geowissenschaften der Universität Hamburg

auf Grund der Gutachten von
Prof. Dr. Hartmut Graßl
und
Dr. Daniela Jacob

Hamburg, den 10. Dezember 2008
Prof. Dr. Jürgen Oßenbrügge
Leiter des Departements für Geowissenschaften

ISSN 1614-1199

On biogeophysical interactions between vegetation phenology and climate simulated over Europe

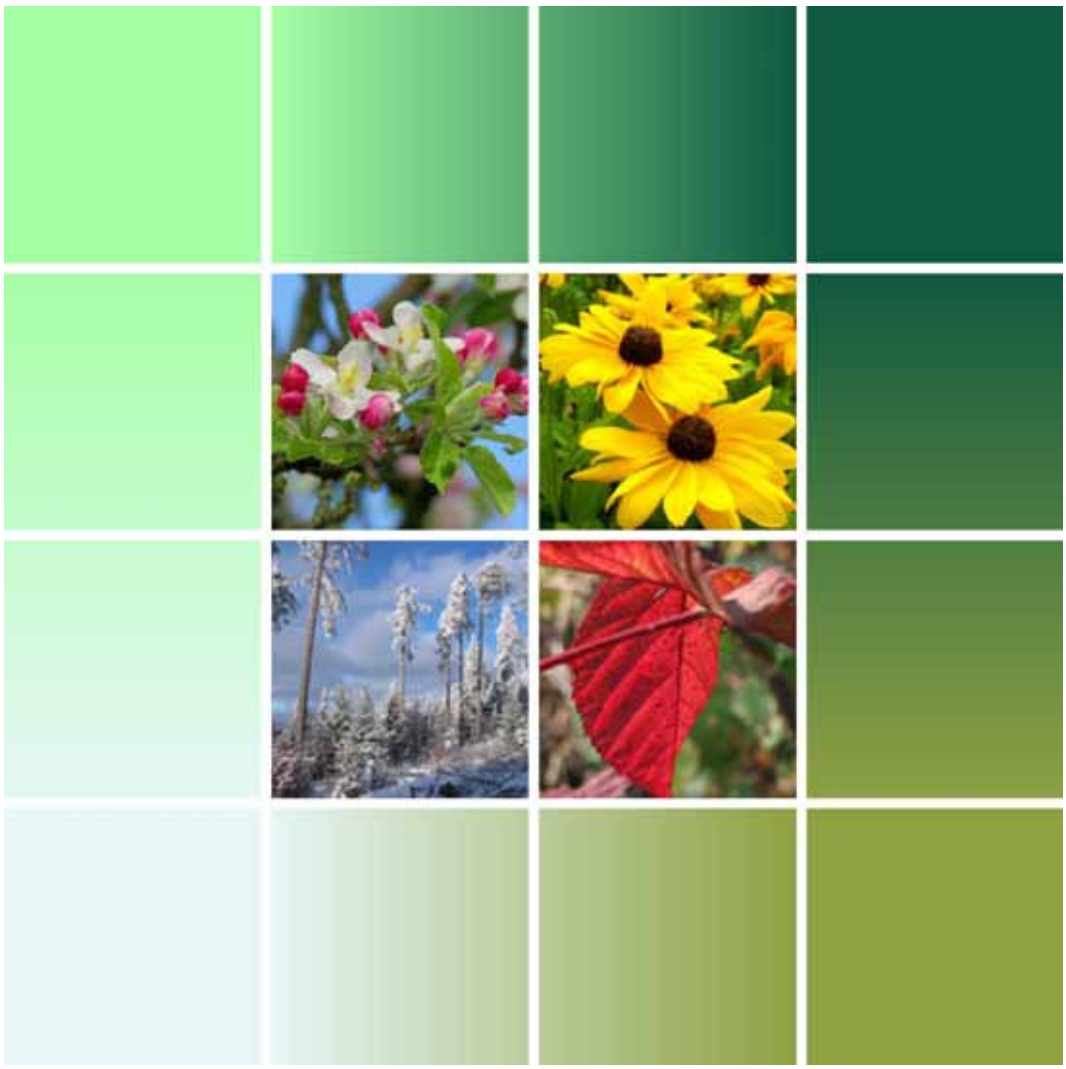

Diana Rechid

Hamburg 2008

Contents

Contents

Abstract

This thesis investigates biogeophysical interactions between plant phenology and climate simulated over Europe. The investigations are mainly done on a regional scale with focus on Europe. The simulations are carried out with the regional climate model REMO. An additional study is done on a global scale using the global climate model ECHAM5. The investigations are done on seasonal timescales for present-day climate conditions with an additional study for future climate conditions. Vegetation phenology is implemented into the regional climate model REMO and its impacts on the simulated regional climate are studied by analysing several climate model simulations. The work is done within 3 steps: 1. Implementation of monthly varying vegetation fields into the land surface scheme of REMO as lower boundary condition for the atmosphere, and investigation of its influence on the regional climate simulations. 2. Parameterisation of snow-free land surface albedo variability as a function of vegetation phenology on the basis of remotely-sensed data, and investigation of its influence on the regional climate simulated by REMO, and on the global climate simulated by ECHAM5. 3. Design of the vegetation phenology scheme PHENO, which relates the species-averaged parameter leaf area index (LAI) directly to the simulated climate parameters of near surface heat and moisture conditions, and fully coupling to the regional climate model REMO in order to study the dynamic interactions between vegetation phenology and climate variability.

Seasonal vegetation variability strongly affects the water and energy fluxes at the land surface. The strongest effects occur over eastern and central Europe during the summer season. In both, the global and the regional simulations, clear effects caused by snow-free land surface albedo changes occur over Europe, but, in many cases, with contrary responses to the advanced albedo parameterisation. In contrast to the global simulation, where the large-scale atmospheric circulation patterns are changed by the new albedo parameterisation, in the regional simulations, the circulation patterns within the model domain are not influenced. In the regional model simulations mainly local effects occur during the summer season. In the global model simulations, the effects on the simulated climate are not restricted to regions where the land surface albedo is changed, but also occur in remote regions through atmospheric teleconnections. The global results show higher sensitivity to the changed albedo parameterisation with regard to the annual temperature and precipitation cycles. The vegetation phenology model PHENO is capable of representing the interannual variability and the observed long-term trends in vegetation phenology caused by climate variability. Model simulations with PHENO fully coupled to REMO show the feedback of the interannual variability of plant phenology on the simulated climate over Europe. There is a positive feedback on drought conditions during warm and dry summer/autumn periods by intensifying the water limitation of plants, which leads to another decrease in LAI. The use of the PHENO scheme facilitates an improved representation of vegetation in REMO, that may become especially important in future climate change simulations.

Zusammenfassung

Die vorliegende Arbeit untersucht die biogeophysikalischen Wechselbeziehungen zwischen Pflanzenphänologie und Klima in Europa. Die Untersuchungen werden räumlich vorwiegend auf regionaler Skala mit Fokus auf Europa durchgeführt. Für die regionalen Simulationen wird das regionale Klimamodell REMO verwendet. Eine weitere Studie wird auf globaler Skala mit dem globalen Klimamodell ECHAM5 durchgeführt. Die Untersuchungen werden zeitlich auf saisonaler Skala für heutiges Klima ausgeführt mit einer weiteren Studie für zukünftige Klimabedingungen. Die Vegetationsphänologie wird in das regionale Klimamodell REMO implementiert und ihr Einfluss auf das simulierte regionale Klima mittels Durchführung und Auswertung mehrerer Modellstudien untersucht. Die Umsetzung erfolgt in 3 Schritten: 1. Implementierung monatlich variierender Vegetationsparameter in das Landoberflächenschema von REMO als untere Randbedingungen für die Atmosphäre und Untersuchung des Einflusses auf regionale Klimasimulationen. 2. Parameterisierung der Variabilität der Albedo schneefreier Landoberflächen als Funktion der Vegetationsphänologie auf der Basis von Fernerkundungsdaten und Untersuchung des Einflusses auf das regionale Klima simuliert mit REMO und auf das globale Klima simuliert mit ECHAM5. 3. Entwicklung des Vegetationsphänologie-Modells PHENO, das den über Pflanzenarten gemittelten Parameter Blattflächenindex in Abhängigkeit von simulierten Klimaparametern der bodennahen Wärme- und Feuchtebedingungen beschreibt; sowie interaktive Kopplung zum regionalen Klimamodell REMO, um die dynamischen Wechselbeziehungen zwischen Vegetationsphänologie und Klimavariabilität zu untersuchen.

Die jahreszeitliche Variabilität der Vegetation beeinflusst deutlich die Wasser- und Energieflüsse an der Landoberfläche. Die größten Effekte treten im Sommer über Ost- und Mitteleuropa auf. Die Veränderung der Albedo schneefreier Landoberflächen zeigt deutliche Auswirkungen in Europa sowohl in den regionalen als auch den globalen Klimasimulationen, allerdings häufig mit gegensätzlichen Reaktionen auf die erweiterte Parameterisierung der Albedo. Im Gegensatz zu den Globalsimulationen, in denen die großskalige atmosphärische Zirkulation verändert wird, bleiben in den regionalen Klimasimulationen die Zirkulationsmuster innerhalb des Modellgebietes unbeeinflusst. In den regionalen Simulationen treten hauptsächlich lokale Effekte während der Sommerjahreszeit auf. In den Globalsimulationen sind die Auswirkungen auf das simulierte Klima nicht auf die Regionen beschränkt, in denen sich die Oberflächenalbedo verändert hat, sondern sie treten auch in entfernten Gebieten durch atmosphärische Telekonnektionen auf. Der Vergleich der regional und global simulierten Jahresgänge von Temperatur und Niederschlag für verschiedene europäische Regionen zeigt, dass die globalen Modellsimulationen sensitiver auf die veränderte Albedoparametrisierung reagieren als die regionalen Simulationen. Das Vegetations-Phänologie-Modell PHENO ist in der Lage, die klimabedingte interannuelle Variabilität der Pflanzenphänologie und die beobachteten Langzeit-Trends zu simulieren. Die mit dem Regionalmodell gekoppelten Modellsimulationen zeigen das Feedback der interannuellen Variabilität der Pflanzenphänologie auf das simulierte Klima in Europa. Es zeigt sich ein positiver Feedback auf Trockenheitsbedingungen während warmer und trockener Sommer- und Herbstperioden, was die Wasserlimitierung der Pflanzen verstärkt und damit zu einer weiteren Abnahme des Blattflächenindex in der gekoppelten Modellsimulation führt. Die Anwendung des PHENO-Modells verbessert die Repräsentation der Vegetation in REMO, was besonders wichtig für Simulationen möglicher zukünftiger Klimaänderungen ist.

Chapter 1

Introduction

The following chapter provides an insight into the research on vegetation-climate interactions (section 1.1) with focus on the observation and modelling of vegetation phenology in relation to climate variability (section 1.2). The objectives of this thesis are described and an outline is given.

1. 1 Interactions between climate and vegetation

Vegetation as visualisation of the climate - on the global scale, there is a strong correlation between climate and vegetation zones. The moist tropics are associated with rainforests, the dry subtropics with subtropical deserts, regions of temperate climate with temperate and boreal forests, and polar regions with tundra and polar deserts. Alexander von Humboldt as the founder of biogeography with his "*Ideen zu einer Geographie der Pflanzen*" (Humboldt 1807) was among the first geographers analysing the coherences between climate and vegetation in a scientific way. Wladimir Köppen's climate classification system (Köppen 1936) was a first attempt to establish quantitative relationships between climate and vegetation on a global scale.

The climate is the dominant factor that determines the distribution of major vegetation types over the earth (biogeography). Vice versa, the vegetation affects the climate by modifying the physical properties of the land surface like the albedo, roughness, vegetation density and water conductivity (biogeophysical effects). Moreover, vegetation influences the cycle of matter, and thus the atmospheric gas composition, as for example the concentrations of CO_2 and CH_4 (biogeochemical effects). Pielke et al. (1998) reviewed experimental and modelling studies on the influence of biogeophysical, biogeochemical and biogeographical mechanisms on the weather and the climate.

Biogeophysical interactions

This thesis covers biogeophysical interactions between the biosphere and the atmosphere. Biogeophysical mechanisms determine the fluxes of energy, water and momentum between the biosphere and atmosphere at the land surface. The surface albedo influences the short wave radiation budget. Surface roughness changes the wind in the planetary boundary layer. The density of vegetation cover controls the transpiration by leaf stomatal conductance and the evaporation by interception of water on the skin of the canopy. Evapotranspiration

determines the partitioning of the vertical turbulent heat fluxes into latent and sensible heat. The latent and sensible heat fluxes are the main mechanisms to return energy from the surface into the atmosphere. They influence convective processes as well as the boundary layer structure. These surface processes controlled by vegetation properties impact the near surface atmospheric conditions such as the near surface temperature, the near surface humidity and the low level cloudiness. This provides the appropriate feedback mechanisms to other physical processes in the atmosphere. The land surface processes also influence the conditions in the soil like the soil temperature and the soil moisture content. Vice versa, the conditions in the atmosphere and the soil determine the plant growing. The variability of climatic conditions in the atmosphere and the soil determine the temporal and spatial variability of vegetation, which again feeds back to the climate.

Modelling studies

Within this thesis climate modelling studies are carried out to investigate the biogeophysical interactions between vegetation and climate. Modelling studies are an appropriate tool to study vegetation-climate interactions on regional and global scales. In climate models, biogeophysical processes are parameterised by land surface schemes. Land surface parameters specify the land surface properties. The parameter values are, in most cases, allocated by data sets retrieved from satellite observations. Important parameters, which represent vegetation characteristics, are the leaf area index (LAI, ratio of one-sided leaf area to ground area), the stem area index or forest fraction, the green vegetation cover (fraction of photosynthetically active vegetation), the canopy albedo, the roughness length and the water holding capacity due to plant rooting depth.

Over the last decades, many climate modelling studies have shown the sensitivity of the simulated climate to land surface conditions, and therefore suggest the need for their accurate representation (e.g. Shukla & Mintz 1982, Mintz 1984, Sud et al. 1988, Sud et al. 1990, Bonan et al. 1992, Collins & Avissar 1994, Chase et al. 1996, Yang 1999). Garrett (1993) gave a review about the sensitivity of climate simulations to land surface schemes and atmospheric boundary layer treatments, and pointed out the need to include realistic canopy schemes into the climate models. Henderson-Sellers et al. (1993) described the "Project for Intercomparison of Land-surface Parameterisation Schemes" (PILPS) and Pitman et al. (1999) presented the key results and implications from phase 1 of PILPS. They found large differences in how the models simulated the exchange of energy and water at the surface. The review of Yang (2004) about modelling land surface processes in weather and climate studies describes the historical development of land surface models ranging from the early, simple “bucket” models to recent more sophisticated soil-vegetation-atmosphere transfer schemes. Several studies revealed the improvement of current climate simulations by advanced surface schemes (e. g. Cox 1999, Saha et al. 2006, Oleson et al. 2008). The inclusion of canopy processes within the land surface schemes allows for investigations of the impact of the vegetation on the climate (e. g. Niu et al. 2004, Snyder et al. 2004), and how the vegetation variability affects the climate (e.g. Avissar & Liu 1996, Lu & Shuttleworth 2002, Lawrence & Slingo 2004a and 2004b, Koster & Suarez 2004).). Fraedrich et al. (1999) and Kleidon et al. (2000) tried to estimate the maximum effect of vegetation changes on the global climate by performing model simulations using two very different extreme land surface boundary conditions over land, in the first case completely covered by forest ("green planet") and in the other case completely covered by desert ("desert world"). Further applications are model

studies on the impact of land cover changes on the climate (e. g. Bonan 1997, Stohlgreen et al. 1998, Chase et al. 2000, Osborne et al. 2004, Gibbard et al. 2005) with the pioniering works of Charney (1975) in the African Sahel.

To study the complex biosphere-atmosphere feedbacks a two-way coupling of vegetation and climate is needed to consider the bi-directional climate-vegetation interactions. A simple way to couple vegetation and climate is to simulate the climate with fixed land surface parameters, then to feed the simulated climate parameters into a dynamic vegetation model, and finally to simulate the climate again with the changing vegetation fields calculated by the vegetation model. This offline coupling was performed to study the feedback of changing vegetation fields due to climate change conditions on the simulated climate in the Barents Sea Region (Göttel et al. 2008). Schurgers et al. (2007) studied the long-term vegetation-climate interactions for the Eemian interglacial by an interactive coupling of vegetation and climate. They exchanged vegetation and climate parameters between a general atmospheric circulation model and a dynamic vegetation model by using an iterative procedure. Levis et al. (1999 and 2000) used a fully coupled climate-vegetation model to show potential vegetation feedbacks on the climate change.

The above listed modelling studies are just a small selection of a huge amount of investigations on vegetation-climate interactions. In parts, they present different results, which implies additional uncertainty for climate projections (Pitman et al. 1999). Nevertheless, there are some results, on which several studies agree. It has been established that vegetation growth enhances evapotranspiration (Crucifix et al. 2005). Increases in vegetation density result in cooler and moister near-surface conditions (e. g. Bounoua et al. 2000). In the high latitudes, the replacement of shrubs by trees reduces surface albedo due to vegetation masking of snow, which warms the climate (Bonan et al. 1992, Göttel et al. 2008). The northward expansion of the boreal forest in response to the climate warming decreases the land surface albedo, which leads to an additional warming, as shown by Foley et al. (1994). Most of the studies on the impact of land cover changes on the climate in the tropics have demonstrated that large-scale deforestation reduces precipitation and increases temperatures. Voldoire & Royer (2004) showed that tropical deforestation not only impacts the mean climate but also its variability.

Recently, regional climate models have also started to be used for studies on land-atmosphere interactions (Pielke et al. 1999, Pan et al. 2001, Zheng et al. 2002, Vidale et al. 2003, Suh & Lee 2004). Seneviratne et al. (2006) explored an increase in summer temperature variability in eastern and central Europe due to soil-moisture-atmosphere feedbacks. Regional climate models are an appropriate tool to analyse interactions between the biosphere and climate, as many of the aspects of land surface processes are highly related to regional scales. Also the effects of land surface descriptions on the simulated climate have been investigated using regional models (Seneviratne et al. 2002, Maynard and Royer 2004, Pitman & McAvaney 2004). The study of Sánchez et al. (2007) indicated a high sensitivity of summer precipitation processes to vegetation changes at regional scales. The current thesis also uses regional climate model simulations to study the impact of vegetation phenology on the simulated climate in Europe.

Temporal scales

The timescales of biogeophysical vegetation-climate interactions range from one day to 100,000 years. Diurnal cycles of vegetation result from the light dependency of the plants. The annual vegetation cycle outside the tropics is driven by the seasonal variability of climate variables, e. g. radiation, temperature, soil moisture and precipitation, which feeds back to the climate by changes of surface albedo, for example. Typical time scales for changes in the vegetation composition (succession and competition) and its spatial distribution (migration) due to climatic changes are 1 to 1,000 years, which feeds back to the climate due to changes in land surface conditions. The evolution of plants takes place on timescales from 10,000 to 100,000 years as a way to adapt to changing environments. This thesis investigates biogeophysical interactions between climate and vegetation on seasonal to decadal time scales in order to study the annual cycles as well as the interannual variability of vegetation phenology in relation to the climate. Hereby, most studies of this thesis are done for present-day climate conditions with one additional study using a climate projections for the end of the century.

Spatial scales

Vegetation-climate interactions range from microclimates to global scales. At the local scale, microclimates are produced by plants. Vegetation patchiness affects mesoscale climate (1 to 100 km). The global and regional climate determines the spatial distribution of vegetation types. Vice versa, the regional vegetation distribution influences the climate on the regional and even the global scale via atmospheric teleconnections. For example, the climate forcing of land cover changes can be transported by large-scale atmospheric circulations and affect the climate in remote regions (e. g. Saha et al. 2006). The effect of land use changes and vegetation-soil-snow dynamics on the global scale was found to be comparable in magnitude to the radiative effect of carbon dioxide (Chase et al. 2002). This thesis investigates regional vegetation-climate interactions with focus on Europe. An additional study is carried out on global scales.

1. 2 Vegetation phenology and climate variability

Vegetation phenology visualises the interactions between vegetation and climate on seasonal time scales. Additionally, it shows interannual variability and trends in relation to climate variability. Phenology comprises the study of “life cycle phases or activities of plants and animals in their temporal occurrence throughout the year” (Lieth 1974) in relation to climate (Schnelle 1955). Recognising its value as an integral bio-indicator for climate change, the interest in plant phenological observations increased in the context of climate change research (Menzel 2002).

Ground observations

Phenological networks were established, extended and standardised collecting considerable data archives as the German Weather Service (Bruns 2007) and the International Phenological Gardens (IPG) in Europe (Chmielewski 1996). Many studies analyse those phenological observations to determine spatial variations, interannual variability and temporal trends in plant phenology in relation to climate data (Ahas 1999, Menzel & Fabian 1999, Jaagus & Ahas 2000, Menzel 2000, Rötzer et al. 2000, Chmielewski & Rötzer 2001, Defila & Clot 2001, Menzel et al. 2001, Ahas et al. 2002, Chmielewski & Rötzer 2002, Scheifinger et al. 2002, Sparks & Menzel 2002, Menzel 2003, Menzel et al. 2003, Studer et al. 2005, Menzel et al. 2006). For detecting regional trends of phenological phases and finding their relation to climate changes Rötzer & Chmielewski (2001) computed phenological maps of Europe showing long-term means, trends and annual timings of phenological phases. In high and mid-latitudes phenological phases were found to depend strongly on temperature conditions. As a consequence of climate change many studies show evidence of a shift in plant development towards an earlier onset of spring and a lengthening of the growing season in Europe (Menzel 2000, Defila & Clot 2001, Menzel et al. 2001, Ahas et al. 2002, Menzel et al. 2003) and in Northern America (Beaubien & Freeland 2000, Schwartz & Reiter 2000, Cayan et al. 2001). Menzel et al. (2006) found an average advance of spring phases of 2.5 days per decade for 21 European countries from 1971 - 2000. Changes in autumn are not so easily to detect (Menzel et al. 2001, Sparks & Menzel 2002) and the signal is ambiguous (Menzel et al. 2006). Spring and summer phenological phases, such as leaf unfolding and flowering, strongly correlate with temperature of the preceding months (e. g. Chmielewski & Rötzer 2001, Ahas et al. 2002). The spring phenological anomalies also correlate with the Northern Atlantic Oscillation Index (NAO) of January to March (e. g. Scheifinger et al. 2002, Menzel 2003).

Remotely sensed observations

Whereas ground observations of plant phenology are often site- and/or species-specific, satellite data can provide spatially and species-averaged information on the start and end of the growing season as Normalised Difference Vegetation Index (NDVI) or derived leaf area index data (Myneni et al. 1997, Tucker et al. 2001, Zhou et al. 2001, Schwartz et al. 2002, Zhang 2003). Chen et al. (2000) analysed the relation between ground phenology observations and remote sensing derived measures of greenness to determine the growing season of land vegetation on the regional scale.

Application in climate modelling

During the last decades, consistently processed satellite-derived NDVI and LAI data became available providing spatially averaged information of land surface vegetation on the regional and global scale for the consideration of current plant phenology variations within climate modelling. While using satellite-derived LAI data in the land surface schemes of climate models, Buermann et al. (2001) studied the impact of interannual variability of phenology on climate. Bonan et al. (2002) studied the impact of spatial variability of phenology on climate simulations. Lawrence and Slingo (2004a, 2004b) prescribed an annual vegetation cycle on the basis of satellite-estimated LAI to a global climate simulation and found a reduction in surface temperatures in extra-tropical regions during both the summer and winter season.

Where the magnitude of LAI values is enhanced, precipitation increases. In the study of Lu & Shuttleworth (2002), vegetation phenology was assimilated into the climate version of a regional atmospheric modelling system also in the form of LAI estimates. They concluded that the effect of enhanced heterogeneity dominates over the effect of an reduced magnitude in LAI fields.

Vegetation phenology modelling

Phenology modelling approaches vary from statistical analyses (e. g. Gálan et al. 1998, Dose & Menzel 2006) to more mechanistic models with plant physiologically based approaches (e.g. Hänningen 1990, Chuine et al. 2003, Schaber & Badeck 2003). Several phenological bud burst models for forest tree species have been published (Hänninen 1994, Kramer 1994 and 1995, Rötzer et al. 2004), which are, however, limited to single species and/or geographic areas. For trees, the onset of greenness has been successfully modelled using a simple cumulative thermal summation (e. g. Murray et al. 1989, Hari & Häkkinen 1991, Hänningen et al. 1993). White et al. (1997) developed predictive phenology models on a continental scale and their application revealed extensive interannual variability in the timing of onset and offset of greening in the United States. To quantify the effects of climate change on forest growth, different phenological models for the growth of boreal, temperate and Mediterranean forest ecosystems were developed and coupled to a forest model by Kramer et al. (2000). Chmielewski et al. (2005) investigated the possible impacts of future climate change on natural vegetation in Saxony using simple phenological models in relation to regional climate scenarios, but still only driven by temperature. Relatively little research has been performed on the relation between water availability and phenology (Loustau et al. 1992 and 1996, Kramer et al. 2000). In most dynamic global vegetation models (DGVMs) prognostic phenology schemes are already included (Cramer et al. 2001), but often run uncoupled from general circulation models (GCMs). During recent years work focused on executing DGVMs coupled to GCMs (Foley et al. 1998, Levis 1999, Krinner 2005) with a review about coupling techniques by Foley et al. (2000). But it is still not common to run DGVM-GCMs routinely, especially because of the high demand on computational efforts. Most studies are done on coarse horizontal resolutions. Another problem arises if there are large differences between the land surface schemes of the GCM and the DGVM. To overcome such inconsistencies, the approach of Bonan et al. (2003) is to be mentioned. They add dynamic vegetation processes from a DGVM directly to the land component of a climate model.

1. 3 Objectives of this study

The overall objective of this thesis is to investigate biogeophysical interactions between seasonal vegetation variability and climate on the regional scale with a focus on Europe. Thereby, the primary interest is on how the atmosphere responds to vegetation phenology. The modelling studies were performed using the regional climate model REMO (REgional MOdel, Jacob et al. 1997 and 2001). One study on global scales is done by global climate model simulations using the general circulation model ECHAM5 (Roeckner et al. 2003). Vegetation phenology was implemented into the land surface scheme of REMO following

three steps and all advancements were extensively tested and its influence on the climate simulations investigated. The individual working steps refer to the following hypotheses:

1 Vegetation phenology influences the simulated regional mean climate.

2 The seasonal albedo variability of snow-free land surfaces (background albedo) can be described as a function of vegetation phenology, and it influences the simulated climate.

3 The variability of the regional climate causes variability of vegetation phenology, which feeds back to the simulated regional climate.

The corresponding working steps are:

1 Implementation of monthly varying vegetation fields into the land surface scheme of REMO as lower boundary condition for the atmosphere and investigation of its influence on the simulated regional climate over Europe

2 Parameterisation of surface background albedo variability as a function of vegetation phenology on the basis of remotely-sensed data, application in the RCM REMO (and the GCM ECHAM5) and investigation of its impact on the regional (and global) climate simulations

3 Development of a plant phenology scheme and implementing it into the regional climate model REMO in order to study the dynamic interactions between vegetation phenology and climate variability

During the studies the focus was on the following questions:

- How is the near-surface climate affected by seasonal vegetation variability? What are the impacts on vertical surface fluxes, near-surface temperature and precipitation?

- Is the effect of vegetation phenology on climate varying with regard to different regions of Europe and with respect to the different seasons?

- Does the vegetation effect on climate simulations depend on the spatial horizontal resolution of the climate modelling grid?

- Do the advanced vegetation treatments improve the climate model simulation results with regard to observations?

- How strong is the effect of seasonal albedo variations caused by vegetation phenology on the simulated near-surface climate? Do the global and the regional climate model simulations respond differently to the advanced albedo parameterisation?

- Is a simple phenology model capable of representing the interannual variability and temporal trends in vegetation phenology caused by climate variability?

- How is vegetation phenology affected by climate warming conditions simulated by a future climate projection for the end of the century?

- What is the feedback effect of interannual variability of vegetation phenology on the simulated regional climate?

1. 4 Outline

This thesis is structured according to the three main hypotheses and working steps described in chapter 1. 3. Step 1 is presented in chapter 2, step 2 is split into the chapters 3 and 4 and step 3 is outlined in chapter 5. Each chapter is a journal publication and includes a short summary, introduction, model descriptions, results and conclusions, some recurrences may occur:

Chapter 2 studies the impact of a mean annual vegetation cycle on the simulated regional climate over Europe and is published as: *Rechid D, Jacob D (2006) Influence of monthly varying vegetation on the simulated climate in Europe. Meteorol Z, 15, 99-116.*

Chapter 3 describes the parameterisation of snow-free land surface albedo variability as a function of vegetation phenology on the basis of remotely-sensed data. It is published as: *Rechid D, Raddatz TJ, Jacob D (2008a) Parameterization of snow-free land surface albedo as a function of vegetation phenology based on MODIS data and applied in climate modelling. Theor Appl Climatol, DOI 10.1007/s00704-008-0003-y.*

Chapter 4 investigates the influence of the advanced background albedo parameterisation on regional and global climate model simulations. It is published as: *Rechid D, Hagemann S, Jacob D (2008b) Sensitivity of climate models to seasonal variability of snow-free land surface albedo. Theor Appl Climatol, DOI 10.1007/s00704-007-0371-8.*

Chapter 5 presents the simple plant phenology model PHENO and investigates the impact of climate on the interannual variability and temporal trends of vegetation phenology and its feedback on the simulated regional climate. It is submitted to *Climate Dynamics* as: *Rechid D, Jacob D (2008) Dynamic interactions between plant phenology and climate variability simulated by the regional climate model REMO over Europe.*

Chapter 6 composes the main conclusions of this thesis and gives a short outlook regarding ongoing research activities and future perspectives.

Chapter 2

Influence of seasonally varying vegetation on the simulated climate in Europe[1]

Abstract

In this study the regional climate model of the German Max-Planck-Institute for Meteorology (REMO) is used to analyse the effect of monthly varying vegetation on the simulated climate in Europe. For this investigation the annual cycle of vegetation is implemented in the land surface parameterization scheme of REMO. As input data source a new global dataset of land surface parameters is used. It contains monthly varying vegetation parameter values for leaf area index, fractional vegetation cover and background surface albedo. This dataset is adapted to both standard REMO model domains at 0.5 degree and 0.l6 degree horizontal resolution focusing Europe. For both resolutions present-day climate simulations are performed to examine the sensitivity of REMO to the modified vegetation parameterization. The simulation results are compared to corresponding reference simulations where vegetation parameter values are held constant in time. A validation is done by the comparison of the model results with several gridded observational datasets. A significant influence of monthly varying vegetation on the regional climate can be demonstrated. Vertical surface fluxes, near surface temperature and precipitation are strongly affected. The temporal analysis of the results reveals that the vegetation effect on the simulated climate occurs mainly in the summer season. In general, the simulated near-surface climate becomes cooler and wetter during the growing season. Concerning the spatial resolution, main effects can be detected in eastern Europe and the Hungarian lowlands. In these regions the more realistic vegetation treatment improves the simulated mean annual cycles of 2m temperature and precipitation with respect to the observations.

2. 1 Introduction

Vegetation strongly modifies the earth surface characteristics. They determine the exchange processes of water, energy and momentum between the land surface and the atmosphere. To

[1] *Rechid D, Jacob D (2006) Influence of monthly varying vegetation on the simulated climate in Europe. Meteorol Z, 15, 99-116*

specify some important processes: The surface albedo influences the short wave radiation budget. Surface roughness changes the wind in the planetary boundary layer. The density of vegetation cover controls transpiration by leaf stomatal conductance and evaporation by interception of water on the skin of the canopy. Evapotranspiration determines the partitioning of the vertical turbulent heat fluxes into latent and sensible heat. They are the main mechanisms to return energy from the surface into the atmosphere and influence convective processes and the boundary layer structure. These surface processes controlled by vegetation properties are responsible for near surface atmospheric conditions, such as surface temperature, near surface humidity and low level cloudiness and provide the appropriate feedback mechanisms to other physical processes in the atmosphere. Numerous studies demonstrate the importance of land surface characteristics for surface-atmosphere interactions and the relevance of these processes for climate at all scales in space and time (e.g. Avissar and Verstraete 1990, Sellers 1991, Pielke et al. 1998). Several investigations address the significance of different surface parameters in atmospheric modelling (e.g. Shukla and Mintz 1982, Mintz 1984, Sud et al. 1988, Sud et al. 1990, Rowntree 1991, Henderson-Sellers 1993, Pielke et al. 1997). Sensitivity studies (Collins and Avissar 1994, Rodriguez-Camino and Avissar 1998) estimate the relative importance of land-surface parameters. The vegetation properties leaf area index (LAI), roughness length and surface albedo turned out to be dominant parameters for climate model simulations.

A number of recent studies analyse the feedback of vegetation variability on the climate system. How land use change can influence the simulated climate is examined for example by Bonan (1997), Stohlgreen et al. (1998) or Chase et al. (2000). Bounoua et al. (2000) investigate the sensitivity of climate to changes in vegetation density induced by natural decadal climate variability using a coupled biosphere-atmosphere model. They find that increases in vegetation density result in cooler and moister near-surface climate. In climate models themselves, the temporal variability of vegetation is often not explicitly specified or simulated. Recent efforts to consider the annual cycle of vegetation in a global climate model are done by Lawrence and Slingo (2004a, 2004b). They prescribe the vegetation annual cycle on the basis of satellite estimates of LAI and they adjust some model parameters in several sensitivity studies to strengthen the relationship between evaporation and vegetation state. They find that an annual cycle of vegetation reduces surface temperatures in extratropical regions during both the summer and winter season. Where the magnitude of LAI values is enhanced, precipitation increases. In the study of Lu and Shuttleworth (2002), vegetation phenology is assimilated into the climate version of the regional atmospheric modelling system (ClimRAMS) in the form of LAI estimates derived by the normalized difference vegetation index (NDVI). They conclude that the effect of enhanced heterogeneity dominates over the effect of an reduced magnitude in LAI fields.

In the present study a mean annual cycle of vegetation is prescribed to the regional climate model of the German Max-Planck-Institute for Meteorology (REMO) as temporally varying boundary condition. It is derived from a global dataset of land surface parameters constructed by Hagemann et al. (1999) and Hagemann (2002), that contains monthly fields of fractional vegetation cover, LAI and background surface albedo, which is the albedo over snow-free land areas. They are adapted to the regional model. The modified model version of REMO enables us to investigate the impact of seasonally varying vegetation on the simulated climate in Europe.

2. 2 Model description

2. 2. 1 Basic characteristics

The regional climate model REMO (Jacob and Podzun 1997, Jacob et al. 2001) is based on the "Europamodell", the former numerical weather prediction model of the German Weather Service (Majewski 1991). Further development of the model took place at the Max-Planck-Institute for Meteorology, where the physical parameterizations from the global climate model ECHAM4 (Roeckner et al. 1996) were implemented. The prognostic variables are surface pressure, temperature, horizontal wind components, specific humidity and cloud water. Their calculations are based on the hydrostatic approximation. The model equations are formulated in a rotated spheric coordinate system. The model can be used in the forecast mode or in the climate mode. In the climate mode continuous runs for long time periods up to decades are carried out with updates of the lateral boundaries every 6 hours (Jacob 2001). The regional model is nested into the driving fields. These lateral boundary conditions are provided by analysis/reanalysis data or by global climate model results. A relaxation scheme according to Davies (1976) is used to adjust the prognostic variables prescribed by the boundary fields in a zone of the 8 lateral grid rows. As lower boundary values land surface characteristics, sea surface temperature and sea ice distribution are prescribed during the whole model simulation (for more details about initialization and boundary conditions see Semmler et al. 2004). The horizontal discretization is done on the Arakawa-C-grid. The generally used horizontal resolutions are 0.5 degree and 0.16 degree corresponding approximately to 55 km and 18 km grid size, respectively. The vertical discretization is done in a hybrid coordinate system (Simmons and Burridge 1981). The time-stepping is leap-frog with semi-implicit correction and Asselin-filter.

2. 2. 2 Land surface parameterizations

In REMO version 5.0, which is used for the model simulations in the present study, thermal and hydrological processes in the soil are based on parameterization schemes of ECHAM4 (DKRZ 1993, Roeckner et al. 1996). Soil temperatures are calculated from diffusion equations solved in five discrete layers with zero heat flux at the bottom (10m depth) according to the scheme of Warrilow et al. (1986). The heat diffusion in the soil depends on heat capacity and thermal conductivity of the soil. Soil hydrology is parameterized in three water budget equations for the temporal alteration of water storage in the soil related water reservoirs, namely snow, vegetation and bare soil. The runoff-scheme is based on catchment considerations including sub-grid scale variations of field capacity over inhomogeneous terrain (Dümenil and Todini, 1992). The vertical turbulent surface fluxes are calculated from Monin-Obukhov similarity theory (Louis, 1979) with a higher order closure scheme for the transfer coefficients of momentum, heat, moisture and cloud water within and above the planetary boundary layer.

The land surface processes are controlled by physiological vegetation properties. In REMO they are represented by the vegetation parameters leaf area index (LAI, here the ratio of one-sided leaf area to ground area), fractional vegetation cover (here fraction of photosynthetically active vegetation), background surface albedo, surface roughness length due to vegetation, forest ratio and water holding capacity. In the present study, monthly varying fields are introduced to the parameters LAI, fractional vegetation cover and background surface albedo.

Water holding capacity (depending on plant rooting depths) and forest ratio (used as a constant stem index) are not or only marginally affected by the annual vegetation cycle. Surface roughness length is kept constant. A possible impact of temporally varying roughness length due to vegetation is planned to be investigated in a further study. We don't expect any significant effects on the simulated climate, because total surface roughness length is dominated by the orographic variance in most regions.

To provide a basis for later discussions of the study results, surface processes related to the modified parameters are now briefly introduced. The background surface albedo is the albedo over snow-free land areas. Over snow and sea, surface albedo is modified by surface conditions during the model integration time. It determines the short-wave radiation budget at the earth surface. The vegetation cover ratio C_v is assigned to each surface grid box. It determines the fraction of grid area where vegetation properties take effect on surface exchange processes. The LAI in particular affects interception and evapotranspiration through stomatal conductance. Intercepted water goes into the skin reservoir, which determines the wet skin fraction C_l:

$$C_l = min\left(1, \frac{W_l}{W_{lmx}}\right) \qquad (2.1)$$

with

$$W_{lmx} = W_{lmax}((1 - C_v) + C_v \cdot LAI) \qquad (2.2)$$

W_l is the prognostic variable for the skin reservoir content, W_{lmx} is the maximum skin reservoir content and W_{lmax} is the maximum amount of water that can be held on one layer of leaf or bare ground. It is taken to be 0.2 mm. Evaporation from the skin reservoir (E_l) is at the potential rate:

$$E_l = \rho \cdot C_h \cdot |v_h| \cdot (q_v - q_s) \qquad (2.3)$$

ρ is the air density, C_h is the transfer coefficient for heat and v_h the horizontal velocity. q_v is the specific near-surface humidity and q_s is the saturation specific humidity at surface temperature and surface pressure. Evaporation from dry vegetated areas is called transpiration. It is proportional to the evaporation efficiency e:

$$E_v = e \cdot \rho \cdot C_h \cdot |v_h| \cdot (q_v - q_s) \qquad (2.4)$$

Based on Sellers et al. (1986), the evaporation efficiency e is expressed as a function of stomatal resistance R:

$$e = (1 + C_h \cdot |v_h| \cdot R)^{-1} \quad (2.5)$$

with

$$R = \frac{R_0}{F(W_s)} \quad (2.6)$$

The water stress factor $F(W_s)$ is an empirical function of the available water in the root zone. R_0 is the minimum value of the stomatal resistance:

$$\frac{1}{R_0} = \frac{1}{k \cdot c} \cdot \left(\frac{b}{d \cdot PAR} \cdot \ln\left(\frac{d \cdot e^{k \cdot LAI} + 1}{d + 1} \right) - \ln\left(\frac{d + e^{-k \cdot LAI}}{d + 1} \right) \right) \quad (2.7)$$

where

$$d = \frac{a + b \cdot c}{c \cdot PAR} \quad (2.8)$$

The photosynthetically active radiation (PAR) is taken as 55% of the net surface short wave radiation and the standard parameter values are: k=0.9, a=5000 Jm^{-3}, b=10 Wm^{-2}, c=100 sm^{-1}.

2. 3 Study design

In this study the annual cycle of vegetation is implemented in the regional climate model REMO. The vegetation cycle is derived from a global dataset of land surface parameters (Hagemann et al. 1999, Hagemann 2002). These data fields are based on the global distribution of major ecosystem types according to the definitions given by Olson (1994a, 1994b). This global dataset of land use classes was derived from Advanced Very High Resolution Radiometer AVHRR data at 1 km resolution supplied by the International Geosphere-Biosphere Program (Eidenshink and Faundeen 1994) and constructed by the U.S. Geological Survey (1997, 2002). For each land use class parameter values for background surface albedo, fractional vegetation cover, leaf area index, forest ratio, roughness length and soil water holding capacity are allocated. The global datafields are adapted to the 0.5 degree and 0.16 degree standard model domains of REMO focusing on Europe (Rechid 2001). The monthly vegetation values for fractional vegetation cover, LAI and background surface albedo are estimated by a global data field of the monthly growth factor, which determines the growth characteristics of the vegetation at a horizontal resolution of 0.5 degree (Hagemann

2002). This method enables the preparation of an annual vegetation cycle that remains consistent with all land surface parameter values used in the model. These monthly vegetation fields are prescribed to the model as temporally varying boundary conditions. During the model simulation, the monthly values are interpolated for the 5 minutes model time step at 0.5 degree horizontal resolution and for the 2 minutes model time step at 0.16 degree resolution.

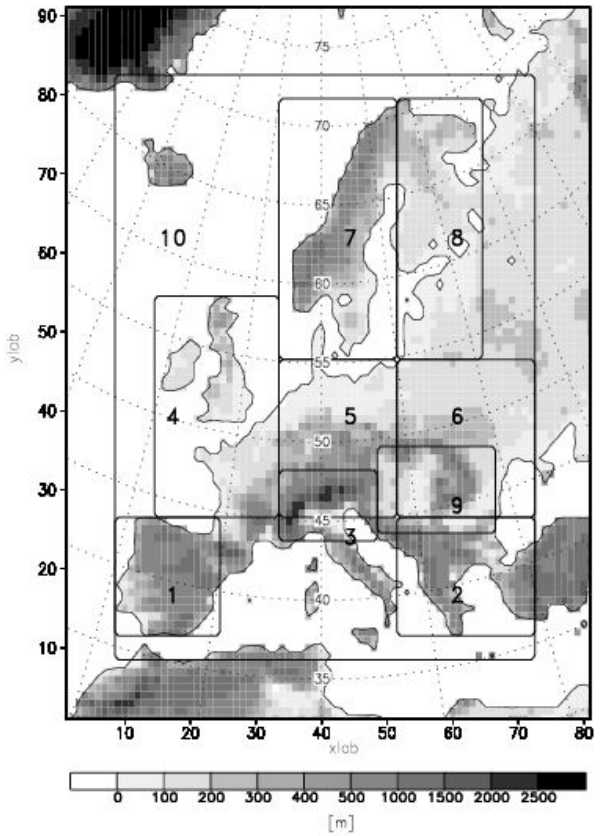

Figure 2.1: REMO model orography [m] at 0.5 degree resolution with European subdomains: 1 Iberian peninsula, 2 south-eastern Mediterranean, 3 Alpine region, 4 western Europe, 5 central Europe, 6 eastern Europe, 7 eastern Baltic, 8 western Baltic, 9 Hungarian lowlands, 10 model domain area without the 8 boundary grid boxes.

To investigate the sensitivity of the regional model to the modified vegetation parameterization model simulations for both horizontal resolutions with 20 vertical atmosphere levels are performed. The model run at 0.5 degree resolution (VEG-0.5) simulates 15 years of today's climate (1979-1993) driven by lateral boundary conditions and sea surface temperatures from the European Centre for Medium-Range Weather Forecasts (ECMWF) Reanalysis Project (ERA-15). The 0.16 degree resolution run (VEG-0.16) simulates 5 years (1984-1988) driven by the 0.5 degree run results. The simulation results are compared to corresponding reference runs with temporally constant vegetation input (REF-0.5 and REF-0.16). The evaluation of VEG-0.5 is done for several subdomains representing different European climate regions. The 0.5 degree model domain and the European subdomains superposed on the model orography are presented in figure 2.1. For all data analyses only the land area of the different regions is considered.

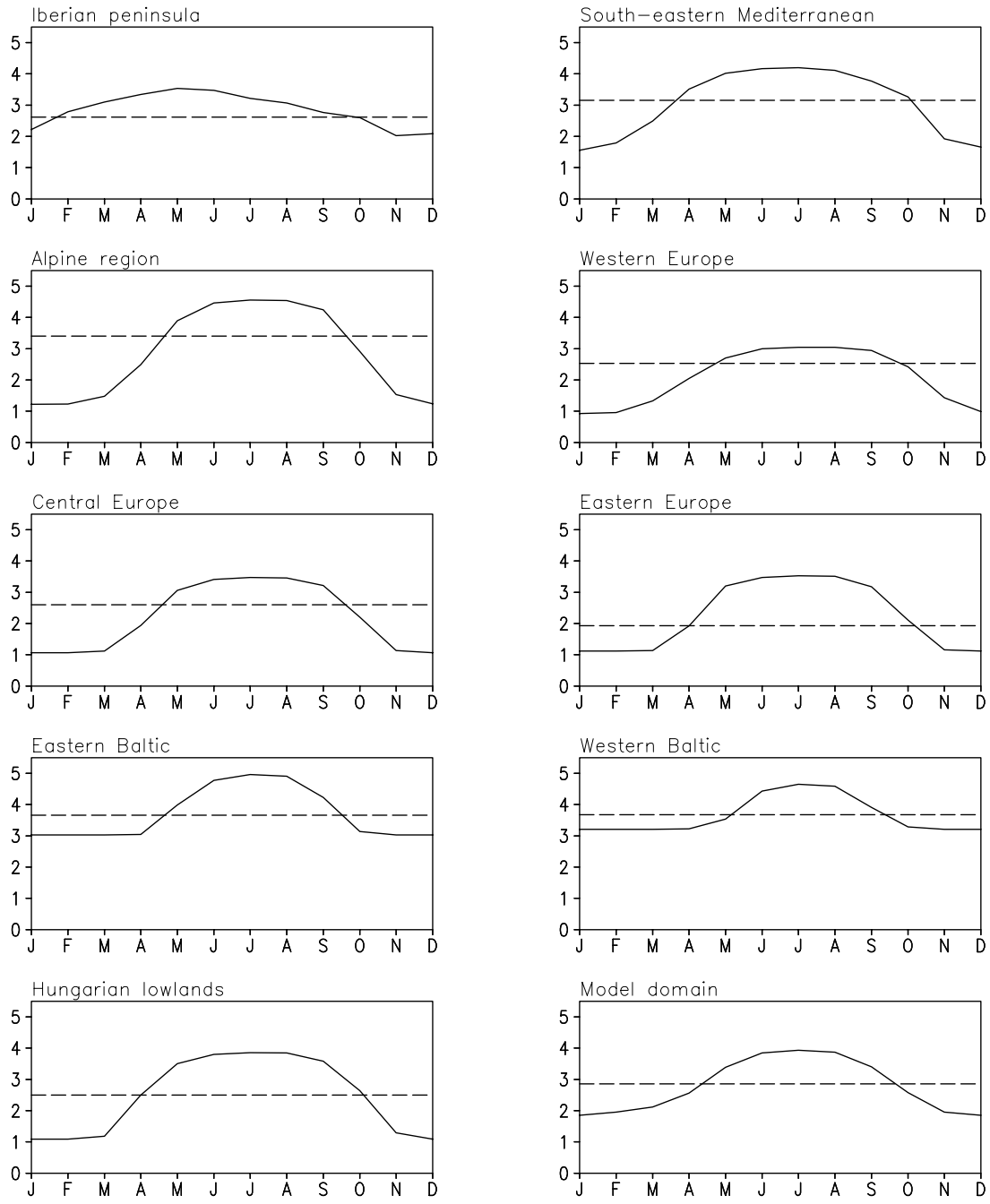

Figure 2.2: New annual cycle of leaf area index compared to reference constant value area-averaged over the European subdomains.

As example the new annual cycle of LAI for all European subdomains in comparison to the former annual mean LAI value is presented in figure 2.2. In all European subdomains the LAI shows lower values during winter and higher values during summer in comparison to the former mean LAI values. The largest differences in summer season occur in eastern Europe. The constant annual mean value of the reference simulation is slightly different from the temporal average of the varying LAI because the minimum and maximum LAI values are corrected for some ecosystem types (Hagemann 2002). But as the annual LAI cycles still

exhibit a realistic variation compared to the reference constant annual means with clearly lower values in summer and larger values in winter, the influence on the regional climate can be attributed to the monthly varying vegetation.

2. 4 Results and discussion

To analyse the simulation results, time series of monthly means are calculated and averaged over the 15 years simulation time period in terms of mean annual cycles and seasonal means. Mean annual cycles are plotted in area-averages calculated for the model domain and the European subdomains introduced in figure 2.1. For all investigated regions only land surface area is considered. To examine the influence of resolution some selected results of VEG-0.5 are compared to VEG-0.16 and their respective reference runs.

2. 4. 1 Seasonal means

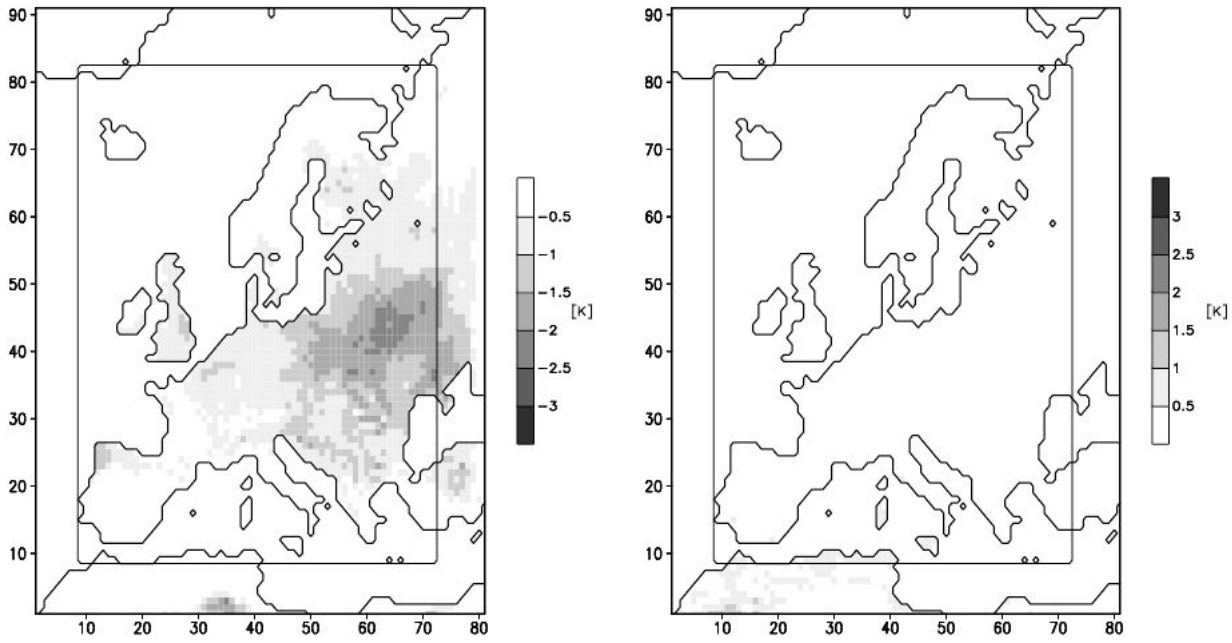

Figure 2.3: Seasonal mean JJA 1979-1993 of negative (left panel) and positive (right panel) change in surface temperature [K] due to monthly varying vegetation. The difference VEG-0.5 - REF-0.5 is plotted.

During the summer season (June-July-August, JJA) the effect of the annual vegetation cycle reduces the mean surface temperatures in the north-west of Spain, in central and especially in eastern Europe up to -2 K (figure 2.3). In winter time (December-January-February, DJF) the surface temperature is almost not affected by temporally varying vegetation (not shown). The seasonal means of precipitation are also mostly unaffected in winter time (not shown), but in the summer season a substantial increase in precipitation over the land surface area of the

whole model domain can be detected, up to 40 mm/month in eastern Europe and the Alps (figure 2.4). As in the case of surface temperature and precipitation all investigated parameters respond to temporally varying vegetation mainly during the summer season. In summer vertical exchange processes dominate advective processes. High solar radiation input to the earth surface leads to intensive exchange processes of energy at the land surface which are strongly controlled by land surface characteristics. In contrast, during the winter season low solar radiation input, dominant large-scale weather conditions and snow cover deactivate the control of land surface processes by vegetation properties. Over sea areas there is only a slight change in precipitation. This indicates, that the vegetation effect is mainly restricted to the land area, where the vegetation parameter values are modified. The effect on large-scale atmospheric circulations is marginal. We also analysed the mean sea level pressure and the 850 hPa geopotential (not shown). The new vegetation treatment does not cause any noticeable changes in these parameters. Moreover, the biases compared to the input data from the ECMWF reanalyses are even larger with one order of magnitude in some regions (not shown). Altogether, the new vegetation scheme has no impact on the large scale pressure regimes.

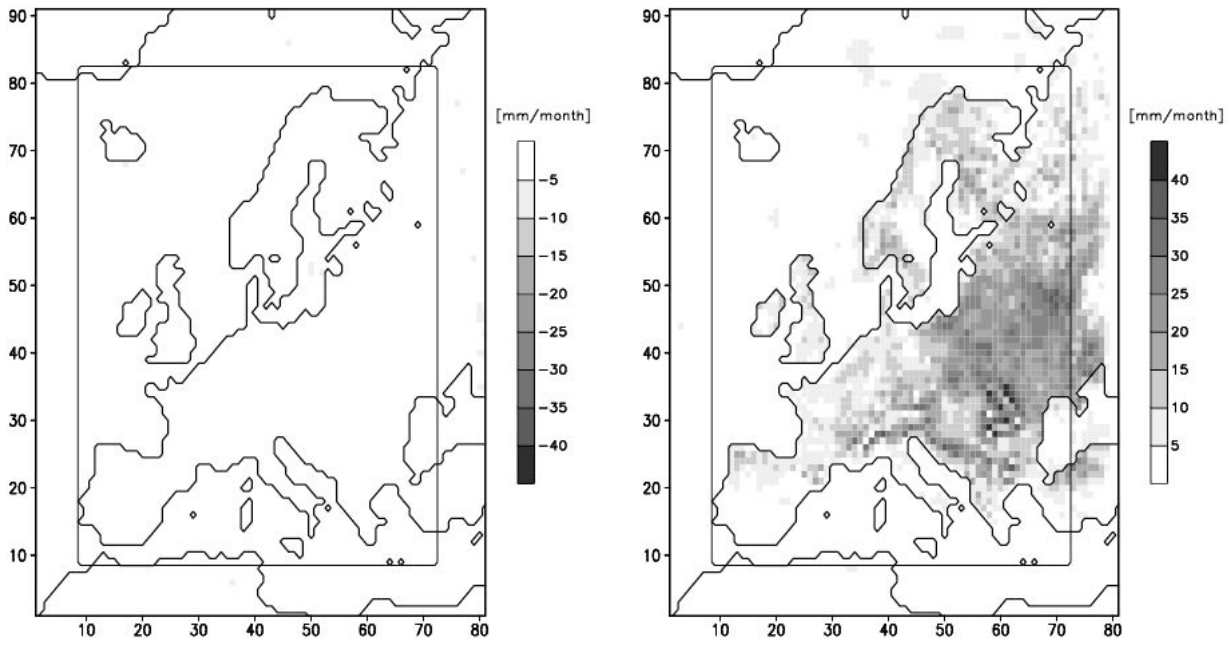

Figure 2.4: Seasonal mean JJA 1979-1993 of negative (left panel) and positive (right panel) change in precipitation [mm/month] due to monthly varying vegetation. The difference VEG-0.5 - REF-0.5 is plotted.

As described in section 2.2 fractional vegetation cover and LAI directly control the evapotranspiration processes. During the summer season increased values of fractional vegetation cover and LAI raise transpiration. The simulated surface evapotranspiration (figure 2.5) does significantly increase over major parts of the land surface. Strongest changes occur in regions, where the LAI shows significantly higher values compared to reference (figure 2.2). Accordingly, the surface latent heat flux is increased over major parts of the European land area whereas the surface sensible heat flux is decreased. Soil wetness is reduced over some parts of Europe up to 25 % (not shown), because more water leaves the soil through

transpiration. Together, raised evapotranspiration and latent heat flux decrease surface temperature and the water content in the soil and increase water vapour in the atmosphere and therefore precipitation.

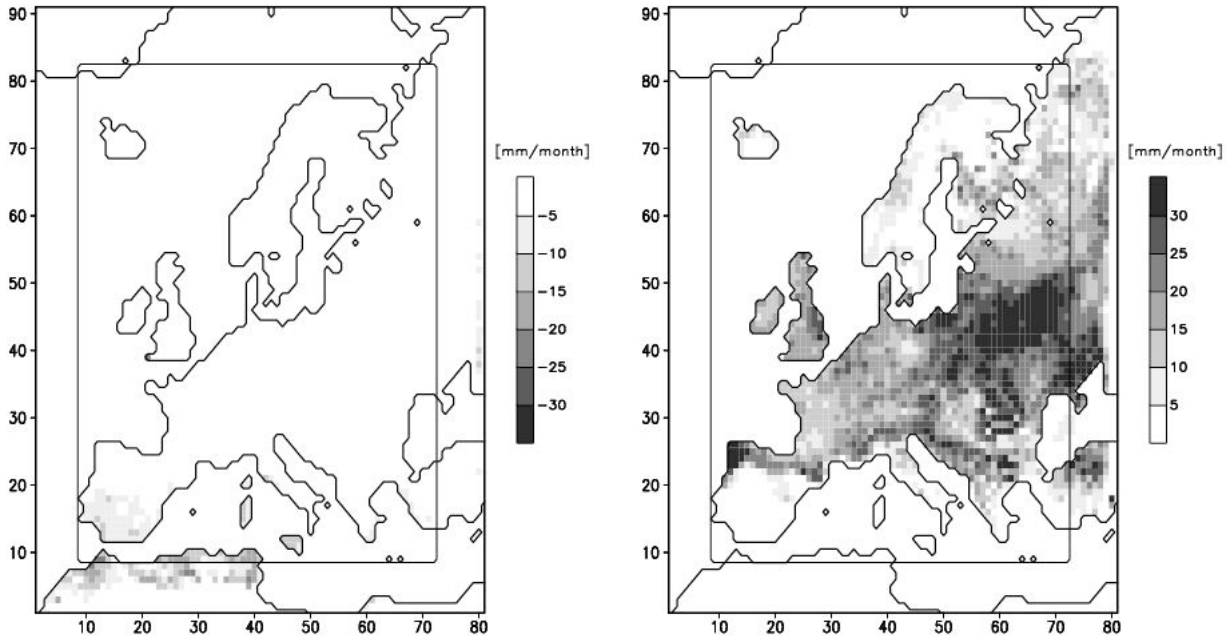

Figure 2.5: Seasonal mean JJA 1979-1993 of negative (left panel) and positive (right panel) change in evapotranspiration [mm/month] due to monthly varying vegetation. The difference VEG-0.5 - REF-0.5 is plotted.

2. 4. 2 Mean annual cycles

The temporally varying vegetation directly modifies the mean annual cycles of the vertical fluxes of humidity and heat at the surface. Higher LAI values in summer strongly increase evapotranspiration over land (as presented in chapter 2.4.1 and figure 2.5). This raises latent heat fluxes during the summer months up to 30 W/m^2 (not shown). Accordingly, sensible heat fluxes are reduced and surface temperatures decrease. Figure 2.6 presents the differences in the mean annual cycles of surface temperatures caused by the temporally varying vegetation. Most European regions show lower temperature values during the summer season whereas temperature in winter is only slightly affected. Strongest changes occur in eastern Europe and the Hungarian lowlands with differences up to -1.7 K in June. As illustrated in figure 2.2 these are the regions with the largest LAI differences in summer. Besides, the continental climate in eastern Europe is characterised by relatively high temperatures and low precipitation in summer. High solar radiation input leads to intensive vertical exchange processes at the earth surface which are determined by the surface properties. Thus, the altered vegetation parameter values strongly influence the simulated climate in this European region.

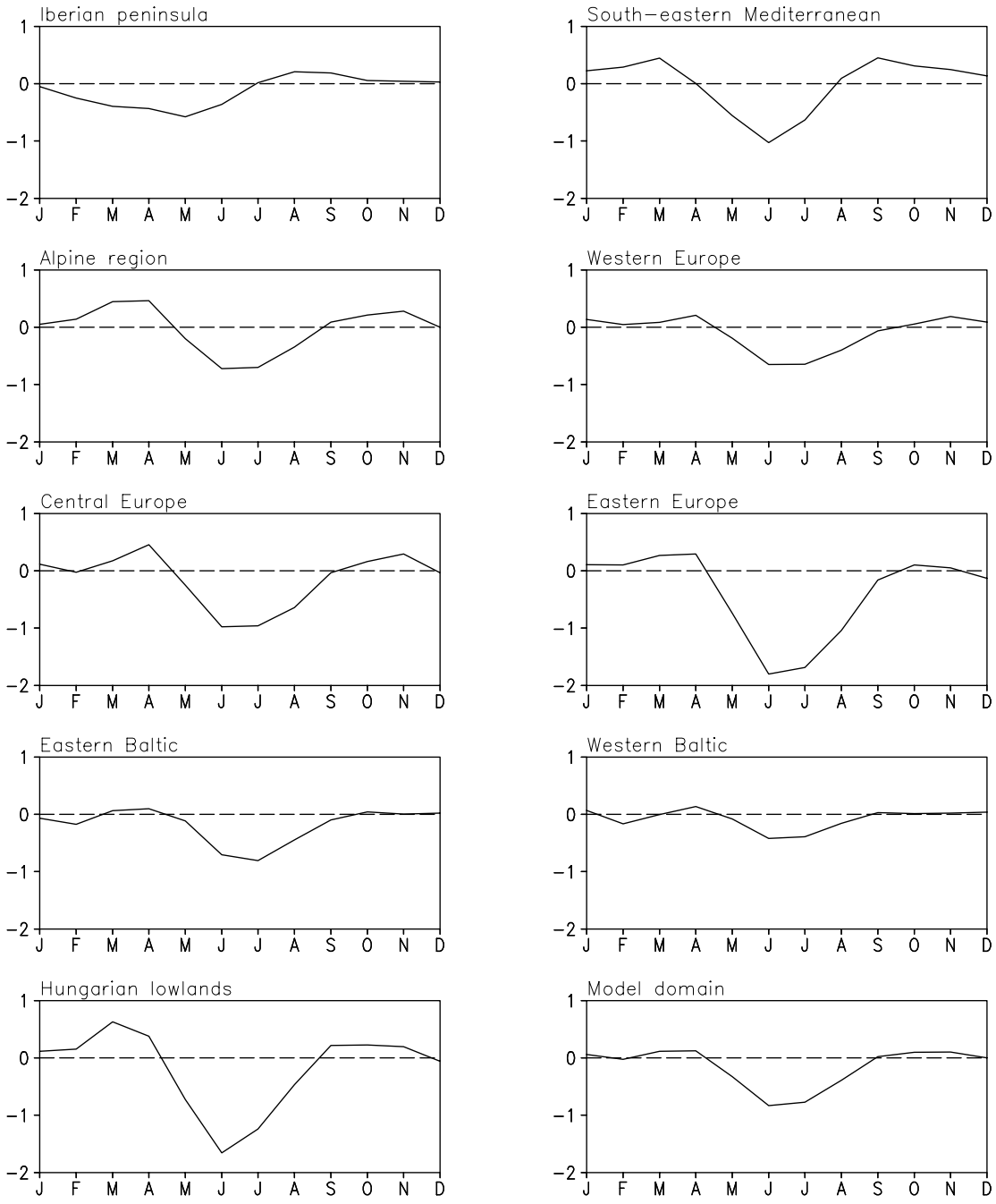

Figure 2.6: Mean annual cycle 1979-1993 of change in surface temperature [K] due to monthly varying vegetation area-averaged over the European subdomains. The difference VEG-0.5 - REF-0.5 is plotted.

On the Iberian peninsula, the largest differences in surface temperature appear in May. In this region, summer season starts earlier and accordingly, maximum vegetation is already reached in May. In western Europe and the western Baltic area surface temperatures are almost not affected. In the case of western Europe, this can be explained by minor LAI changes in summer (figure 2.2). In the western Baltic land area, in contrast, the LAI values are enhanced. But here, the modified vegetation has only slight effects because this area is close to the sea. The annual temperature cycle is less distinctive than in other European regions and the

summer magnitude of near-surface temperatures is discernable lower. Evapotranspiration and latent heat fluxes are less affected by vegetation due to the lower saturation deficit of water vapour in the atmosphere. This results in lower temperature differences between VEG-0.5 and REF-0.5. Besides, the strongest effect of the westerly winds on Europe occur on the Norwegian coast. Thus, the western Baltic area is dominated by large scale weather conditions and regional surface characteristics are of secondary importance.

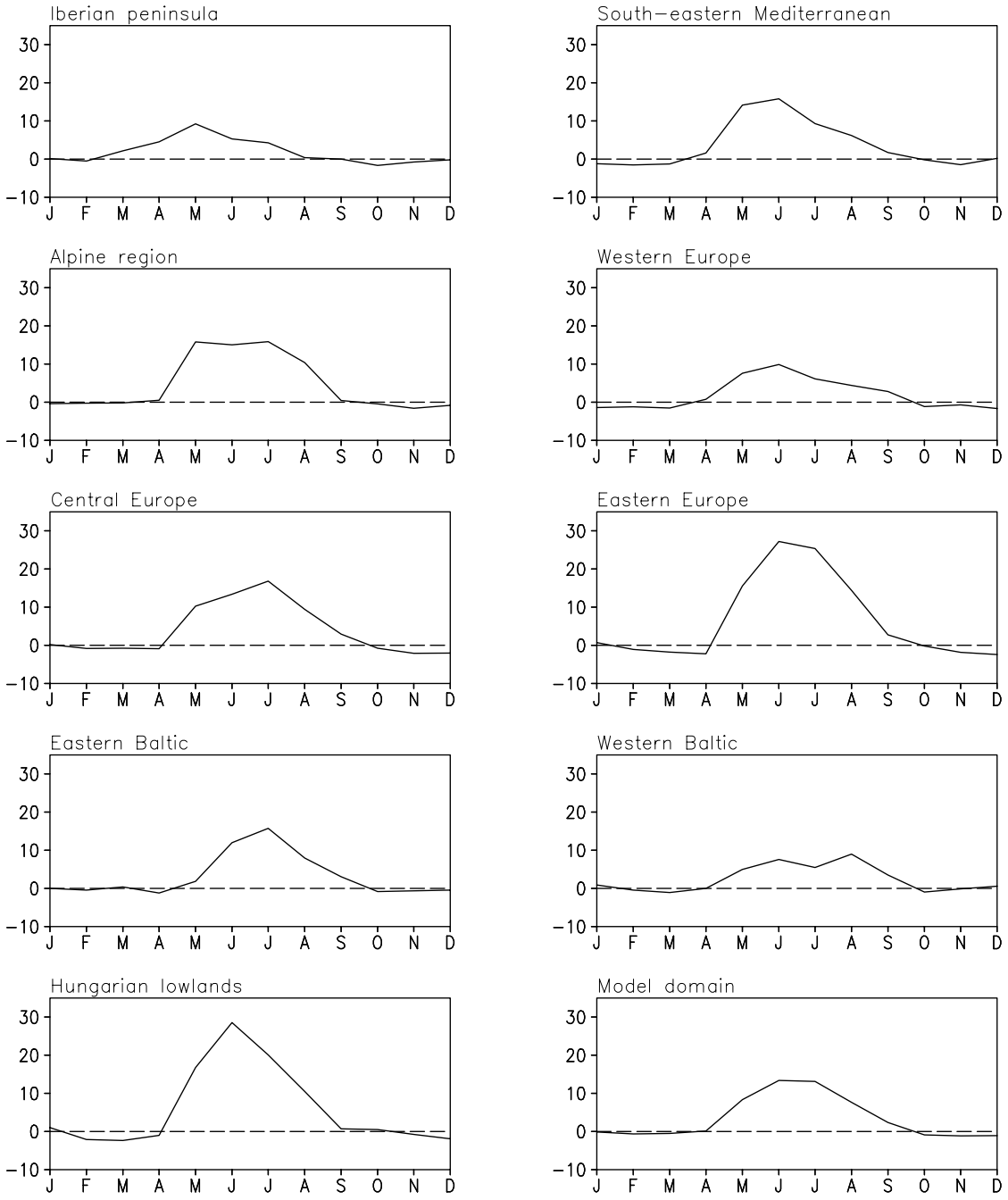

Figure 2.7: Mean annual cycle 1979-1993 of change in precipitation [mm/month] due to monthly varying vegetation area-averaged over the European subdomains. The difference VEG-0.5 - REF-0.5 is plotted.

The new vegetation treatment strongly influences the simulated annual precipitation cycle in Europe (figure 2.7). In all European subregions precipitation increases during the summer months, whereas winter precipitation is not affected. The strongest effects here also occur in the continental climate zones. In eastern Europe the largest precipitation differences reach up to + 30 mm in June. In this region with intensive vertical exchange processes at the surface insummer the influence of the annual vegetation cycle becomes most visible.

To explain the vertical interactions between soil-vegetation-atmosphere several parameters for eastern Europe are composed in figure 2.8. In plot 2.8a and 2.8b precipitation is separated into large scale precipitation and convective precipitation. It becomes evident that the precipitation change is only caused by the convective part, whereas the large scale precipitation is not influenced. This means, that vegetation properties have local effects on the vertical exchange processes but not on the large scale atmospheric conditions. The higher LAI values in summer increase evapotranspiration up to a difference of 30 mm in June (2.8d). More leaves intercept more water on the canopy which can evaporate from there at the potential rate (see also chapter 2.2.2). Increased evapotranspiration raises the latent heat flux by up to 30 W/m^2 (2.8e). The sensible heat flux decreases by up to 15 W/m^2 (2.8f). The soil heat flux is also decreased which becomes evident by lower surface temperature (2.8c). The surface thermal radiation is reduced by 8 W/m^2 (not shown). Whereas the water flux into the atmosphere is higher, less water is stored in the soil (2.8g). In April after the spring runoff peak the soil water content is filled up almost to the same level as in the reference simulation, but during the following summer months less water reaches the soil due to increased interception and more water leaves the soil through transpiration. The maximum changes in evapotranspiration and precipitation occur in June. During the following summer months, the soil water in the upper layers is depleted and limits evapotranspiration. The increased water content in the atmosphere does not lead to higher fraction of cloud cover (2.8h) , but is raising precipitation. Altogether, the water storage in the soil is reduced and the hydrological cycle is intensified.

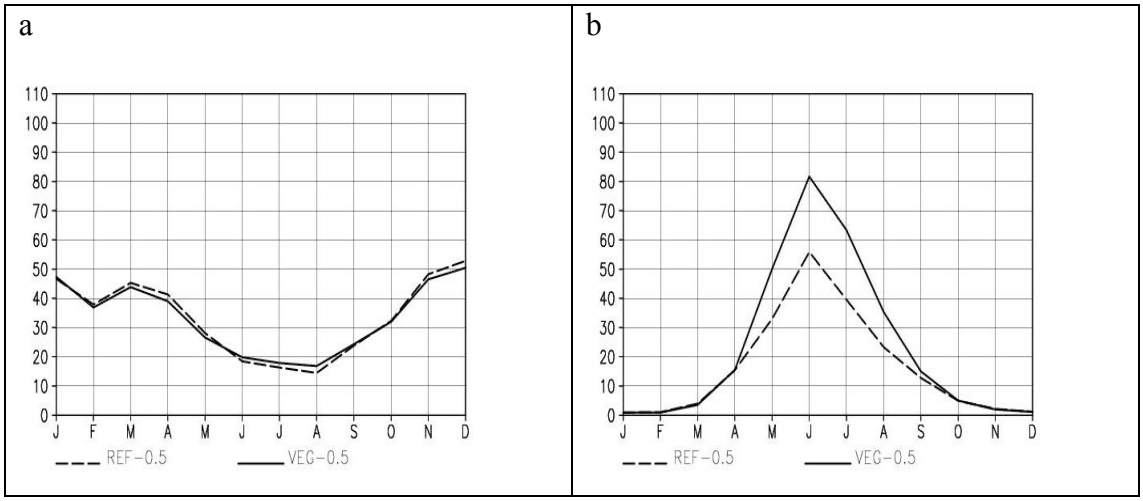

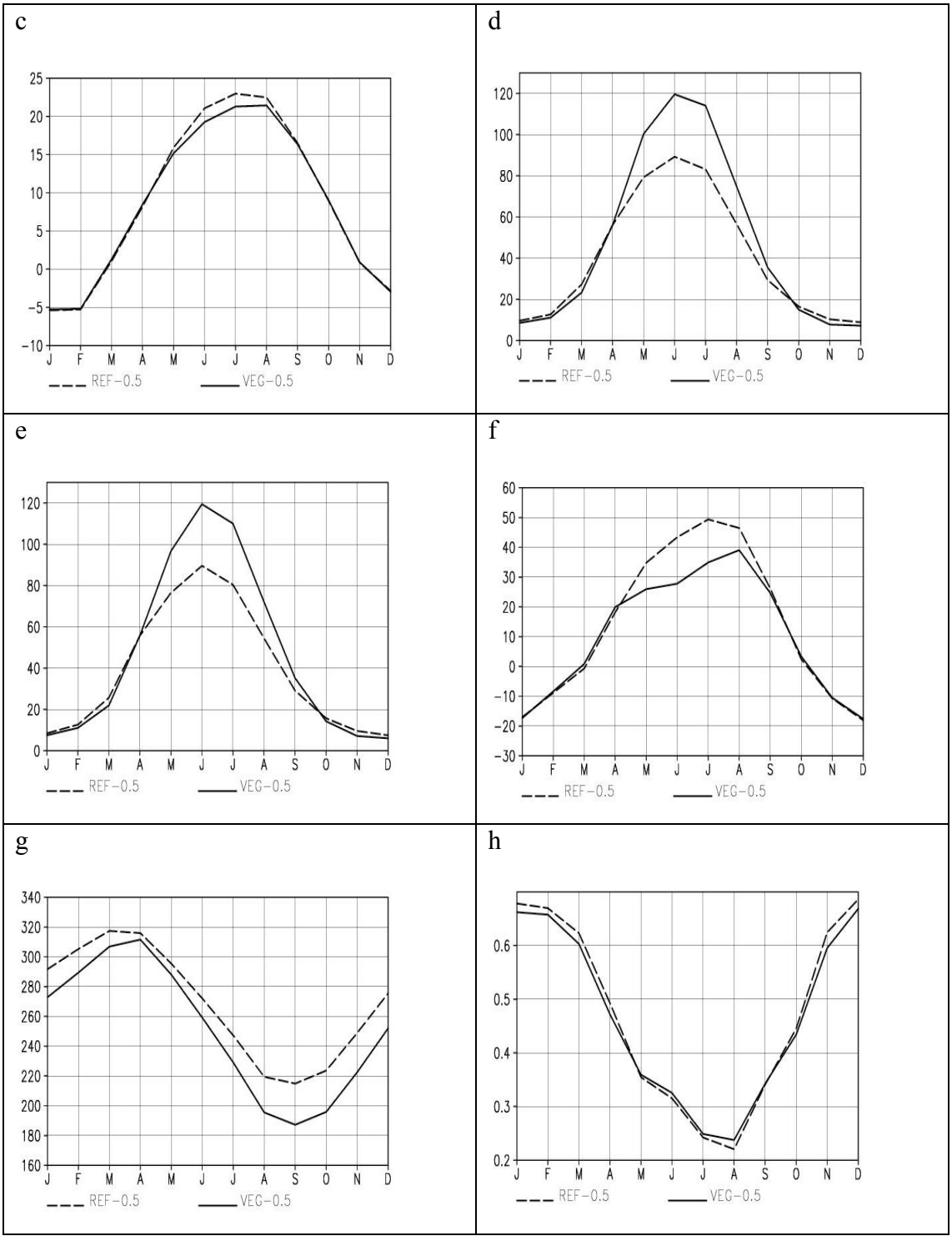

Figure 2.8: Mean annual cycles 1979-1993 of reference run REF-0.5 and simulation VEG-0.5 area-averaged over eastern Europe: a) large scale precipitation [mm/month], b) convective precipitation [mm/month], c) surface temperature [°C], d) evapotranspiration [mm/ month], e) latent heat flux [W/m^2], f) sensible heat flux [W/m^2], g) soil wetness [mm], h) fractional cloud cover [0,1]

2. 4. 3 Influence of horizontal resolution

To investigate the influence of the horizontal model resolution to the modified vegetation parameterization a 5 year long REMO simulation at 0.16 degree resolution is performed. The 0.16 degree model domain superposed on the model orography is presented in figure 2.9. To obtain the mean annual cycles of the simulation results timeseries of monthly means are calculated and averaged over the time period 1984-1988. For the 0.5 degree run the same temporal average for these 5 years is calculated. The subdomain central Europe and the model domain area are chosen exemplarily to compare results of VEG-0.16 and VEG-0.5 in terms of area-averaged annual cycles.

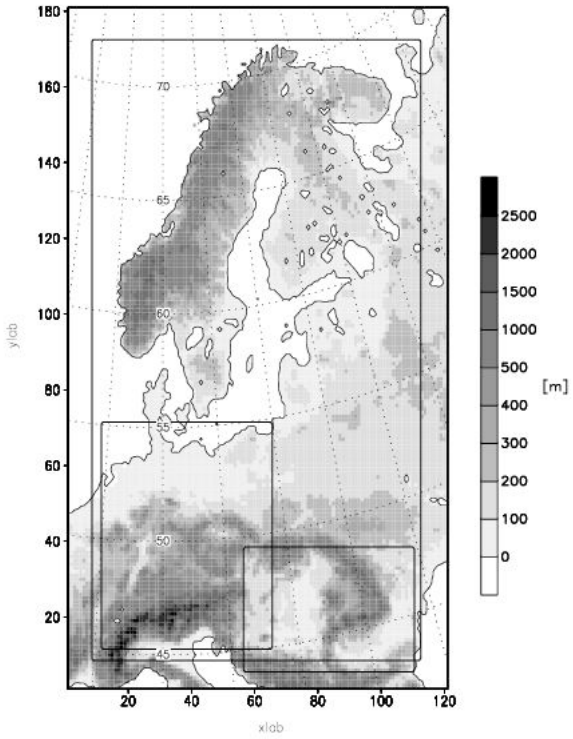

Figure 2.9: REMO model orography [m] at 0.16 degree resolution with subdomain central Europe and model domain without boundary zone.

The mean annual cycles of temperature and precipitation indicate no significant deviations. In summer, the temperature differences between VEG-0.16 and REF-0.16 are slightly lower than the differences between VEG-0.5 and REF-0.5 (figure 2.10). In the study at 0.16 degree resolution, the maximum precipitation change is also slightly lower and in the case of the model domain-average the maximum change in precipitation is reached one month earlier at 0.16 degree resolution (figure 2.11). The upper and lower curves in figure 2.10 and 2.11 show the temperature and precipitation changes +/- the standard deviations of the area averages, respectively. In all cases, the spatial variability increases in summer, but without noticeable differences caused by the different horizontal resolutions. Together, the influence of the horizontal model resolution on the area-averaged mean temperature and precipitation cycles of the European regions is only marginal.

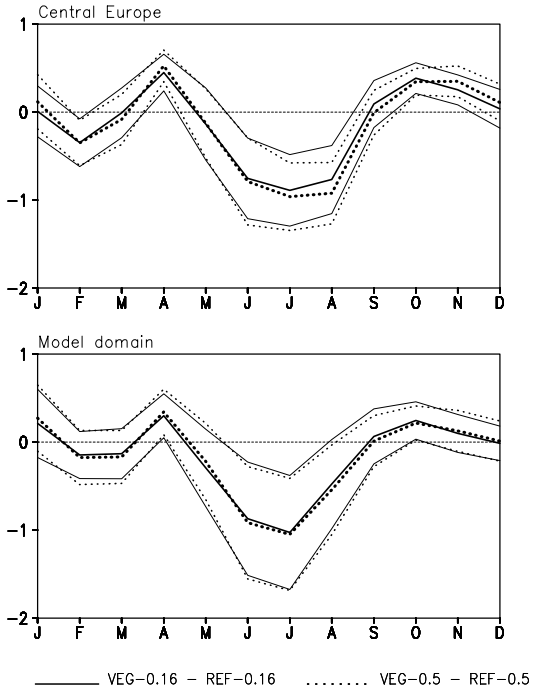

Figure 2.10: Mean annual cycle 1984-1988 of change in surface temperature [K] due to monthly varying vegetation area-averaged over central Europe (upper panel) and over the whole model domain (lower panel). The differences between VEG-0.16 and REF-0.16 and between VEG-0.5 and REF-0.5 are plotted. The upper and lower curves show the temperature change +/- the standard deviations of the area averages, respectively.

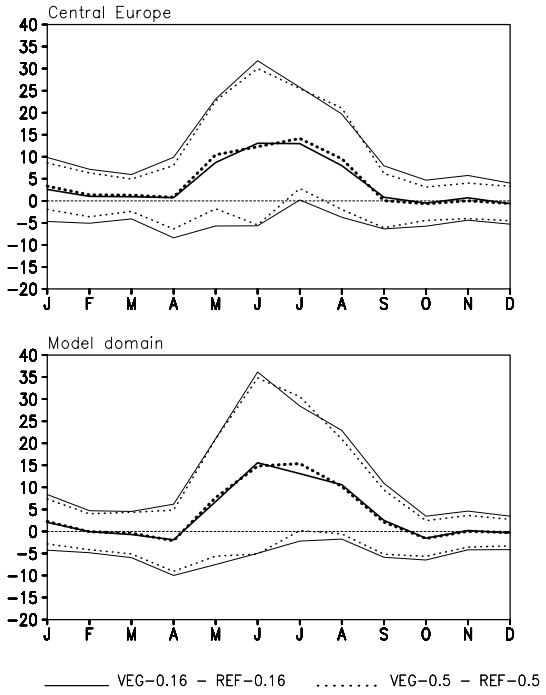

Figure 2.11: Mean annual cycle 1984-1988 of change in precipitation [mm/month] due to monthly varying vegetation area-averaged over central Europe (upper panel) and over the whole model domain (lower panel). The differences between VEG-0.16 and REF-0.16 and between VEG-0.5 and REF-0.5 are plotted. The upper and lower curves show the precipitation change +/- the standard deviations of the area averages, respectively.

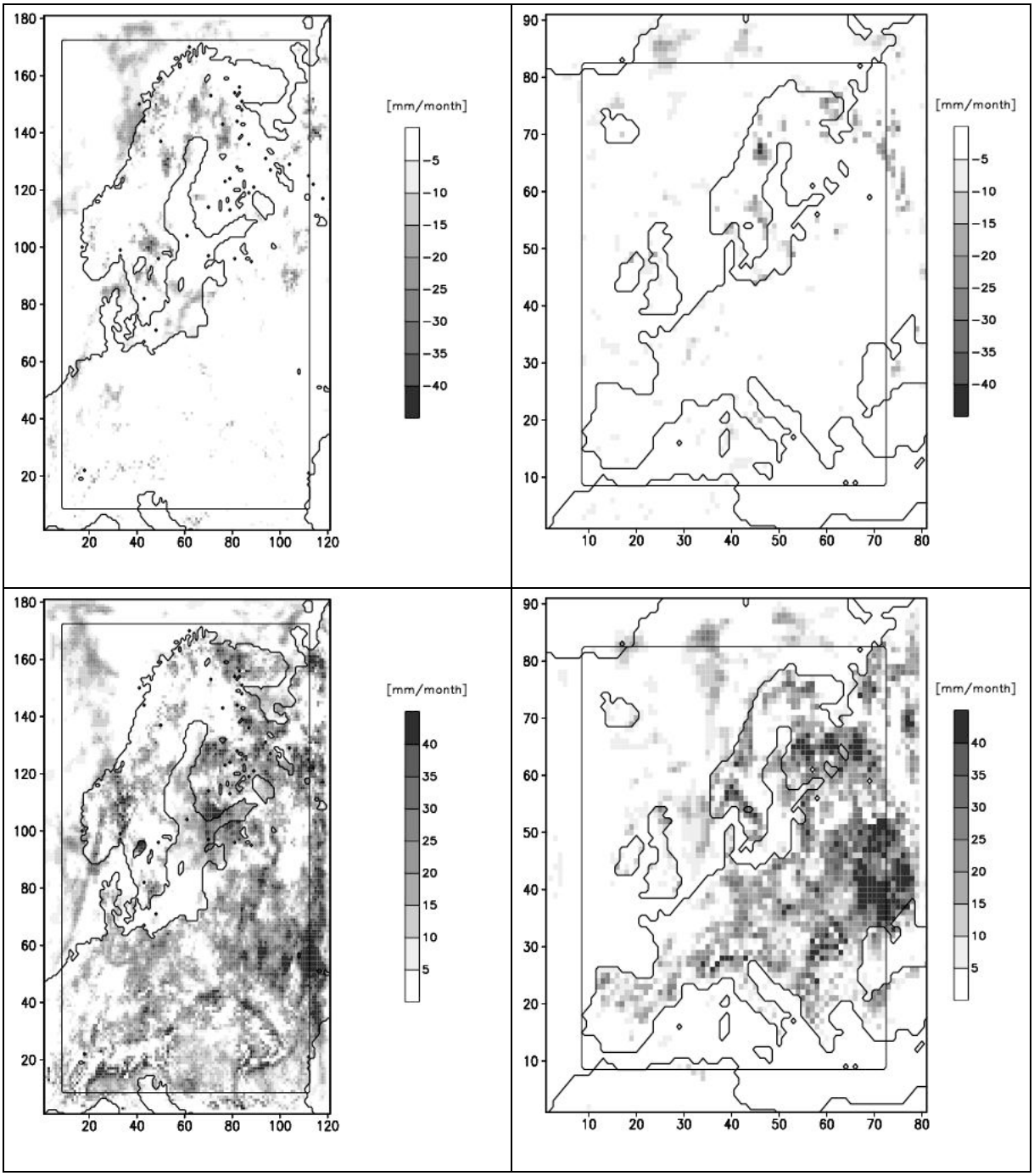

Figure 2.12: Monthly mean July 1984-1988 of negative (upper panels) and positive (lower panels) change in precipitation [mm/month] due to monthly varying vegetation. The differences VEG-0.16 - REF-0.16 (left panels) and VEG-0.5 - REF-0.5 (right panels) are plotted.

Looking at smaller areas, the horizontal resolution in combination with the annual vegetation cycle does affect the simulation results. In figure 2.12, the horizontal plots of the precipitation differences between VEG-0.16 and REF-0.16 for July are posed next to the corresponding difference plots of VEG-0.5 and REF-0.5. The comparison shows similar results for central and eastern Europe, in mountainous regions they are more structured at 0.16 degree resolution. In the Alpine region there are several grid points with lower precipitation values in the VEG-0.16 simulation, which do not appear at 0.5 degree resolution. Clear differences

caused by horizontal resolution occur in northern Europe. In northern Finland and especially at the Norwegian coast over sea precipitation is decreased in VEG-0.16, which is not the case at 0.5 degree resolution. The positive changes in precipitation are differently distributed on the Scandinavian peninsula and over the Baltic Sea in the simulation at 0.16 degree resolution. In some cases, they seem to be displaced eastward. In Scandinavia, the vegetation effect is superposed by the synoptic scale weather conditions strongly affected by the westerly winds. Here, the horizontal model resolution in combination with the modified vegetation treatment leads to changes in the mesoscale atmospheric circulation.

2. 4. 4 Validation

Observational datasets used for validation purposes are extracted from the Climate Research Unit analyses version 2.0 (CRU, Mitchell et al. 2003, New et al. 2000) and the Global Precipitation Climatology Project version 2.0 (GPCP, Huffmann et al. 1997).

The CRU dataset provides global 2m temperature and precipitation fields in terms of time series of monthly means for the time period 1901-2000 at 0.5 degree horizontal resolution for land surface area. The temperature and precipitation fields are based on gauge measurements. The GPCP precipitation dataset is globally gridded data at 2.5 degree resolution based on gauge measurements over land and satellite data over sea. The GPCP precipitation values are corrected for undercatch of gauge stations. Time series of monthly means are available for 1979-2000. By using area averages we expect to reduce uncertainties in the observations that are caused by location, exposure and altitude of the stations.

Figure 2.13 presents mean annual cycles of the differences in 2m temperature between the simulation results and the CRU observations. For all European subregions the temperature annual cycle is improved due to monthly varying vegetation with respect to the observations. Generally, the simulated annual cycle of 2m temperature is characterised by a larger amplitude, but due to the vegetation effect summer temperatures of VEG-0.5 decrease and come to a better agreement with the observations. In eastern Europe temperature values move about 1.5 K closer to CRU data.

The validation results for precipitation are presented in figure 2.14. The mean annual cycles of precipitation for the simulation results of VEG-0.5 and REF-0.5 and the observational data of CRU and GPCP are plotted. Together, the model simulations reproduce the characteristics of the individual precipitation annual cycles in the different European subdomains. However, some noticeable underestimations in precipitation are simulated in the Alpine region in autumn and in the south-eastern Mediterranean in the winter season. In the western Baltic area precipitation is discernable overestimated in spring. During the summer season in central and eastern Europe, the change in precipitation due to temporally varying vegetation causes an overestimation of the maximum precipitation. But regarding the whole annual cycle, the vegetation effect leads to a better agreement with the observations. A clear improvement of the precipitation annual cycle can be detected in the Hungarian lowlands. Here the vegetation effect produces the correct maximum precipitation and an improved annual precipitation cycle. In this region, an artificial summer drying problem is simulated by many climate models (Hagemann et al. 2001, Seneviratne et al. 2002). With the more realistic treatment of vegetation the summer drying is reduced, but in late summer and autumn, it remains.

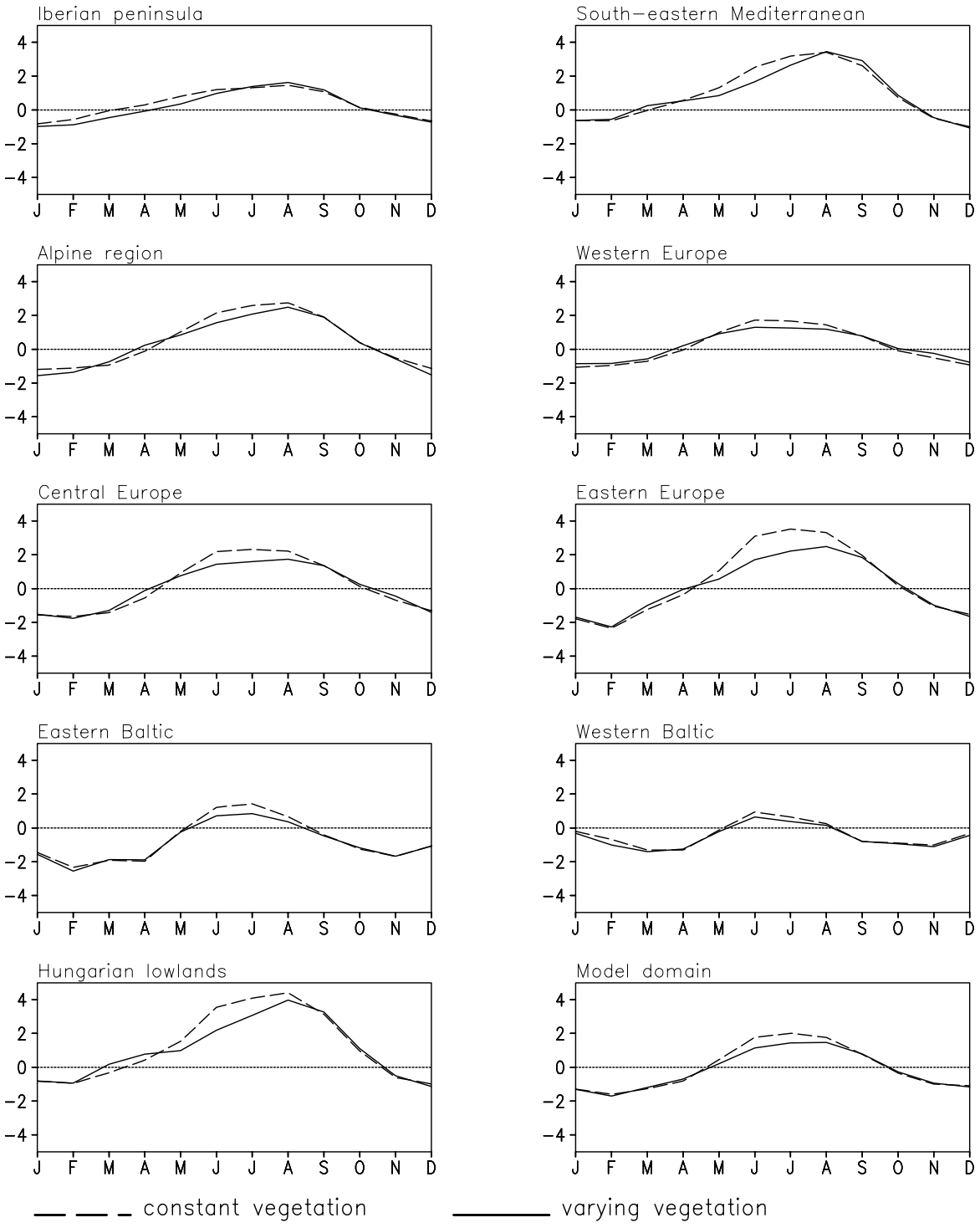

Figure 2.13: Mean annual cycles 1979-1993 of differences in 2m temperature [K] between VEG-0.5 and CRU and REF-0.5 and CRU, area-averaged over the European subdomains.

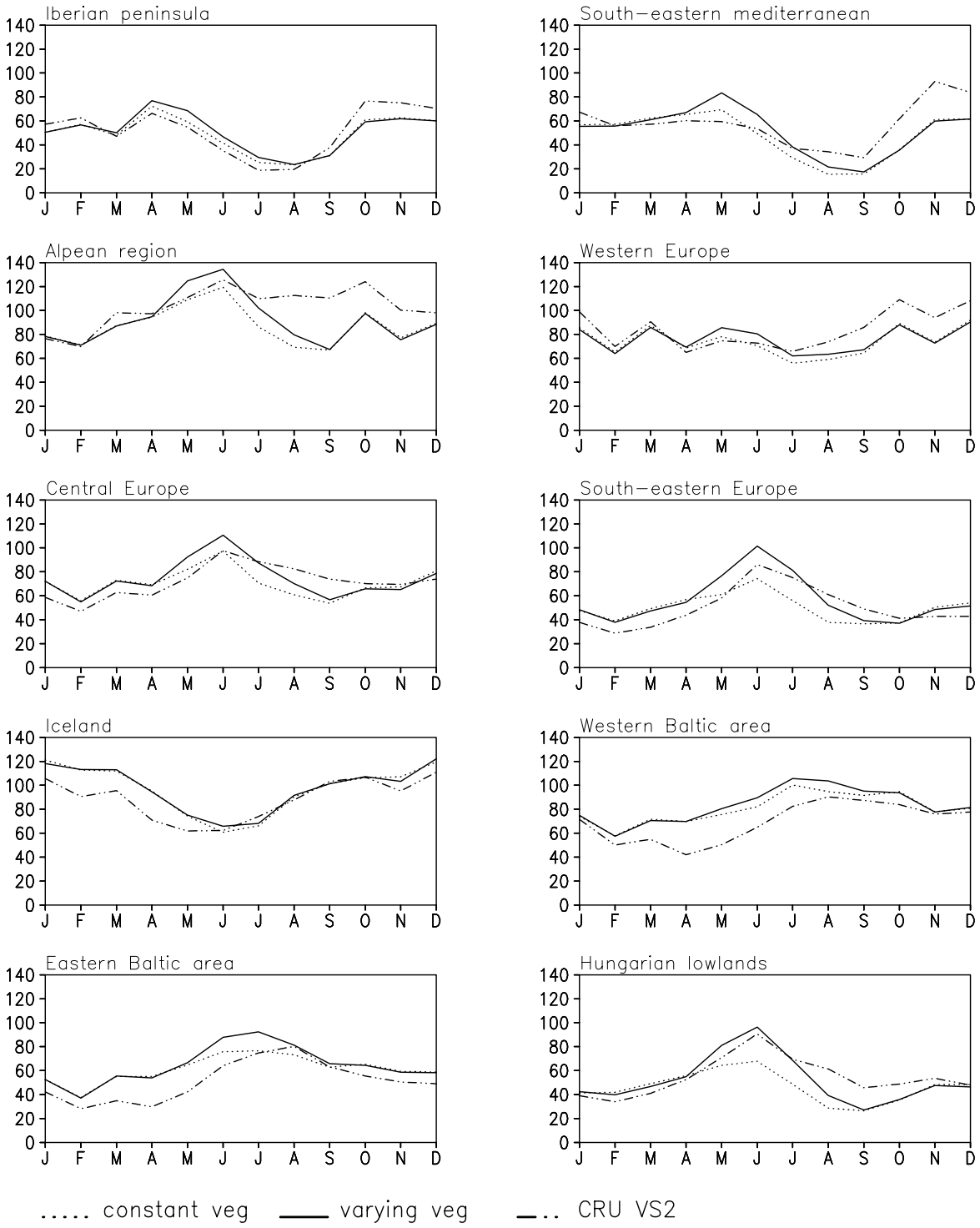

Figure 2.14: Mean annual cycles 1979-1993 of precipitation [mm/month] for model results of VEG-0.5 and REF-0.5 and observational data of CRU and GPCP, area-averaged over the European subdomains.

To quantify the validation results presented in figure 2.13 and 2.14, the mean absolute deviations (d) between the model results (m) and the observations (o) are calculated:

$$d_{xy} = \frac{1}{n} \sum_{i=1}^{n} |m_{xyi} - o_{xyi}| \qquad (2.9)$$

$$d = \frac{\sum_{xy} (\cos(lat(x,y)) \cdot d_{xy})}{\sum_{xy} \cos(lat(x,y))} \qquad (2.10)$$

d_{xy} is the mean absolute deviation for the timeseries of monthly means at each grid point. The indices x and y specify the graduating and n gives the month of the annual cycle. To determine the area averages for the European subdomains, the mean absolute deviations are weighted by the cosine of the grid point latitude (lat). The significance of the vegetation effect on the simulation results can be estimated by the standard error (Δd) of the mean absolute deviation. The standard error for the timeseries at each grid point (Δd_{xy}) of monthly means is the quotient of standard deviation and square root of the number of time steps. The standard error Δd for the area averages over divers grid points is calculated from the error of the timeseries $\Delta d_{xy}$with error propagation:

$$\Delta d_{xy} = \sqrt{\frac{1}{n(n-1)} \cdot \sum_{i=1}^{n} (|m_{xyi} - o_{xyi}| - d_{xy})^2} \qquad (2.11)$$

$$\Delta d = \sqrt{\sum_{xy} \left(\frac{\cos(lat(x,y))}{\sum_{xy} \cos(lat(x,y))} \cdot \Delta d_{xy} \right)^2} \qquad (2.12)$$

The results are composed in figure 2.15. The vegetation effect leads to a significant improvement in 2m temperature for all European subdomains except for the Iberian peninsula and the Alpine region. On the Iberian peninsula the mean absolute deviation increases as winter 2m temperatures are underestimated. In the Alpine region the mean absolute deviation becomes smaller, but not significantly. Here, the effect of vegetation phenology is overpowered by the synoptic scale weather conditions. Concerning precipitation, the deviations increase in the Baltic and the Mediterranean area; central and eastern Europe including the Hungarian lowlands show improved results.

Iberian peninsula

	REF−0.5	VEG−0.5
P:CRU2	12.47/0.21	13.74/0.23
P:GPCP	14.03/0.24	15.21/0.26
T:CRU2	0.96/0.014	1.01/0.015

South−eastern Mediterranean

	REF−0.5	VEG−0.5
P:CRU2	18.42/0.32	19.14/0.35
P:GPCP	21.12/0.34	22.35/0.37
T:CRU2	1.64/0.028	1.56/0.026

Alpine region

	REF−0.5	VEG−0.5
P:CRU2	34.48/0.57	33.77/0.59
P:GPCP	30.27/0.52	31.62/0.56
T:CRU2	1.72/0.033	1.69/0.033

Western Europe

	REF−0.5	VEG−0.5
P:CRU2	19.64/0.33	19.37/0.34
P:GPCP	15.05/0.23	15.51/0.23
T:CRU2	0.95/0.012	0.80/0.011

Central Europe

	REF−0.5	VEG−0.5
P:CRU2	19.26/0.23	18.34/0.23
P:GPCP	20.57/0.23	19.87/0.23
T:CRU2	1.47/0.015	1.26/0.014

Eastern Europe

	REF−0.5	VEG−0.5
P:CRU2	14.17/0.14	13.03/0.15
P:GPCP	13.93/0.15	12.82/0.15
T:CRU2	1.92/0.019	1.57/0.016

Eastern Baltic

	REF−0.5	VEG−0.5
P:CRU2	15.47/0.14	16.37/0.15
P:GPCP	14.39/0.15	15.02/0.15
T:CRU2	1.43/0.012	1.33/0.013

Western Baltic

	REF−0.5	VEG−0.5
P:CRU2	17.50/0.21	18.80/0.22
P:GPCP	18.10/0.24	19.05/0.23
T:CRU2	1.21/0.014	1.18/0.013

Hungarian lowlands

	REF−0.5	VEG−0.5
P:CRU2	15.52/0.30	13.77/0.25
P:GPCP	19.18/0.25	18.00/0.27
T:CRU2	1.94/0.032	1.71/0.027

Model domain

	REF−0.5	VEG−0.5
P:CRU2	17.22/0.073	17.63/0.079
P:GPCP	17.45/0.074	18.03/0.078
T:CRU2	1.49/0.006	1.37/0.006

Figure 2.15: Statistical parameters of the mean annual cycles (1979-1993) of 2m temperature and precipitation for VEG-0.5 and REF-0.5 in comparison to CRU and GPCP, area-averaged over the European subdomains. P:CRU2: mean absolute deviation/error in precipitation for REF-0.5 and VEG-0.5 compared to CRU, P:GPCP: mean absolute deviation/error in precipitation for REF-0.5 and VEG-0.5 compared to GPCP, T:CRU2: mean absolute deviation/ error in 2m temperature for REF-0.5 and VEG-0.5 compared to CRU.

2. 5 Summary and conclusions

This study shows that including the annual cycle of vegetation in the regional climate model REMO does influence the simulated climate in Europe. The more realistic description of vegetation variability strongly affects the water and energy fluxes at the land surface. The raised LAI values and fractional vegetation cover during the growing season directly increase evapotranspiration and therefore latent heat flux, whereas sensible heat flux is decreased. These changes lead to lower surface temperatures and increased precipitation during the summer season. In all European regions the vegetation effect occurs mainly in the summer season when exchange processes of mass and energy at the land surface are most intensive and strongly controlled by land surface properties. The simulated climate for the winter season is only slightly affected. The spatial analysis of the results show main effects in eastern Europe and the Hungarian lowlands, where the continental climate with intensive vertical exchange processes at the land surface during summer is strongly determined by the altered vegetation parameter values. The simulated climate in the western European regions close to the sea are less affected by the modified vegetation parameterization due to dominating large scale weather conditions. The evaluation of the model simulation at 1/6 degree resolution shows approximately the same vegetation effect on the area-average climate. In the horizontal view, the results are more structured and in some regions the spatial precipitation distribution is changed due to the higher resolution. Especially in northern Europe the mesoscale atmospheric circulation is affected by the horizontal model resolution in combination with the modified vegetation treatment. The validation of the modified model version shows that the simulation results are generally in good agreement with the observations. The statistical analysis of the vegetation effect indicates a significant improvement of the annual 2m temperature cycle. Concerning precipitation, central and eastern Europe including the Hungarian lowlands show significantly improved results. But in southern and northern Europe the deviations slightly increase, especially the summer maximum precipitation values are overestimated. This may point to deficiencies in physical parameterizations. Numerous sensitivity experiments with regard to physical parameterizations are performed by the regional climate modelling group at MPI-M at this time. In most cases, the effects on precipitation and temperature are of the same order of magnitude as the effect of the altered vegetation parameterization (not shown). The implementation of an annual vegetation cycle improves the representation of vegetation in the model. However, its effect can be superposed by uncertainties due to deficiencies in other model parameterizations as for example in aerosol processes or in the treatment of convective clouds.

The vegetation effect on the simulated climate is outside the internal model variability, because changes do not show spatial or temporal fluctuations on the considered scale but go clearly in one direction. In summer, precipitation changes are positive and temperature changes are negative in all European subregions. Giorgi and Bi (2000) demonstrate that internal model variability only minimally affects the mean annual cycle of precipitation and temperature. In our case, we have strong effects which can be attributed to the modified vegetation parameters.

Generally, the results of this study are in line with previous global studies on the influence of interannual vegetation variability on the simulated climate (Bounoua et al. 2000, Lawrence and Slingo 2004a, 2004b). In these experiments larger LAI values also result in cooler and moister near-surface climate. Our regional study focusing on Europe now demonstrates that the climates of the European subregions are affected by the annual vegetation cycle in varying degrees. Related to this work, the study results of Lu and Shuttleworth (2002) are quite

interesting. Their NDVI-derived values introduce more spatial heterogeneity to LAI fields and reduce the magnitude of LAI values in comparison to their default model version. In contrast to our study they reduce LAI values in summer, but in spite of this they simulate cooler and wetter climate conditions. They separated the effect of reduced LAI from enhanced heterogeneity which leads to warmer and dryer near-surface summer climate. But reduced LAI in combination with enhanced heterogeneity lead to cooler and wetter climate conditions. Thus, their conclusion is that the introduction of increased spatial heterogeneity is the primary cause of the cooler and wetter summer climate. In future REMO model studies it would be quite interesting to perform a similar sensitivity study with NDVI-derived LAI fields.

Chapter 3

Parameterization of snow-free land surface albedo as a function of vegetation phenology based on MODIS data and applied in climate modelling[2]

Abstract

The aim of this study was to develop an advanced parameterization of the snow-free land surface albedo for climate modelling describing the temporal variation of surface albedo as a function of vegetation phenology on a monthly time scale. To estimate the effect of vegetation phenology on snow-free land surface albedo, remotely sensed data products from the Moderate-Resolution Imaging Spectroradiometer (MODIS) on board the NASA Terra platform measured during 2001 to 2004 are used. The snow-free surface albedo variability is determined by the optical contrast between the vegetation canopy and the underlying soil surface. The MODIS products of the white-sky albedo for total shortwave broad bands and the fraction of absorbed photosynthetically active radiation (FPAR) are analysed to separate the vegetation canopy albedo from the underlying soil albedo. Global maps of pure soil albedo and pure vegetation albedo are derived on a 0.5 degree regular latitude/longitude grid, re-sampling the high-resolution information from remote sensing-measured pixel level to the model grid scale and filling up gaps from the satellite data. These global maps show that in the northern and mid-latitudes soils are mostly darker than vegetation, whereas in the lower latitudes, especially in semi-deserts, soil albedo is mostly higher than vegetation albedo. The separated soil and vegetation albedo can be applied to compute the annual surface albedo cycle from monthly varying leaf area index. This parameterization is especially designed for the land surface scheme of the regional climate model REMO and the global climate model ECHAM5, but can easily be integrated into the land surface schemes of other regional and global climate models.

3. 1 Introduction

Land surface albedo is the ratio of solar radiation flux reflected at the surface to the total incoming solar radiation flux. It determines the energy budget of the earth's surface, which in

[2] *Rechid D, Raddatz TJ, Jacob D (2008a) Parameterization of snow-free land surface albedo as a function of vegetation phenology based on MODIS data and applied in climate modelling. Theor Appl Climatol, DOI 10.1007/s00704-008-0003-y*

turn modifies hydrological processes and regulates circulation patterns. Thus, it is an important parameter in modelling climate processes. Modelling studies have shown complex interactions between surface albedo, climate and the biosphere (Dickinson & Hanson 1984, Rowntree & Sangster 1986, Lofgren 1995, Berbet & Costa 2003). Surface albedo is determined by the surface properties, depending on the angular and spectral distributions of the incident solar radiation. Bare soil albedo depends on the soil moisture content, surface roughness and soil texture. The soil texture is determined by soil mineral composition and organic deposition. Vegetation canopy albedo depends on leaf area index (LAI), leaf angle distribution, leaf transmittance and reflectance. The land surface albedo shows not only spatial variability but also temporal variations. This can be observed by field studies (Song, 1999) and examined by remotely sensed data (Zhou et al. 2003). The largest temporal and spatial variations of surface albedo are caused by snow cover. In this study we solely refer to the albedo over snow-free land surfaces called "background albedo".

This study is focused on the monthly time scale. Over vegetated surfaces, the monthly variability of albedo is mainly caused by seasonally varying vegetation characteristics. In the study of Song (1999) the relationship between albedo and plant phenology was examined by field observations in prairie grassland and agricultural crops. The observed albedo showed clear changes during the phenology phases from green-up to peak greenness, dry down and senescence or harvesting stage. The study of Song (1999) also showed the difficulty to distinguish the seasonal variations in albedo caused by phenological changes from those caused by solar zenith angle depending on land cover type. To reduce the confounding effects of the seasonal varying solar zenith angle on surface albedo one should compare albedo values at the same solar zenith angle. In this study, these overlying effects on seasonal albedo changes are not distinguished. Only the white-sky albedo is analysed to yield surface albedo as a function of vegetation phenology. The variability due to plant phenology is determined by the optical contrast between the vegetation canopy and the underlying soil surface. Over bright-coloured soils vegetation cover reduces surface albedo whereas plants on dark soils increase surface albedo. During the annual cycle of vegetation development the vegetation density is changing. This can be expressed by the leaf area index (LAI), which is the projection of the one-sided leaf area to the ground area. Our motivation is to describe land surface background albedo as a dynamic function of the LAI, which is applied in most climate models to describe spatial and temporal variability of vegetation properties.

The land surface schemes of climate models often use background albedos without temporal variations. Thus, in the general circulation model (GCM) ECHAM5 (Roeckner et al. 2003) and the regional climate model (RCM) REMO (REgional MOdel, Jacob et al. 1997, Jacob et al. 2001) the albedo over snow-free land surfaces was prescribed by tabular values only depending on land cover type (Hagemann et al. 1999). During the last years, the availability of high-quality satellite data with high spatial and temporal resolution increased which provides the opportunity to develop advanced land surface parameterizations. For example the Moderate Resolution Imaging Spectroradiometer (MODIS) measurements facilitate the retrieval of surface albedo products and consistent products of vegetation characteristics (Lucht et al. 2000, Schaaf et al. 2002). The aim of this study was to develop a more realistic parameterization of the snow-free land surface albedo for the REMO RCM describing the monthly varying surface albedo as a function of vegetation phenology using MODIS data. At the same time a study of Liang et al. (2005) also used MODIS data to develop an improved dynamic-statistical parameterization for snow-free land surface albedo. This parameterization was designed for the Common Land Model (CLM, Dai et al. 2003, Bonan et al. 2002, Zeng et al. 2002). The CLM albedo scheme is quite complex and considers for the direct beam and

diffuse radiation the visible and near-infrared spectral bands using several parameters depending on soil and land cover type. The surface albedo parameterization of this study was especially designed for the land surface scheme of the REMO RCM and the ECHAM5 GCM, but can also be applied to other climate models with similar albedo schemes.

To estimate the effect of vegetation phenology on snow-free land surface albedo remotely sensed data from the Moderate-Resolution Imaging Spectroradiometer (MODIS) on board the NASA Terra platform measured during 2001 to 2004 are used. We analysed MODIS products of the white-sky albedo for total shortwave broad bands and the fraction of absorbed photosynthetically active radiation (FPAR) as a parameter describing the temporal variability of vegetation characteristics. A linear regression method enables us to separate the vegetation albedo from the underlying soil albedo. Global maps of pure soil albedo and pure vegetation albedo are derived on a 0.5 degree regular latitude/longitude grid, which can be applied to compute the annual surface albedo cycle from monthly varying leaf area index. To sum up, our intention is to apply MODIS data products to develop an advanced parameterization of the snow-free land surface albedo for climate modelling re-sampling the high-resolution information from remote sensing-measured pixel level to the model grid scale and filling up gaps from the satellite data. The temporal variation of snow-free surface albedo is described as a function of vegetation phenology on a monthly time scale.

The paper is organised as follows: In section 3.2 the data products from MODIS used in this study are presented. The data are prepared and analysed in section 3.3 and applied to estimate the annual albedo cycle for climate modelling in section 3.4. In section 3.5 we give conclusions and a short outlook.

3. 2 Data

3. 2. 1 MODIS albedo

Remotely sensed global land surface albedos are routinely provided by the Moderate-Resolution Imaging Spectroradiometer (MODIS) aboard the NASA Terra platform. The MODIS albedo algorithm adopts the linear Bidirectional Reflectance Distribution Function (BRDF) model to characterize the anisotropy of the global surface. The standard 1-km resolution MODIS BRDF/albedo products (called MOD43B) are documented in Strahler et al. (1999), Lucht et al. (2000), Schaaf et al. (2002) and in the MOD43 User's Guide, available at http://geography.bu.edu/brdf/userguide/. These products are provided to the user community by the Earth Resources Observation System (EROS) Data Center in the equal Integerized Sinusoidal projection (ISIN) and can be downloaded from http://edcdaac.usgs.gov/modis/dataproducts.asp. These 1-km standard products are reprojected and aggregated to a latitude/longitude projection at 0.05° resolution (called MOD43) and analysed by Gao et al. (2005). Validation results show good agreement with field measurements within 10 % (Liang et al. 2002, Jin et al. 2003a, 2003b, Wang et al. 2004). Here, we use the white-sky albedo for total shortwave broad bands (MOD43C1), which is provided globally for every 16-day period from March 2000 to present. MODIS albedo observations are cloud-cleared and atmospherically corrected accompanied by quality flags that include the percentage of snow cover.

3. 2. 2 MODIS FPAR

The seasonal variation of vegetation cover is detected by the fraction of absorbed photosynthetically active radiation (FPAR) data from the same instrument MODIS/Terra. The MODIS LAI/FPAR products are composited over an 8-day period at 1 km spatial resolution projected on a sinusoidal grid (MOD15A2). Validation results show reasonable performance of the MODIS LAI/FPAR algorithm (Tan et al. 2005, Privette et al. 2002). For the retrieval of LAI and FPAR from surface reflectance an algorithm based on the physics of radiative transfer in vegetation canopies was developed and implemented for operational processing with MODIS aboard Terra (Myneni et al. 2002). The data are distributed by the EROS Data Center from February 2000 to present time. For each 1 km pixel the product file provides LAI, FPAR and two quality control variables. LAI and FPAR values are related to the land fraction of each pixel. A detailed description is available at http://cybele.bu.edu/modismisr/products/modis/-userguide.pdf.

3. 3 Method

3. 3. 1 Data preparation

The MODIS land surface albedo data includes snow and water albedo of surfaces covered with snow, inland water or coastal water. But for our method we need the albedo only related to snow-free land surfaces. Thus, snow and water albedos need to be excluded. First, the MODIS albedo data is reprojected to a 0.5 degree regular grid. The accompanying quality flag containing information about snow cover is used to mask out snow pixels. The information of land-sea distribution is taken from the GLCCD (U. S. Geological Survey 1997, U. S. Geological Survey 2002). If the land fraction of a grid point is below 0.2, the grid point is excluded from the analysis. For grid cells ranging between 0.2 and 0.8 land fraction, albedo values of the surrounding land grid points are interpolated with the inverse distance weighting method. If land fraction exceeds 0.8, the albedo value is kept unchanged.

MODIS FPAR data is transferred from the 1-km ISIN to a regular latitude/longitude grid at 0.5° resolution. Myneni et al. (2002) advise users of the provisional nature of the products of year one of MODIS operation in view of changes to calibration, geolocation, cloud screening and atmospheric corrections. Therefore, we use the MODIS data from day 65 of the year 2001 to day 65 of the year 2004.

3. 3. 2 Data analysis

Up to 70 pairs of snow-free surface broadband albedo and FPAR values for every 16-day period are obtained for all global grid points, where data are available. The correlation between albedo and FPAR values is shown in figure 3.1. Positive correlations marked with red colours indicate regions, where increasing vegetation cover raises surface albedo. Negative correlations marked with blue colours identify regions, where increasing vegetation cover reduces surface albedo. Uncoloured grid points refer to non-vegetated regions or missing data.

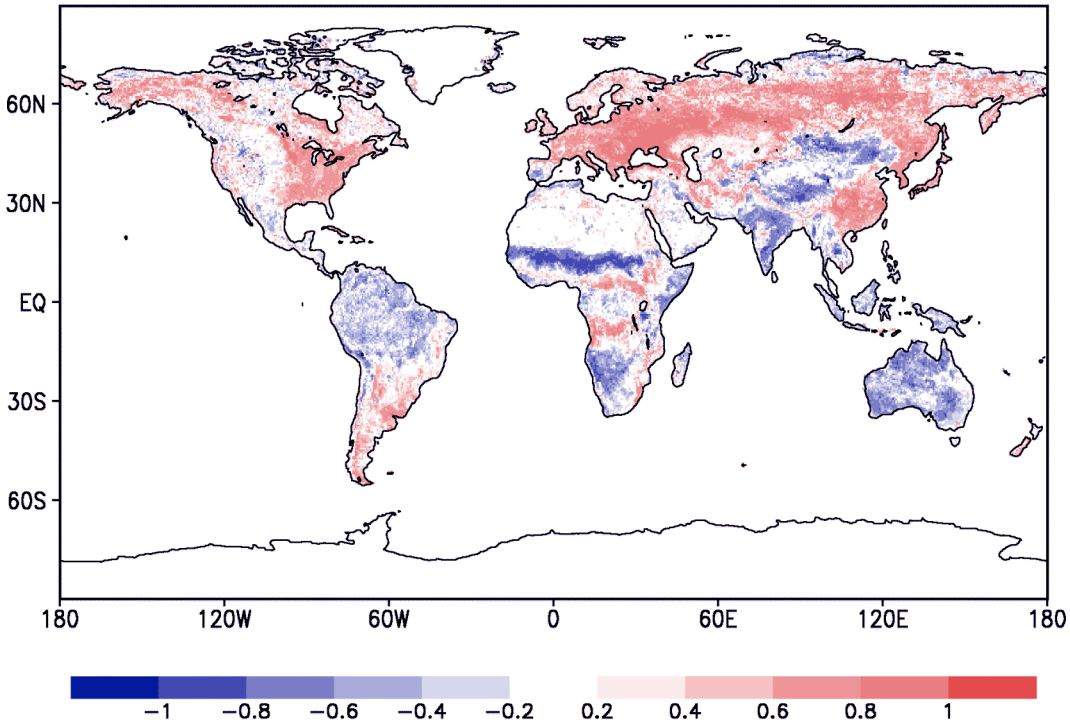

Figure 3.1: Correlation between FPAR and albedo data from MODIS/Terra 2001-2004

In our method, the FPAR value is used as an indicator of the presence of vegetation. The total background surface albedo (a) results from the vegetation albedo (a_{canopy}), where vegetation is present, and the albedo of the soil (a_{soil}), where the underlying surface is visible:

$$a = a_{soil} \cdot (1 - fpar) + a_{canopy} \cdot fpar \qquad (3.1)$$

By linear regression of MODIS FPAR and total surface albedo data the vegetation albedo and soil albedo can be estimated. If there is no vegetation (FPAR=0), surface albedo is equal to soil albedo. If vegetation is present, the contrast between vegetation albedo and soil albedo defines the slope of albedo change.

The regression method delivers reasonable results under the following premises and predefined limits: The method is only applied at grid points, where at least three pairs of albedo and FPAR values are available and the absolute FPAR value changes at least by 0.1. Otherwise, the grid point is excluded from the method due to high uncertainty of the results. If no vegetation is present (FPAR always 0), soil albedo is set to the mean MODIS albedo. In the case of minor vegetation cover (FPAR always below 0.2), the linear regression method is used to estimate the soil albedo and vegetation albedo is set to missing value. In the case of major vegetation cover (FPAR always beyond 0.8), no information about the soil albedo can be observed from the satellite. Here, soil albedo is set to missing value and vegetation albedo is set to mean MODIS albedo. If the regression provides unrealistic results exceeding the lower limit 0.07 for water or the upper limit 0.7 for glacier ice, the respective grid points are also excluded from the method. The resulting global map of the soil albedo is presented in

figure 3.2. All missing grid points that are excluded from our method remain in white colour. Of a total of 60606 ice-free vegetated land grid points 7869 grid points remain undefined, for 87 % of the total grid points the method can be applied.

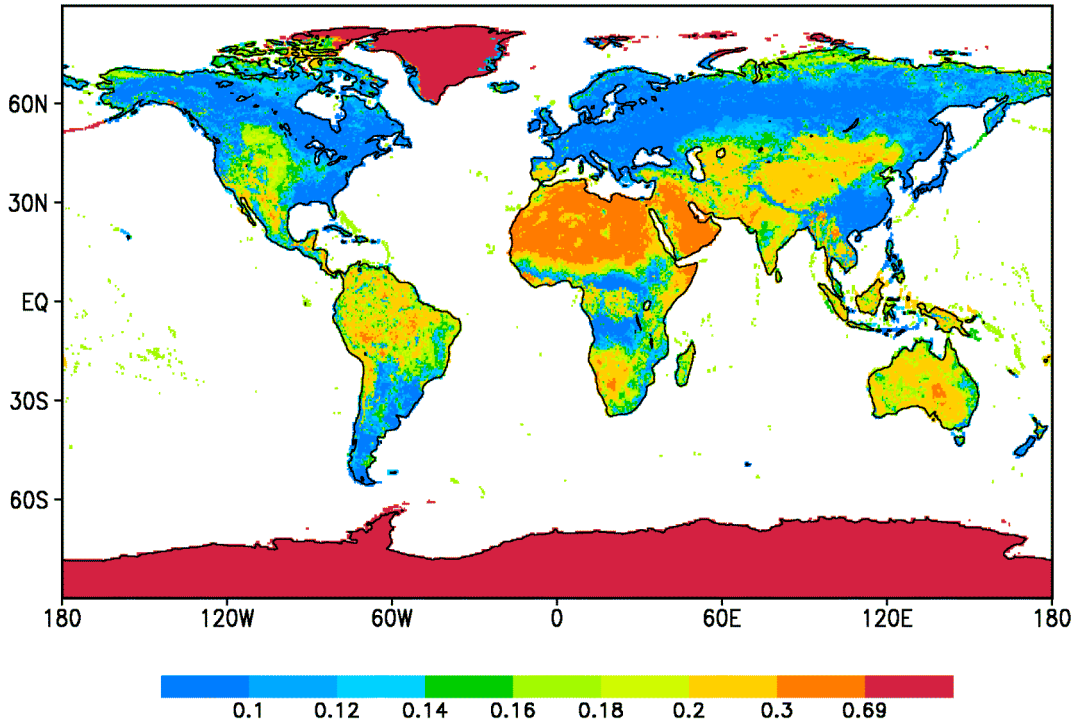

Figure 3.2: Global distribution of soil albedo at 0.5 degree resolution

As climate models require surface information for each grid cell, soil albedo needs to be defined for all grid points. To complete our global map, grid points covered with glacier ice are identified by the Olson land cover types (Olson 1994a, 1994b) and set to 0.7. Missing soil albedo values for grid points without glacier ice are spatially interpolated from the surrounding grid cells by inverse distance weighting method. The same method is applied for missing vegetation albedo at vegetated grid points (FPAR beyond 0.2).

The soil albedo map shows that soils in the northern and mid-latitudes are predominantly dark with low albedo values. This can be understood by noting that low solar energy input and low surface temperatures in these regions slow down the decomposition of plant material and much organic material is stored in the soils. In contrast, surfaces in the lower latitudes often feature higher albedo values. In these regions, high input of solar radiation and high surface temperatures accelerate the mineralization of dead plant material and the content of organic material in the soils is quite low. Altogether, the soil albedo map shows realistic results, except for the northern part of South America. Here, in some places, soils show unrealistically high albedo values. This is possibly caused by undetected cloud and haze contaminations in the satellite data. But vegetation density is typically high in this region, so that nonetheless the total albedo is realistic. Figure 3.3 presents the result for the vegetation albedo. Most vegetation canopies feature albedo values between 0.1 and 0.15. But where grasses and crops

are predominant (as in the mid-latitudes), vegetation canopies show higher albedo values. The boreal forests and the rain forests, in contrast, show quite low albedo values.

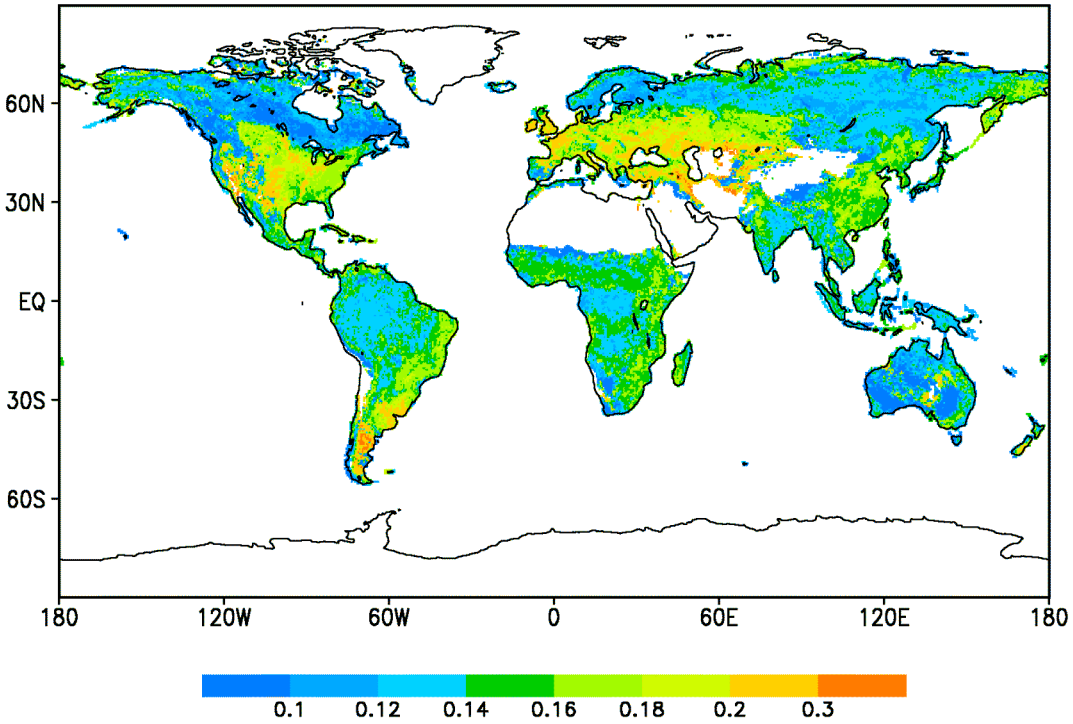

Figure 3.3: Global distribution of vegetation albedo at 0.5 degree resolution

3. 4 Annual background albedo cycle for climate modelling

The global distributions of soil and vegetation canopy albedo can be applied in climate modelling to describe the annual background albedo cycle as a function of vegetation phenology. In this study this method is adapted to the REMO RCM and the ECHAM5 GCM to prepare both models for testing the new albedo parameterization scheme both on the regional and the global scale.

3. 4. 1 Land surface representation and background albedo in REMO and ECHAM5

The general circulation model ECHAM5 and the regional climate model REMO use similar land surface schemes. The REMO RCM is based on the physical parameterizations of the ECHAM4 GCM. The land surface properties are represented by the same global dataset of land surface parameters LSP2 (Hagemann et al. 1999, Hagemann 2002). The LSP2 dataset is based on a global distribution of major ecosystem types (Global Land Cover Characteristics

Database; GLCCD) according to a classification list of Olson (1994a, 1994b). In REMO and ECHAM5 74 land use classes of the total 96 Olson ecosystem types are used (Hagemann 2002). The Olson ecosystem types were derived from Advanced Very High Resolution Radiometer AVHRR data at 1 km resolution supplied by the International Geosphere-Biosphere Program (Eidenshink & Faundeen 1994) and constructed by the U.S. Geological Survey (1997, 2002). For each land cover type mean parameter values for background surface albedo, fractional vegetation cover, minimum and maximum leaf area index and other vegetation properties are allocated. This information is aggregated to the model grid scale averaging the vegetation parameters of all land cover types, which are located in one model grid cell.

Together, so far, in ECHAM5 and REMO the albedo over snow-free land surfaces is defined by mean tabular values only depending on land cover type without temporal variability caused by changing soil properties as moisture content or changing vegetation properties as LAI or leaf colours. They are prescribed to the climate models as a lower boundary condition and remain constant during the whole model simulation.

The total surface albedo of a model grid box is the area-weighted linear average of the background albedo over the fraction with snow-free land, the albedo over the water fraction and the albedo over snow-covered grid area. The albedo over snow-covered land surfaces is a function of snow cover, temperature, forest fraction, subgrid-scale orography and in ECHAM5 also of the sky view factor depending on LAI.

In both the REMO RCM and the ECHAM5 GCM the total land surface albedo is the ratio of the solar radiation flux reflected at the surface to the total incoming solar radiation flux. So far, there is no spectral distinction for the reflection of the solar radiation at the surface, only the total shortwave broadband surface albedo is used. So, this spectral dependency is not considered in this study. Influencing the net radiation budget, the surface albedo has impact on the simulated vertical energy exchange at the earth's surface modifying surface heat fluxes and temperatures as well as hydrological processes. How the advanced albedo scheme will affect surface processes in the climate models is the topic of a further study (Rechid et al. 2008b). There, the sensitivity of the simulated climate parameters in REMO and ECHAM5 to the new background albedo parameterization is evaluated in several global and regional climate simulations. The study investigates the individual performance of both models and how differently the new land surface background albedo scheme affects the simulations on the global and the regional scale.

The new background albedo parameterization describes the monthly varying background surface albedo as a function of vegetation phenology. In ECHAM5 and REMO vegetation phenology is represented by the same monthly varying values of the leaf area index LAI (Roeckner et al. 2003, Rechid & Jacob 2006). These temporal varying vegetation fields are taken from the global dataset of land surface parameters LSP2 designed by Hagemann (2002). The seasonal variation of the LAI between minimum and maximum values is estimated by a global data field of the monthly growth factor, which is defined by climatologies of 2m temperature and FPAR (Hagemann 2002). In regions with water availability being the limiting growing factor, the FPAR climatology is applied which considers indirectly the mean soil moisture conditions within the LAI variability. Together, this dataset provides a mean climatology of the annual LAI cycle without inter-annual variability.

So far, this mean seasonal LAI cycle was not related to temporal variability of snow-free land surface albedo. The LSP2 dataset also includes monthly fields of background albedo. This mean annual albedo cycle was derived by a method, which was designed for regions with bright soils where vegetation decreases the surface albedo. But this is not appropriate for the European region, the domain, where the REMO model is frequently applied. Here, dark soils are dominant, where vegetation increases the surface albedo (Bremicker 1998).

3. 4. 2 New background albedo scheme in REMO and ECHAM5

In ECHAM5 and REMO vegetation phenology is represented by a climatology of monthly varying values of the leaf area index LAI. Thus, we modify equation (3.1) converting the FPAR to LAI using a simple Beer's Law approach (Jarvis & Leverez 1983, cited in Turner et al. 2005):

$$fpar = 1 - e^{-K \cdot LAI} \qquad (3.2)$$

K is the canopy light extinction coefficient. As a simple approach K is assumed to be 0.5 for all vegetation types in this study. More sophisticated transformation algorithms are available (Chen et al. 1997; Gower et al. 1999), if they can be consistently parameterized within the land surface scheme of the climate model.

According to equation (3.1) we get the following function for the total land surface background albedo:

$$a = a_{soil} \cdot e^{-0.5 \cdot LAI} + a_{canopy} \cdot (1 - e^{-0.5 \cdot LAI}) \qquad (3.3)$$

In figure 3.4 the resulting annual mean of the climatological land surface background albedo for the climate models is presented. For comparison, the MODIS annual mean snow-free land albedo averaged over the whole period 2001-2004 is shown in figure 3.5. For the MODIS picture the annual means are displayed only for those grid points, where values are available for all months of the year. For the following comparisons between the annual background albedo cycles of the climate models and of MODIS only those defined MODIS grid points are comprised in the area-averages for the selected world regions, which are also presented in figure 3.4 and figure 3.5. For northern Asia no albedo cycle is computed as for this region almost no MODIS data are available for the winter season. The annual mean background albedos of the models and MODIS show quite good agreement except for Australia and the northern part of southern America, where the values are underestimated at many grid points by our method. A more detailed analysis of these results will be done while evaluating the annual albedo cycles of the models and MODIS area-averaged over the selected regions.

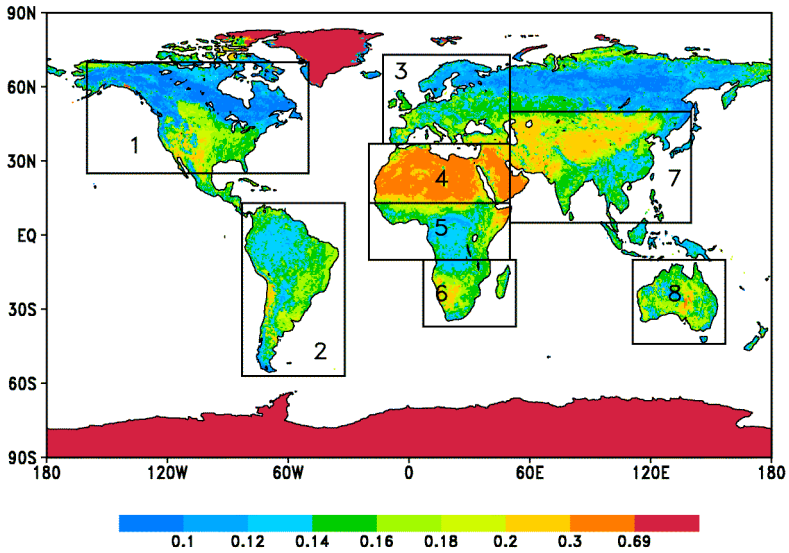

Figure 3.4: Resulting annual mean of global background surface albedo climatology at 0.5 degree horizontal resolution for the climate models. The selected world regions are numbered for: 1 northern America, 2 southern America, 3 Europe, 4 northern Africa, 5 central Africa, 6 southern Africa, 7 southern Asia, 8 Australia

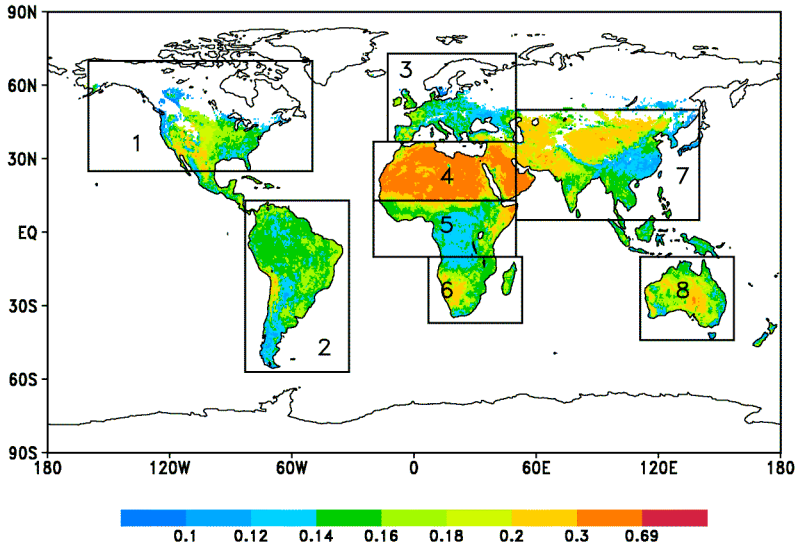

Figure 3.5: Annual mean of global snow-free land surface albedo averaged over the whole period 2001-2004 at 0.5 degree horizontal resolution of MODIS. The selected world regions are numbered as in Fig.4. Values are only plotted at grid points, where MODIS is available for all months of the year.

As examples the mean annual cycle of the leaf area index climatology and the resulting mean annual background albedo cycles of Europe and Australia, respectively, are shown in figure 3.6. The values of LAI and albedo are horizontal area-weighted averages for both regions. The pictures indicate that in Europe soils are mainly darker than vegetation; hence, albedo is increasing with increasing LAI. In Australia, in contrast, soils are brighter than vegetation and albedo is decreasing with increasing LAI.

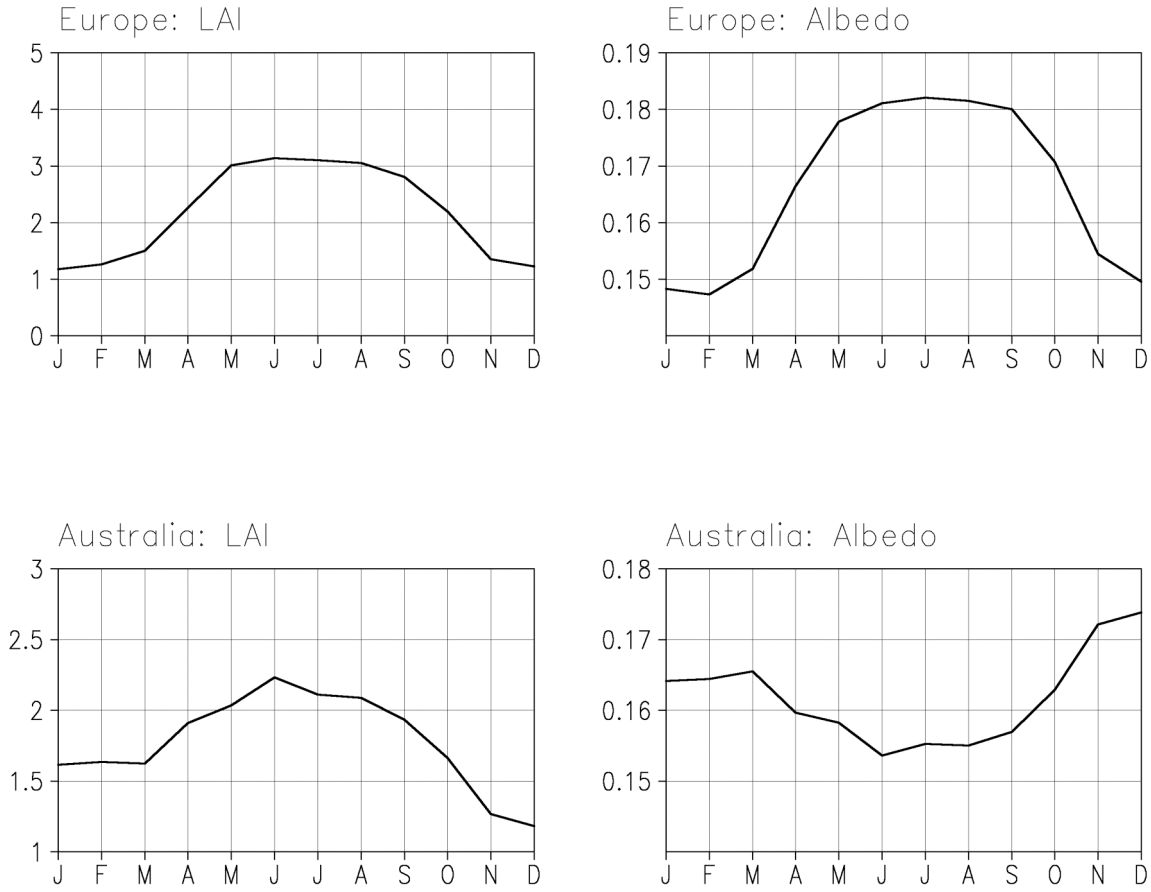

Figure 3.6: Mean annual cycles of background albedo and LAI climatologies for Europe and Australia

The resulting mean annual background albedo cycles for the selected world regions are compared to the mean annual snow-free land albedo cycles of MODIS from 2001-2004 in figure 3.7. Additionally, the so far used annual mean background albedo of REMO and ECHAM5 from the LSP2 dataset is also displayed. In comparison to MODIS the mean background albedo is overestimated by the LSP2 data. Hence, in almost all regions the new mean background albedo of the models is lower than the old LSP2 mean, which introduces partly a stronger change to the model albedo than the seasonal albedo variation.

Together, the observed MODIS albedo and the derived model albedo values show satisfying agreement. Especially, in all African sub-regions and in southern America the background albedo values of the climate models fit very well to the MODIS albedo values. These are regions with only low temporal albedo variability. Moreover, these regions are dominated by natural land use types with low anthropogenic influence, which can be captured better by our method than regions with high anthropogenic influence. The other regions presented in figure 3.7 show some differences which shall be analysed and discussed in the following.

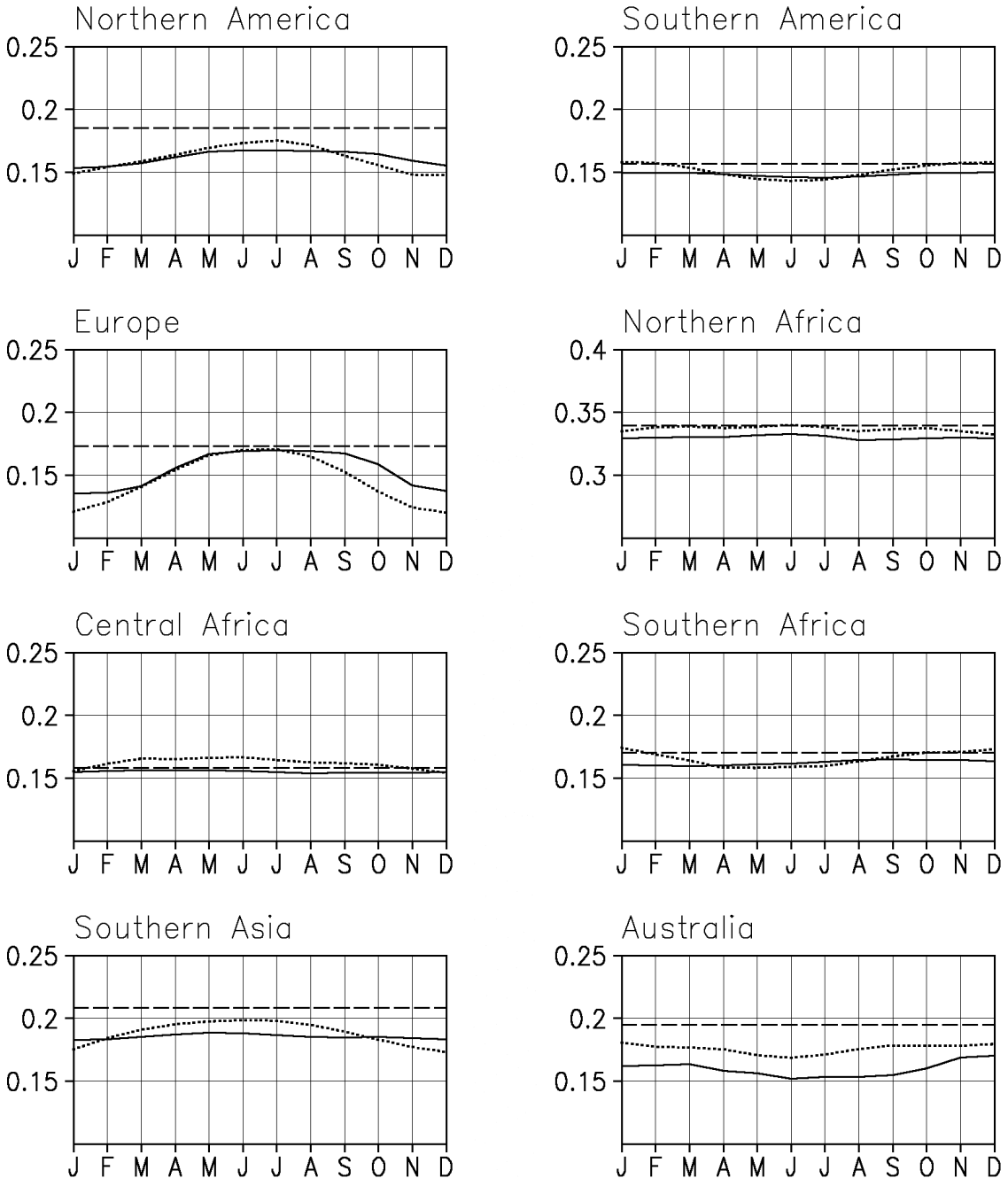

Figure 3.7: New annual mean of the climatological background surface albedo cycle (solid line) in comparison to MODIS annual mean background surface albedo cycle averaged over the whole period 2001-2004 (dotted line) and LSP2 mean (dashed line) area-averaged over the land areas of the selected world regions

Over Australia, the mean background albedo cycle is underestimated by our method for all month of the year. The temporal distribution is very similar, which means that the temporal variability of the LAI is correct. But there is an offset between the observed and the derived albedo cycle of about 0.02. This obviously results from an underestimation of the pure vegetation albedo in Australia by our method (compare figure 3.3).

In northern America, Europe and northern Asia albedo is increasing during the summer months with increasing LAI. In southern Asia the observed annual cycle of MODIS albedo is quite similar to that observed in northern America. The new albedo scheme correctly captures the annual mean albedo, but the annual cycle is not in agreement with the observed temporal variability. To analyse this we look at different parts of this region. In the northern parts with desert regions the background albedo is correct with constant values over the year. In south-east Asia the albedo is increasing with higher LAI values during the summer month which is captured quite good by our method (not shown). The problem occurs over India. Here, the LAI is also increasing in summer with high precipitation during the Indian summer monsoon from June to September. As figure 3.2 and figure 3.3 show, in this region the pure vegetation albedo is lower than the underlying soil albedo. Additionally, the contrast is intensified due to the higher moisture content. This means, that albedo would decrease with increasing vegetation density. But neither the observed MODIS albedo nor the derived model albedo values decrease during summer. Here, possibly the MODIS data overestimates albedo due to undetected clouds with even increasing albedo values during the monsoon season. Thus, the derived albedo with constant values over the year is firstly satisfying.

The strongest seasonal albedo variations can be seen in Europe, where the optical contrast between the dark soils and the brighter vegetation canopy of grasses and crops is quite strong. But the new albedo keeps high during late summer, whereas MODIS albedo data is decreasing earlier. This is possibly due to variable vegetation albedo (changing colours of the leafs, for example), which cannot be considered by our method. Moreover, dominating agricultural land use types with high anthropogenic influence are difficult to capture within the albedo scheme as well as within the models' phenology scheme. This causes differences between the observed and the derived model albedo especially in Europe and also in northern America.

3. 5 Conclusions and outlook

Here, a method is developed to integrate high-resolution satellite information about the earth's surface consistently into the land surface schemes of the climate models REMO and ECHAM5. The annual albedo cycle of snow-free land surfaces is dynamically described as a function of the monthly varying LAI. This method can also be applied to vegetation models or to coupled climate - vegetation models within a fully dynamic phenology parameterisation.

We assumed that the monthly variation of land surface albedo is mainly caused by changes in vegetation cover. Another important factor causing seasonal variability of surface albedo is the soil moisture content. In our method, this is not explicitly considered. But in most cases, its effect is correlated with the vegetation cover. Thus, it is considered indirectly by the vegetation effect on surface albedo. If the satellite products would also provide soil wetness data, this information could be included in our method to verify this assumption. A weak point of this study is, that only the "white-sky albedo" for the bi-hemispherical reflectance is taken into account while neglecting the "black-sky albedo" for the directional hemispherical reflectance, which strongly depends on the diurnal and seasonal variations of the solar zenith angle. Furthermore, albedos of different land cover types depend on the solar radiation spectrum. Whereas green canopies absorb much solar radiation in the visible interval (0.4-0.7

mm), they reflect and transmit most of the incident radiation in the near-infrared band (0.7-4.0 mm). So far, in the regional climate model REMO only the total shortwave broadband surface albedo is used. So, this spectral dependency is not considered in this study. But for land surface schemes, that distinguish visible and near-infrared surface albedos, the introduced method can be applied separately for the two spectral bands to advance the albedo parameterization.

In this study the introduced method is adapted to the REMO RCM and the ECHAM5 GCM to prepare both models for testing the new albedo parameterization scheme both on the regional and the global scale. The resulting mean annual background albedo cycles of the climate models are compared to the snow-free land surface albedos of MODIS averaged over the whole time period from 2001-2004. Together, the comparison between MODIS and the new seasonal variations indicates realistic albedo cycles for the selected regions. The results show that the model's LAI is applicable in the introduced method. Applying the method to other models and LAI datasets, respectively, it is crucial to know, that currently available LAI datasets differ strongly, which can lead to quite different results. How the advanced albedo scheme will affect surface processes in the climate models is the topic of a further study (Rechid et al. 2008b). There, the sensitivity of the simulated climate parameters in REMO and ECHAM5 to the new background albedo parameterization is evaluated in several global and regional climate simulations.

Moreover, for the regional climate model REMO a dynamic vegetation phenology scheme for the LAI as a function of the model climate is currently developed. The so far used climatological mean annual LAI cycle does not account for inter-annual variability caused by changing thermal and moisture conditions from year to year. The new approach will no longer prescribe the monthly LAI values as a climatological boundary condition to the climate model but will compute daily LAI values prognostically during the model simulations as a function of the actual simulated temperatures and moisture parameters. As in our method the background albedo is dynamically described as a function of the LAI, the advanced albedo scheme can be applied to this new phenology scheme and is expected to provide more realistic land surface albedo values on the daily time-scale.

Chapter 4

Sensitivity of climate models to seasonal variability of snow-free land surface albedo[3]

Abstract

The seasonal variation of snow-free land surface albedo was integrated into the land surface schemes of the global climate model ECHAM5 and the regional climate model REMO to test the sensitivity of climate models to the advanced surface albedo parameterization. This new albedo parameterization was developed in previous studies describing the monthly varying surface albedo fields as a function of vegetation phenology derived from MODIS data products. Three model simulations were performed, respectively, to study the sensitivity of the simulated climate to the seasonal background albedo variations: 1. control simulation with the old time-invariant surface background albedo, 2. experiment 1 with the new mean time-invariant surface background albedo field, 3. experiment 2 with the monthly varying surface background albedo as a function of the leaf area index. The analysis of the simulation results demonstrates the influence of the new albedo parameterization on the model simulations. Strong effects occur over Europe with the regional and the global model simulations responding differently to seasonal background albedo variations. In contrast to the global simulation, where the large-scale conditions are changed by the new albedo parameterization, in the regional simulations the circulation patterns within the model domain are not influenced. Here, the external forcing via the lateral boundaries of the regional model domain suppresses changes in the large-scale circulation that might occur without the external forcing. In the regional model simulations only local effects occur mainly during the summer season, when the vertical energy exchange at the land surface is enhanced compared to the winter season. The comparison between the regional and global studies for the selected European regions reveals that the global results show higher sensitivity of the simulated annual temperature and precipitation cycles to the changed albedo parameterization. For both the regional and the global study the temperature and precipitation deviations to the observations are larger than the differences between the three model simulations.

[3] *Rechid D, Hagemann S, Jacob D (2008b) Sensitivity of climate models to seasonal variability of snow-free land surface albedo. Theor Appl Climatol, DOI 10.1007/s00704-007-0371-8*

4. 1 Introduction

The land surface albedo is an important parameter in climate modelling. It is defined by the ratio of solar radiation flux reflected at the surface to the total incoming solar radiation flux. It determines the energy budget of the earth's surface, which in turn drives the climate system. Uncertainties in surface albedo translate directly into errors in the calculation of net radiation and energy fluxes (Sellers et al. 1996a, Sellers et al. 1996b).

Land surface albedo is determined by the surface properties and shows not only spatial variability but also temporal variations. This can be observed by field studies (Song, 1999) and examined by remotely sensed data (Zhou et al. 2003). Over vegetated surfaces, the monthly variability of albedo is mainly caused by seasonally varying vegetation characteristics. In the study of Song (1999) the relationship between albedo and plant phenology was examined by field observations in prairie grassland and agricultural crops. The observed albedo showed clear changes during the phenology phases from green-up to peak greenness, dry down and senescence or harvesting stage. The variability due to plant phenology is determined by the optical contrast between the vegetation canopy and the underlying soil surface. Over bright-coloured soils vegetation cover reduces surface albedo whereas plants on dark soils increase surface albedo.

Modelling studies have shown complex interactions between surface albedo, climate and the biosphere (Dickinson & Hanson 1984, Rowntree & Sangster 1986, Lofgren 1995). Many studies found a strong sensitivity of climate to surface albedo variations caused by vegetation changes. The study of Berbet & Costa (2003) demonstrates that most of the spatial and seasonal variability in the simulated climate after a tropical deforestation can be explained by the difference in the radiation reflected by the surface. The conversion from tropical forest to pasture grasses exposes more soil to the atmosphere. If the albedo of the exposed soil surface is different from the vegetation albedo, the seasonality in vegetation cover density causes important variations in surface albedo. Betts (2001) found that the global surface temperature change caused by vegetation changes is mainly due to surface albedo changes. Myhre & Myhre (2003) point at the uncertainty in the radiative forcing due to land use changes and underscore the need for better data on surface albedo values regarding the effects of vegetation changes. Dirmeyer and Shukla (1994) investigated the effects of tropical deforestation on climate simulated by a general circulation model (GCM). It is found that the change in climate is strongly dependent on the change in surface albedo that accompanies deforestation. The increased surface albedo reduces the absorbed energy at the surface and decreases sensible and latent heat fluxes resulting in a reduction in convection and precipitation. In the study of Lin et al. (1996) the sensitivity of climate to seasonal surface albedo variations simulated by a two level GCM at 10° horizontal resolution was examined. They demonstrate the sensitivity of simulated precipitation to surface albedo variations, especially over eastern Asia and the Sahara. They also note that precipitation decreases when the surface albedo is increased. Surface air temperature decreased over eastern Asia but increased over most of the Antarctica in July with the relationship between temperature and surface albedo variations being quite complex.

The aim of this study is to test an advanced land surface albedo parameterization in a regional and a global climate model and to evaluate the influence of the seasonal background albedo variations in the simulated climate. This study continues on conducted work in previous studies. The sensitivity of the simulated climate by the regional climate model REMO (REgional MOdel, Jacob et al. 1997, Jacob et al. 2001) to seasonal vegetation changes was

investigated in the study of Rechid & Jacob (2006). Their results showed a significant influence of monthly varying vegetation properties on the simulated European climate. The vertical surface fluxes, temperature and precipitation are strongly affected. The near-surface climate becomes cooler and wetter during the growing season especially in eastern Europe and regions with predominating continental climate.

So far, in the global climate model ECHAM5 (Roeckner et al. 2003) and the regional climate model REMO the albedo over snow-free land surfaces was prescribed by tabular values only depending on land cover type without temporal variability (Hagemann et al. 1999). In both models vegetation phenology is represented by monthly varying fields of leaf area index (LAI) and fractional vegetation cover (Roeckner et al. 2003, Rechid & Jacob 2006). These temporal varying vegetation fields are taken from a global dataset of land surface parameters called "LSP2" designed by Hagemann (2002). This dataset also includes monthly fields of background albedo. This annual albedo cycle was derived by a method, which was designed for regions with bright soils where vegetation decreases the surface albedo. This is not appropriate for Europe, the standard region of the REMO model. Here, dark soils are dominant, where vegetation like grasses and crops increase the surface albedo.

In the study of Rechid et al. (2008a) an advanced parameterization of the snow-free land surface albedo was developed describing the monthly varying surface albedo as a function of vegetation phenology using data products from the Moderate-Resolution Imaging Spectroradiometer (MODIS). The seasonal albedo cycle was prepared for the application in climate modelling. The advanced albedo parameterization was integrated into the land surface schemes of ECHAM5 and REMO. The purpose of this study is now to test this new albedo parameterization and to investigate the sensitivity of the global climate simulated by ECHAM5 and the regional climate simulated by REMO to the new surface background albedo variations due to seasonal vegetation changes and to compare the regional and the global results.

The paper is organised as follows: section 4.2 gives a short descriptions how the land surface characteristics in ECHAM5 and REMO are represented and a short presentation of the new albedo parameterization scheme. In section 4.3 the results of the global and in section 4.4 the results of the regional sensitivity studies are presented. For both studies an comparison is done in section 4.5. Here, the global and regional simulation results are also compared to observations. In section 4.6 we give conclusions and a short outlook.

4. 2 Background albedo parameterization in ECHAM and REMO

The general circulation model (GCM) ECHAM5 (Roeckner et al. 2003) and the regional climate model (RCM) REMO (REgional MOdel, Jacob et al. 1997, Jacob et al. 2001) use similar land surface schemes. The REMO RCM is based on the physical parameterizations of the ECHAM4 GCM. The land surface properties are represented by the same global dataset of land surface parameters (Hagemann et al. 1999, Hagemann 2002). The vegetation phenology is represented by monthly varying values of the leaf area index. These temporal varying vegetation fields are taken from a global dataset of land surface parameters LSP2 (Hagemann 2002). The LSP2 dataset is based on a global distribution of major ecosystem types (Global

Land Cover Characteristics Database; GLCCD) according to a classification list of Olson (1994a, 1994b). The Olson ecosystem types were derived from Advanced Very High Resolution Radiometer AVHRR data at 1 km resolution supplied by the International Geosphere-Biosphere Program (Eidenshink & Faundeen 1994) and constructed by the U.S. Geological Survey (1997, 2002). For each land cover type parameter values for background surface albedo, fractional vegetation cover, minimum and maximum leaf area index and other vegetation properties are allocated. This information is aggregated to the model grid scale averaging the vegetation parameters of all land cover types, which are located in one model grid cell. The seasonal variation of the LAI between minimum and maximum values is estimated by a global data field of the monthly growth factor, which is defined by climatologies of FPAR (fraction of absorbed photosynthetically active radiation) and 2m-temperature (Hagemann 2002). So far, in ECHAM5 and REMO the albedo over snow-free land surfaces was prescribed by tabular values only depending on land cover type without temporal variability.

The new background albedo parameterization describes the monthly varying surface albedo as a function of vegetation phenology using data products from the Moderate-Resolution Imaging Spectroradiometer (MODIS). The MODIS products of the white sky albedo for total shortwave broad bands and FPAR were analysed by Rechid et al. (2008a) to separate the vegetation canopy albedo from the underlying soil albedo. They derived global maps of pure soil albedo and pure vegetation albedo on a 0.5° regular latitude/longitude grid by re-sampling the high-resolution information from remote sensing-measured pixel level to the model grid scale and filling up gaps from the satellite data. These global maps show that in the northern and mid-latitudes soils are mainly darker than vegetation, whereas in the lower latitudes, especially in semi-deserts, soil albedo is mostly higher than vegetation albedo.

The global distributions of soil albedo a_{soil} and vegetation albedo a_{canopy} can be applied in climate modelling to describe the annual background albedo cycle a as a function of the LAI (Rechid et al. 2008a):

$$a = a_{soil} \cdot e^{-0.5 \cdot LAI} + a_{canopy} \cdot (1 - e^{-0.5 \cdot LAI}) \qquad (4.1)$$

The temporal variation of snow-free surface albedo due to seasonally varying LAI was integrated into the ECHAM5 GCM and the REMO RCM.

4. 3 Global simulations with ECHAM5

4. 3. 1 Model simulations

Three model simulations were performed to study the sensitivity of the simulated global climate to the background surface albedo variability. The simulations are done at T63 horizontal resolution with 31 vertical levels using the AMIP2 SST (http://www-pcmdi.llnl.gov/projects/amip/index.php) as forcing for the period 1978-1999: 1. control simulation with the currently used time-invariant surface background albedo = **CONT**, 2. experiment with the new mean time-invariant surface background albedo field = **EXP1**, 3.

experiment with the time-varying surface background albedo as a function of the leaf area index = **EXP2**. EXP1 with the new annual mean background albedo is carried out to distinguish the effect of the new mean albedo from the effect of the seasonally varying albedo on the simulation results. The horizontal distribution of the new background albedo is presented and discussed in section 4.3.2 together with the results of the model simulation. The model results are evaluated for the 20-year time period from 1979-1999 skipping the first year to pay regard to model spin up.

4. 3. 2 Results

4. 3. 2. 1 Background albedo

Figure 4.1a presents the horizontal distribution of the new annual mean background albedo of EXP1 and figure 4.1b the difference between the new and old annual mean background albedo EXP1-CONT. The new annual mean background albedo values derived from MODIS data exhibit lower values up to differences of -0.05 compared to the old annual mean albedo used in the climate model almost over the whole globe except for the Arabian Peninsula, the tropics in Southern America and some coastal areas. The horizontal differences caused by the seasonal background albedo variability (EXP2-EXP1) for the 20-year seasonal means of December-January-February (DJF) and June-July-August (JJA) are displayed in figure 4.1c and 4.1d. The new annual mean background albedo leads to larger albedo differences compared to the old annual mean (EXP1-CONT) than the seasonal variations of the background albedo (EXP2-EXP1). The main differences caused by the seasonal albedo variability occur in Europe, northern Asia and the eastern part of northern America with higher background albedo values during the summer season and lower values during the winter season compared to the annual mean. In these regions the soils are mainly darker than vegetation, so that the greening up of plants during the growing season leads to higher surface albedos. In parts of eastern Asia, in Australia and in the southern part of South America, the soils are mainly brighter than vegetation so that plants lead to decreasing albedo values.

Together, in comparison to MODIS the mean snow-free land surface albedo is overestimated by the values of the control run. Hence, in almost all regions the new mean background albedo of experiment 1 and 2 are lower than the old mean of the control run. The comparison between MODIS and the new seasonal variations indicates realistic albedo cycles for selected regions of the world (Rechid et al. 2008a).

4.1a. EXP1 4.1b. EXP1-CONT

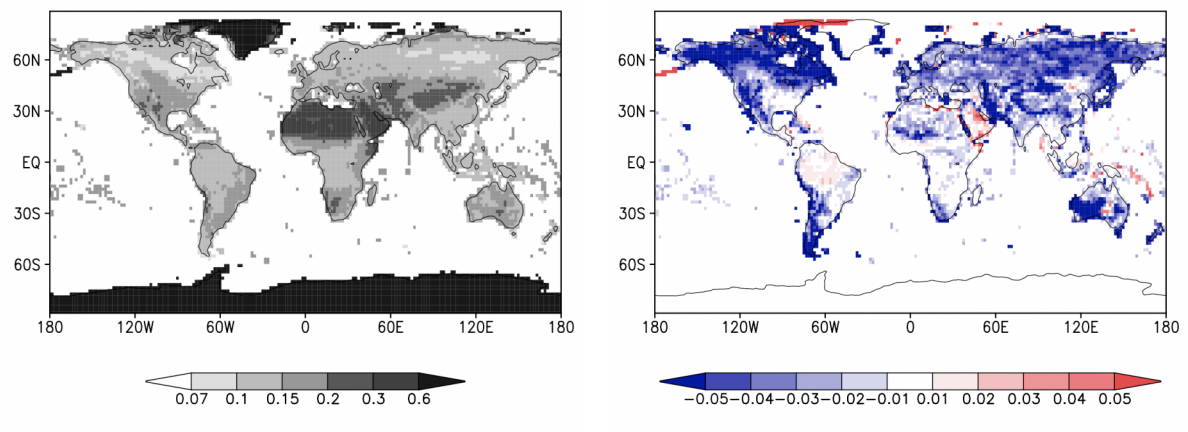

4.1c. DJF, EXP2-EXP1

4.1d. JJA, EXP2-EXP1

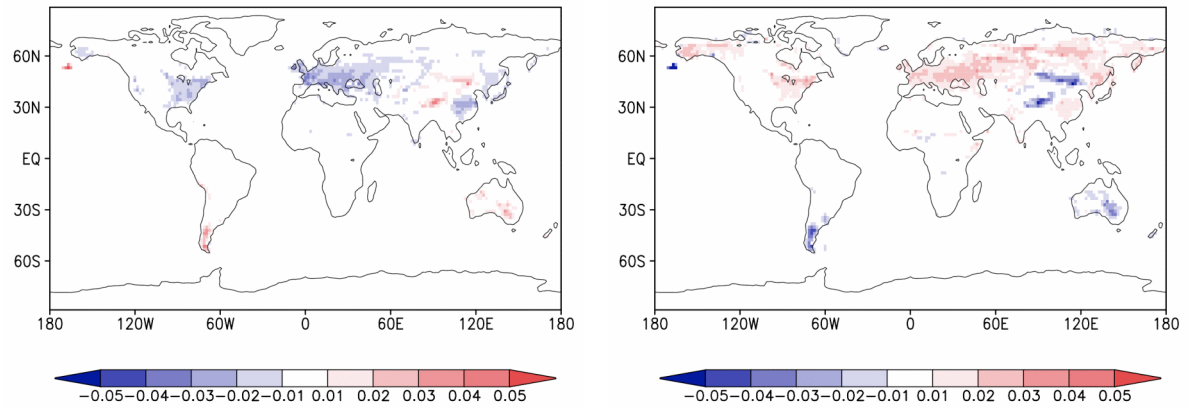

Figure 4.1: New annual mean background albedo of EXP1 (4.1a) compared to the old annual mean EXP1-CONT (4.1b) and seasonal differences for DJF (4.1c) and JJA (4.1d) of temporal varying background albedo compared to the new annual mean EXP2-EXP 1979-1999

4. 3. 2. 2 Total surface albedo

In the following, always the horizontal differences of 20-year seasonal means for JJA and DJF between EXP1-CONT and EXP2-EXP1 are presented and discussed to separate the effects caused by the changes in mean background albedo from the effects caused by the seasonal variability of background albedo on the simulation results. The simulated total surface albedo (figure 4.2) includes albedos of water surfaces and albedos of snow covered fractions of a model grid box. The major differences again result from the new annual mean background albedo (figure 4.2a and 4.2b). In central and eastern Europe during winter season the total surface albedo increases in EXP2 compared to EXP1 in spite of the lower background albedo (figure 4.2c). Here, the differences of the total albedo compared to the background albedo (compare figure 4.1c) are caused by the snow albedo which is a sign of modified snow cover conditions. During JJA (figure 4.2d) the changes in total surface albedo correspond to the seasonal background albedo variations.

4.2a. DJF, EXP1-CONT

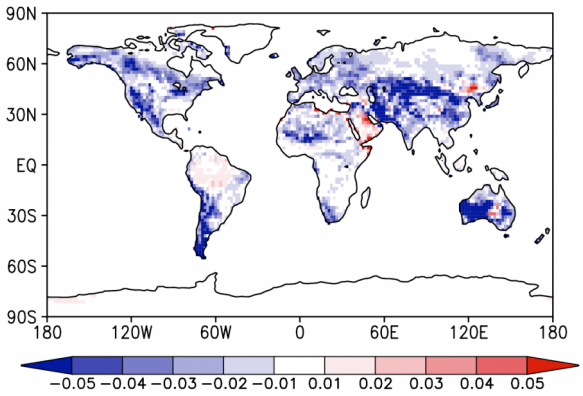

4.2b. JJA, EXP1-CONT

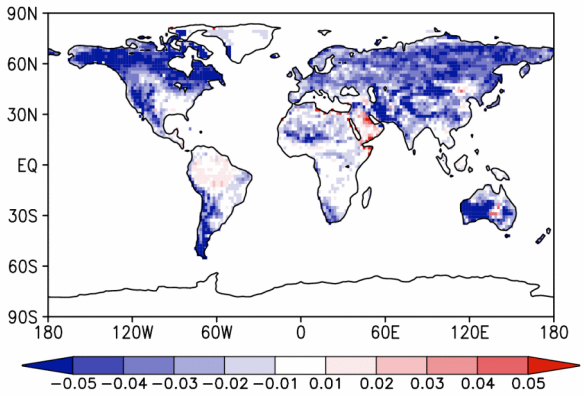

4.2c. DJF, EXP2-EXP1

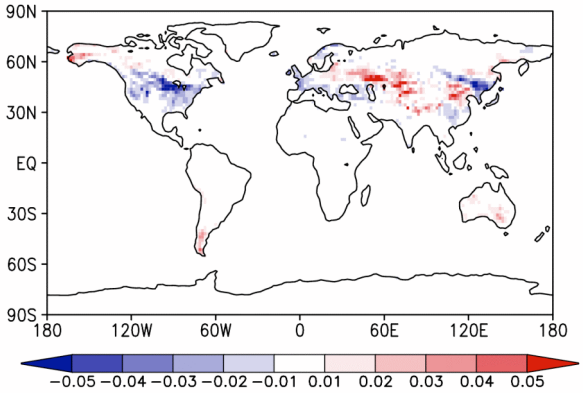

4.2d. JJA, EXP2-EXP1

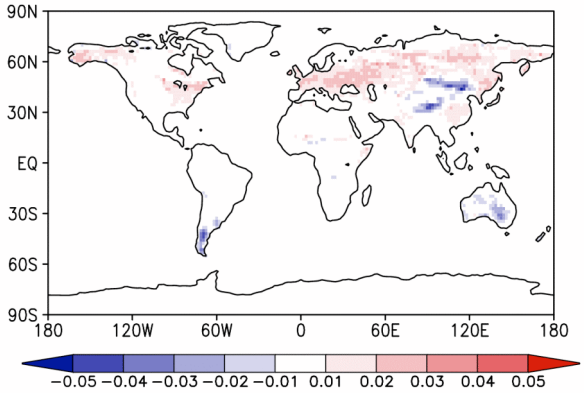

Figure 4.2: Seasonal differences of the total surface albedo (including snow and water albedo) due to the new annual mean background albedo EXP1-CONT (4.2a,b) and due to temporal varying background surface albedo EXP2-EXP1 (4.2c,d) 1979-1999

4. 3. 2. 3 Mean sea level pressure

The simulated mean sea level pressures show clear zonal differences for both experiments compared to the control run up to ±2hPa (figure 4.3). Comparing EXP1 and CONT during DJF (figure 4.3a) a zonal pressure decrease up to -2hPa occurs in the southern high latitudes. Over the northern globe regional differences can be seen with a pressure decrease over central and southern Europe and northern Africa and a slight pressure increase over northern Europe and Siberia. During JJA (figure 4.3b) more regional differences occur with partly reversed conditions compared to the winter season.

In contrast, the new seasonal albedo cycle (EXP2-EXP1) leads to different patterns. Figure 4.3c shows for DJF a zonal increase in mean sea level pressure up to 2hPa for the high latitudes whereas in the mid- and low latitudes the differences are slightly negative to zero. This can lead to modified air flows and circulation patterns. Over the Northern Atlantic, the sea level pressure difference between the Icelandic Low and the Azores High is lower in EXP2. This lower North Atlantic Oscillation (NAO) index weakens the westerlies. For JJA

(figure 4.3d) the pressure increase of +2hPa only occurs in the southern high latitudes, over northern Europe and Siberia the mean pressure also increases but only regionally up to 1hPa. Together, the moderate albedo forcing causes clear differences in mean sea level pressure.

4.3a. DJF, EXP1-CONT

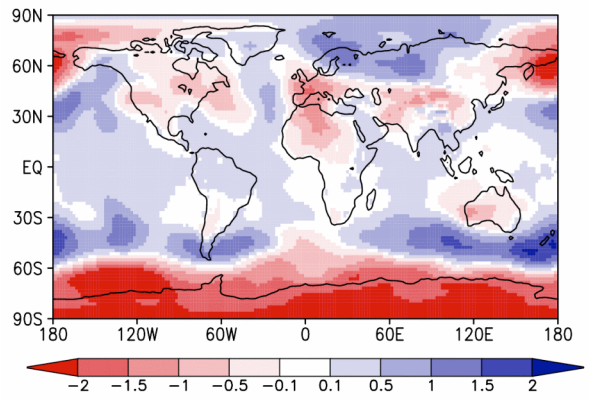

4.3b. JJA, EXP1-CONT

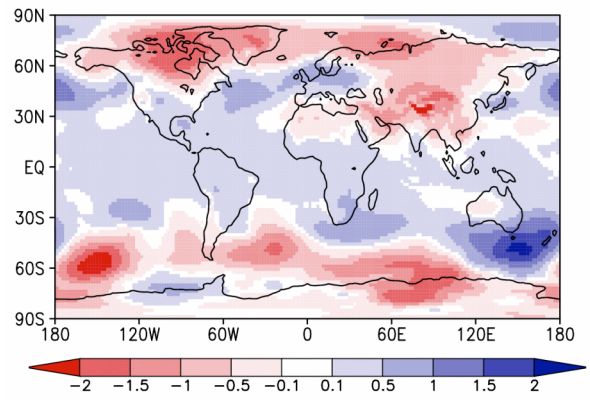

4.3c. DJF, EXP2-EXP1

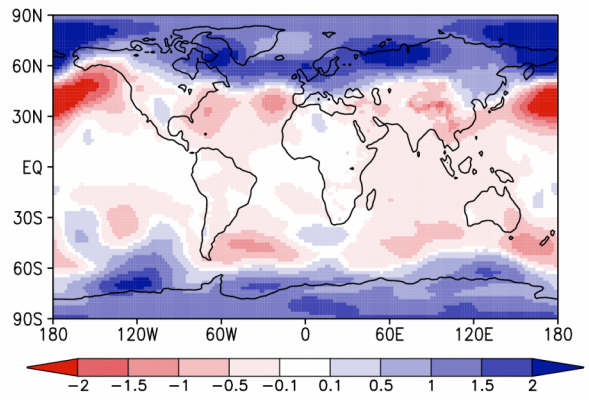

4.3d. JJA, EXP2-EXP1

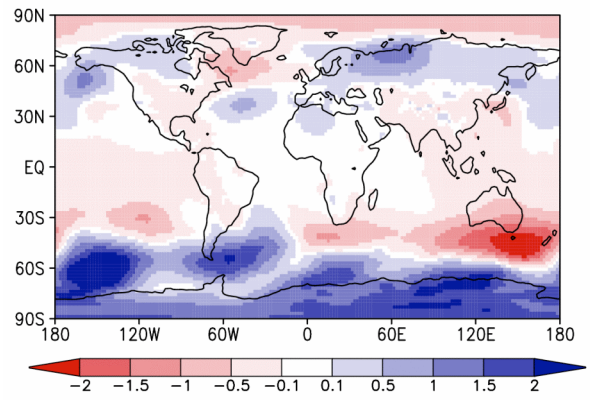

Figure 4.3: Seasonal differences of mean sea level pressure [hPa] due to the new annual mean background albedo EXP1-CONT (4.3a,b) and due to temporal varying background surface albedo EXP2-EXP1 (4.3c,d) 1979-1999

4. 3. 2. 4 Net surface solar radiation

The lower mean albedo of EXP1 compared to the control simulation CONT directly translates into higher net surface solar radiation over the continents in the mid-latitudes, especially when the solar input is high during southern summer season (figure 4.4a) and during northern summer season (figure 4.4b). In contrast, the differences in net surface solar radiation caused by the seasonal variability in background albedo are quite low. The pictures for DJF (figure 4.4c) and JJA (figure 4.4d) look quite patchy. In central and eastern Europe the slightly lower net surface solar radiation is caused by the higher background albedo during summer compared to the constant annual mean albedo (EXP2-EXP1). During the winter season no

effect of the northern hemisphere seasonal albedo variability occurs due to dominating snow cover. In the southern hemisphere over the Pacific between 30S and EQ and between 90W and 180W the net surface solar radiation is noticeably changed in DJF. The difference between EXP1 and CONT (figure 4.4a) shows an increase in seasonal net surface solar radiation in the northern part and a decrease in the southern part of this region. For EXP2-EXP1 (figure 4.4c) the reverse effect occurs. Over the regions with lower net surface solar radiation the total cloud cover is increased up to +5 % and over the regions with higher net surface solar radiation the total cloud cover is decreased up to -5 % (not shown). The seasonal precipitation changes (will be presented in section 4.3.2.6 with more detail) show the same pattern. Over the region with lower net surface solar radiation and higher cloud cover the precipitation is increased up to +40% and vice versa. These are no direct but remote effects of the changes in land surface albedo, which indicate a modification of the large-scale atmospheric circulation.

4.4a. DJF, EXP1-CONT

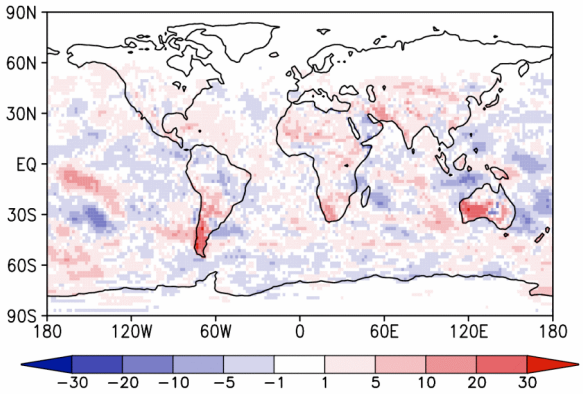

4.4b. JJA, EXP1-CONT

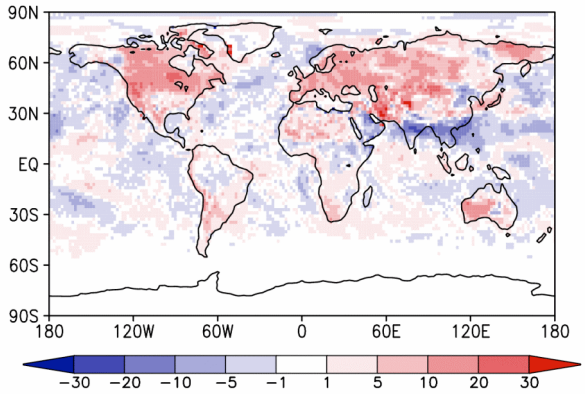

4.4c. DJF, EXP2-EXP1

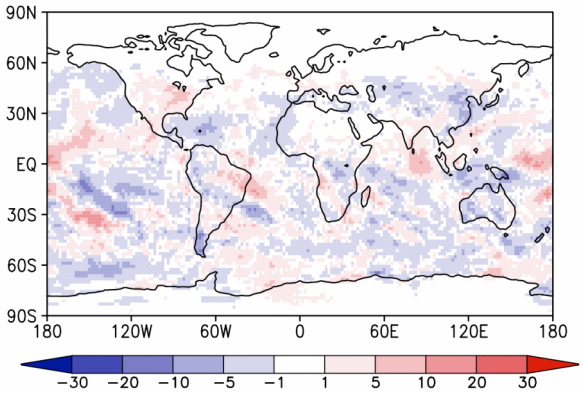

4.4d. JJA, EXP2-EXP1

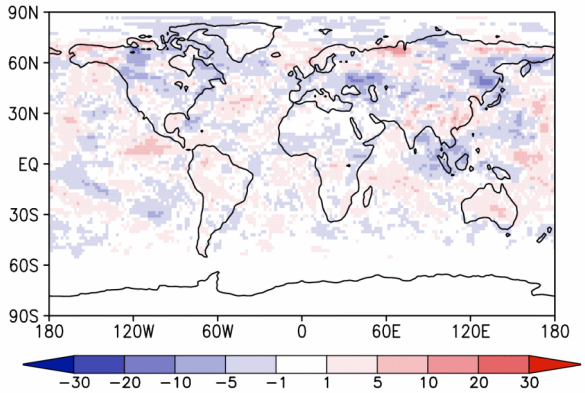

Figure 4.4: Seasonal differences of net surface solar radiation [W/m^2] due to the new annual mean background albedo EXP1-CONT (4.4a,b) and due to temporal varying background surface albedo EXP2-EXP1 (4.4c,d) 1979-1999

4. 3. 2. 5 Surface temperature

4.5a. DJF, EXP1-CONT

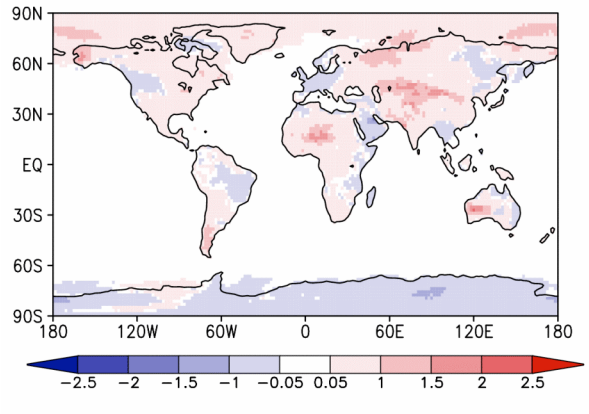

4.5b. JJA, EXP1-CONT

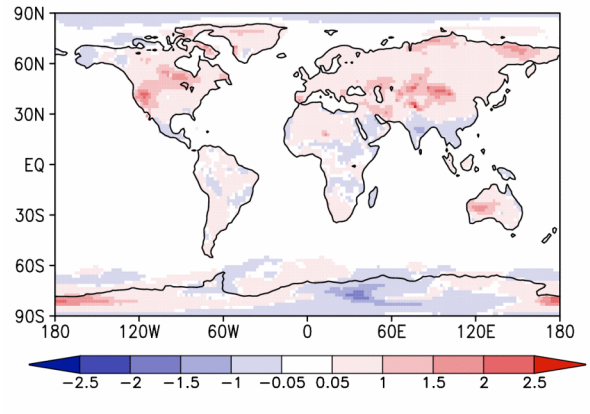

4.5c. DJF, EXP2-EXP1

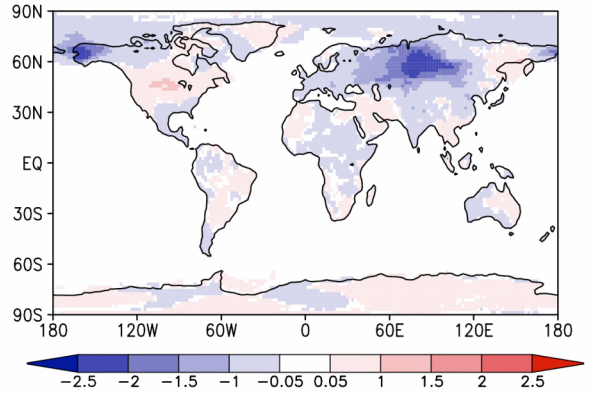

4.5d. JJA, EXP2-EXP1

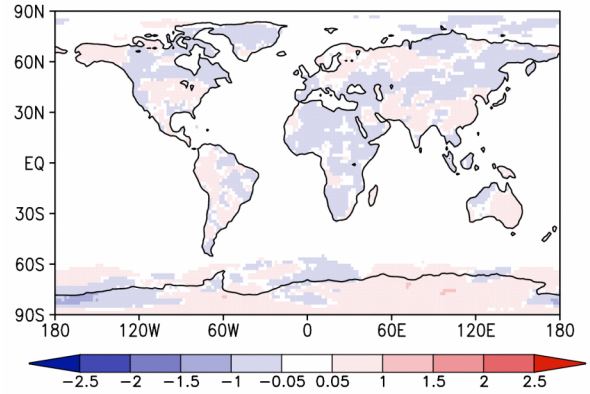

Figure 4.5: Seasonal differences of surface temperature [K] due to the new annual mean background albedo EXP1-CONT (4.5a,b) and due to temporal varying background surface albedo EXP2-EXP1 (4.5c,d) 1979-1999

The simulated surface temperature of the climate model is the temperature of the most upper soil layer at 3.25 cm below the earth surface. The higher net solar radiation input to the land surface caused by the lower albedo mean of EXP1 compared to the control run CONT leads to higher surface temperatures up to 2K in some regions in central Asia, Australia and the western part of northern America especially during the summer season, respectively. (figure 4.5a and 4.5b). There is no significant influence of the seasonal albedo variability on surface temperatures during JJA (figure 4.5d), but during DJF (figure 4.5c), an interesting effect occurs over central Siberia and in the northwest of Alaska. Here, the surface temperatures decrease more than 2K over a large area. The significance of the temperature change was calculated with a one-sided t-test. The temperature decrease over Siberia is significant on the 95% level. This means, that the temperature effect in this region is not caused by natural, internal model variability but can be referred to the seasonal albedo variability. In this region the background albedo didn't change at all, also snow cover and snow albedo show no differences. The same effect occurs over Alaska, where the surface temperature is also

reduced by 2 K. These remote climate impacts of the changed land surface albedo can only be explained by the modification of the planetary-scale atmospheric circulation (compare section 4.3.2.7).

4. 3. 2. 6 Precipitation

4.6a. DJF, EXP1-CONT

4.6b. JJA, EXP1-CONT

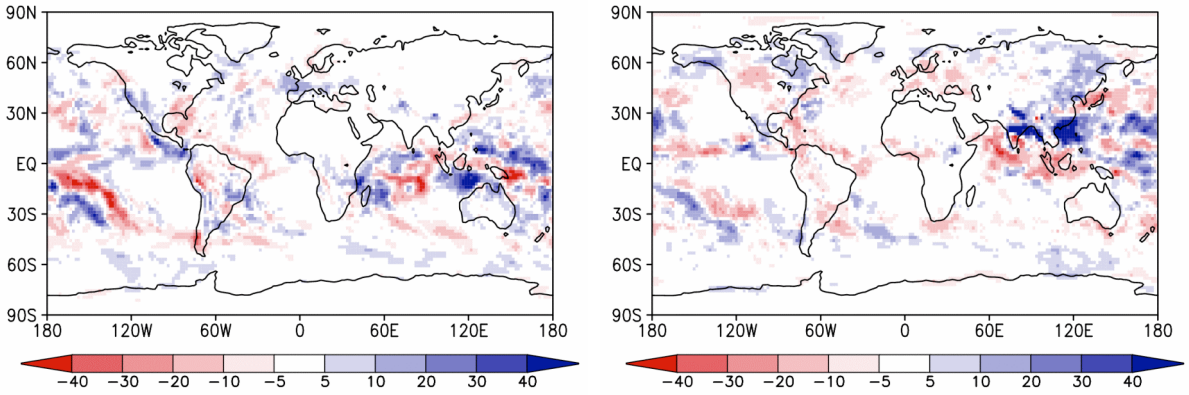

4.6c. DJF, EXP2-EXP1

4.6d. JJA, EXP2-EXP1

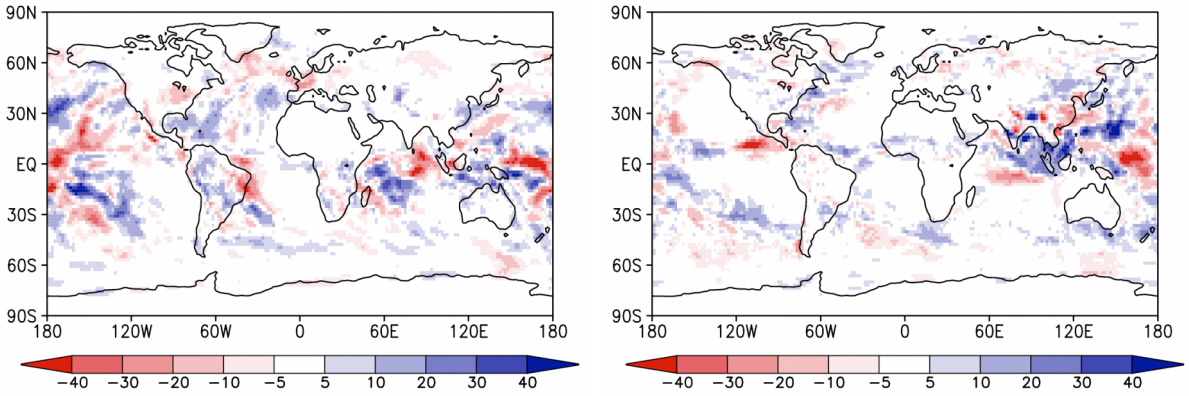

Figure 4.6: Seasonal differences of precipitation [mm/month] due to the new annual mean background albedo EXP1-CONT (4.6a,b) and due to temporal varying background surface albedo EXP2-EXP1 (4.6c,d) 1979-1999

The main changes in precipitation in both experiments occur over the ocean between 30N and 30S (figures 4.6a-d). This remote effect of the new land albedo scheme again indicates a modification of the large-scale atmospheric circulation. Especially during DJF the precipitation over the tropical Ocean is strongly influenced by the new albedo mean (figure 4.6a) and by the seasonal albedo cycle (figure 4.6c). These figures show partly reverse effects on the precipitation patterns as over the Pacific between 120E and 90W (see also section 4.3.2.4), over the Gulf of Mexico and over the Indian Ocean between 60E and 90E. In regions with increased precipitation, in the majority of cases cloud cover is also increased up to +5 %

(not shown) and vice versa. Over land, no significant precipitation changes occur during DJF. A slight decrease in precipitation up to -30 mm/month in Western Europe gives an indication on the weakening of the westerlies, which will be discussed with more detail in section 4.3.2.7.

During JJA the main precipitation changes caused by the new albedo mean occur over the Pacific Ocean between 30N and EQ and between 100E and 150W (figure 4.6b). Here, precipitation is increased up to +40 mm/month with higher cloud cover up to + 5 % (not shown). The precipitation changes in EXP2 compared to EXP1 (figure 4.6d) turned out to be not significant by analysing the relative precipitation differences. Over land during JJA, the simulated differences in precipitation between EXP1 and CONT show an intensification of the monsoon in northern India, possibly through changes in the Hadley and/or Walker circulation (not analysed in this study).

4. 3. 2. 7 Atmospheric circulation

The seasonal changes in mean sea level pressure, net surface solar radiation, surface temperature and precipitation caused by the new land surface albedo scheme indicate a modification of the large-scale atmospheric circulation. The effects on the simulated climate are not restricted to regions where land surface albedo is changed, but also occur in remote regions through atmospheric teleconnections. It is not clear which atmospheric processes lead to these remote climate impacts. Why is the simulated surface temperature up to +2K higher over a large region in Siberia during the winter season where the seasonal surface albedo is not changed at all? Why do the precipitation pattern change over the tropical ocean whereas surface albedo changes are restricted to land? In order to address these issues, simulated model parameters of the air flow in the troposphere are analysed. Some selected results of EXP1 and EXP2-EXP1 during DJF are presented in figure 4.7. The global distribution of wind speed and direction at the lower troposphere (figure 4.7a) show zonal patterns in the low and mid-latitudes with the strong perturbations caused by the continents and their orography. The differences in horizontal wind speed and wind vector at 850 hPa (figure 4.7b) show mainly zonal wind changes in the mid-latitudes in the northern and southern hemisphere. Especially noticeable is the reduced wind speed up to -2 m/s in the west wind zone over the Northern Atlantic and Western Siberia. Considering the vertical zonal mean of wind speed between 60W and 120E (not shown) this wind change pattern can be seen throughout the whole troposphere with stronger changes in the upper levels between 300 hPa and 200 hPa where the jet stream transports weather systems around the globe. The weakening of the westerlies causes less transport of heat and moisture from the Atlantic ocean to the Eurasia land masses. This leads to lower winter temperatures over Europe (figure 4.5c) and also to lower precipitation over the continent (figure 4.6c). Going further east, the influence of the continental land mass becomes more dominant, which is likely to cause the strong temperature decrease over Siberia.. Over the Northern Pacific the wind field is also modified but the strong temperature decrease over Alaska seems to be caused by the intensified inflow of artic cold air into this region.

But which processes lead to the strong modifications of the wind field? Over Northern America and Western Europe the total land surface albedo is reduced (figure 4.2c) in EXP2 compared to EXP1 during the northern winter season. The lower surface albedo increases the net surface solar radiation (figure 4.4c). The higher energy input to the earth surface enhances

the turbulent heat fluxes into the atmosphere. Whereas the latent heat flux is not changed, the sensible heat flux increases over the western part of Northern America. During the winter season with strong vertical temperature gradients this perturbation intensifies and is likely to change the air flow in the whole atmosphere. The global wind field is modified with zonal wind patterns becoming less pronounced. Corresponding to this, the changes in mean sea level pressure (figure 4.3c) show strong zonal patterns, which can also be seen in the fields of geopotential height in the free atmosphere (not shown). The pressure gradients are partly reduced, as over the Northern Atlantic between the Icelandic Low and the Azores High. This means a lower North Atlantic Oscillation (NAO) index and a weakening of the westerlies.

4.7a. Wind speed and vector at 850 hPa [m/s] DJF, EXP1

4.7b. Wind speed and vector at 850 hPa [m/s] DJF, EXP2-EXP1

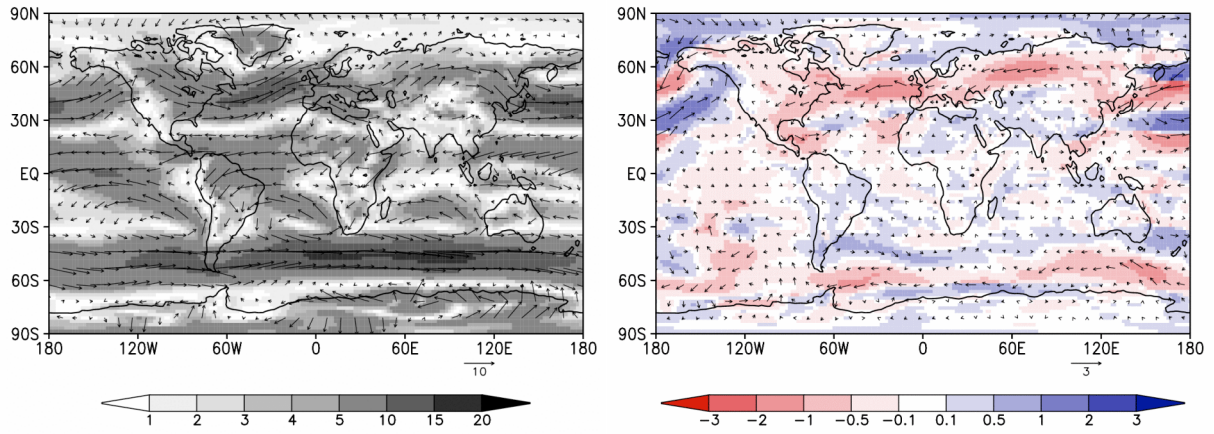

4.7c. Vertical velocity at 500 hPa [hPa/s] DJF, EXP1

4.7d. Vertical velocity at 500 hPa [hPa/s] DJF, EXP2-EXP1

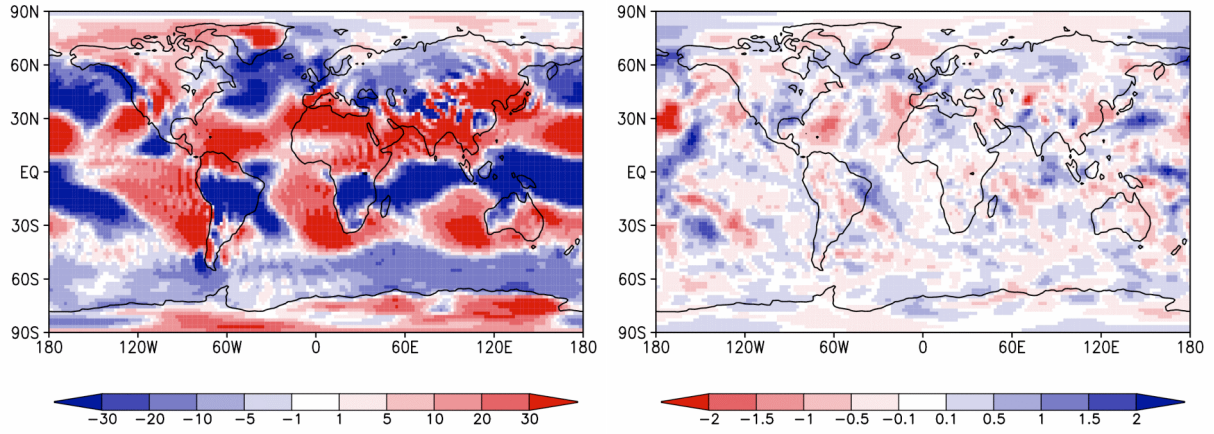

Figure 4.7: Seasonal means of wind speed and direction [m/s] at 850 hPa (4.7a) and vertical velocity [hPa/s] at 500 hPa (4.7c) and seasonal differences due to temporal varying background surface albedo EXP2-EXP1 of wind speed and vector [m/s] at 850 hPa (4.7b) and vertical velocity [hPa/s] at 500 hPa (4.7d) during DJF 1979-1999

During DJF in EXP2 compared to EXP1 the wind patterns between 30N and 30S are hardly changed. But the analysis of the simulation results in the sections before showed remote climate impacts of the land surface albedo changes in the tropics and especially over the tropical ocean. To take a view on the vertical air motion, the changes in vertical velocity in the middle troposphere at 500 hPa are presented in figure 4.7d. To interpret these differences, the vertical velocity of EXP1 is displayed in figure 4.7c. Positive algebraic signs mean sinking air motion and negative signs mean rising air motion. The differences in vertical velocity show the same patterns as the differences in precipitation (figure 4.6c). This is also the case for the changes between EXP1 and CONT (not shown). This means that locations with changes in ascending and descending air motions are consistent with the changes in precipitation, cloud cover and solar radiation (compare also section 4.3.2.4). In regions where the rising air motion is enforced or the sinking air motion is weakened, cloud cover and precipitation are increased and net surface solar radiation is lower. In regions where the rising air motion is weakened or the sinking is enforced, cloud cover and precipitation is reduced and the net surface solar radiation is higher. But why is the vertical air motion modified over the tropics, far away from the regions, where surface albedo is changed? Here, we would like to give a short view on state of the art studies on this question. Tanaka et al. (2005) say that the velocity potential at 200hPa contains information about the overall intensity of the tropical circulation. The changes in velocity potential in our study show partly similar patterns as the precipitation changes over the tropics (not shown). Also the changed streamfunction at 200 hPa (not shown) illustrates clearly modified patterns indicating large-scale modifications of the atmospheric circulation. These planetary-scale perturbations in the velocity potential and streamfunction fields may provide the basis for a possible tele-connection mechanism between the Northern Hemisphere and the Southern Hemisphere (Burke et al. 2000). Chase et al. (1999) state that these planetary-scale changes impact the divergence, and some of the remote climate impacts of land surface changes may result from the vorticity transport set up by this perturbed large-scale divergent field. Vorticity budget studies have shown that the transport of vorticity by the divergent field is an effective transport mechanism, especially for tropical - extra-tropical teleconnections (Sardeshmukh and Hoskins 1987).

4. 4 Regional simulations with REMO

4. 1 Model simulations

As for the global simulations with ECHAM5 three regional model simulations were performed to study the sensitivity of the simulated regional climate to the background surface albedo variability. The simulations are done at 0.44 horizontal resolution with 31 vertical levels for the 15-year time period from 1979-1993 driven by lateral boundary conditions and sea surface temperatures from the European Centre for Medium-Range Weather Forecasts (ECMWF) Reanalysis Project (ERA40, Uppala et al. 2005): 1. control simulation with the currently used time-invariant surface background albedo = **CONT**, 2. experiment with the new mean time-invariant surface background albedo field = **EXP1**, 3. experiment with the time-varying surface background albedo as a function of the leaf area index = **EXP2**. The model domain focusing on Europe is shown in figure 4.8. It presents the model orography superposed by European sub-regions, which are used for some evaluations. The model results are evaluated for the 15-year time period from 1979-1993. The regional model simulations

only cover this 15-year time period performed in the context of further sensitivity studies. For the comparison between the regional and global simulation results in chapter 4.5, the same time period is extracted from the global results.

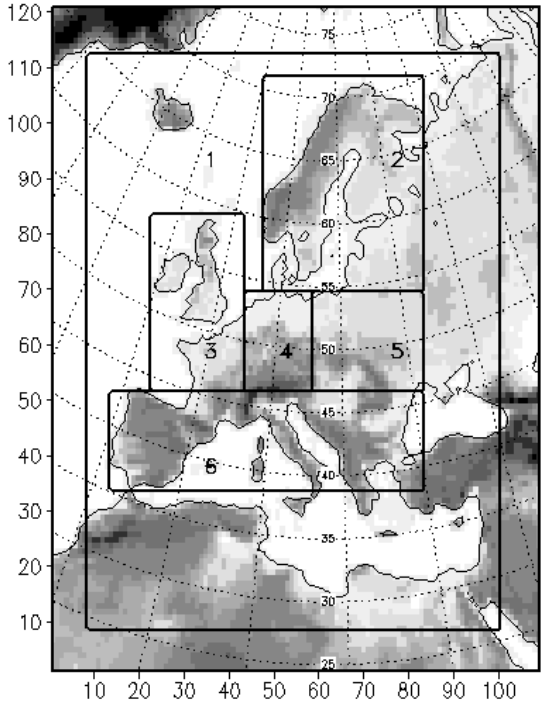

Figure 4.8: REMO model orography [m] at 0.44 degree horizontal resolution with European sub-domains: 1 model domain area without the 8 boundary grid boxes, 2 northern Europe, 3 western Europe, 4 central Europe, 5 eastern Europe, 6 southern Europe.

4. 4. 2 Results

4. 4. 2. 1 Background albedo

For the regional model domain the horizontal differences between the surface background albedos in the three simulations (EXP1-CONT and EXP2-EXP1) in figure 4.9 show the same patterns as for the global experiments (compare section 4.3.2.1), but with more detail. Figure 4.9a presents the regional horizontal distribution of the new annual mean background albedo of EXP1 and figure 4.9b the difference between the new and old annual mean background albedo EXP1-CONT. The new annual background albedo means derived from MODIS data show mainly lower values up to differences of -0.05 over Europe. The seasonal albedo variability leads to higher background albedo values during the summer season (figure 4.9d) and lower values during the winter season (figure 4.9c) compared to the new annual mean. In Europe the soils are mainly darker than vegetation. The greening up of plants during the growing season leads to higher surface albedos, whereas during the dormancy season the darker background soil becomes more visible. Together, the representation of the seasonal surface albedo variations in the regional climate model is clearly improved especially for Europe (Rechid et al. 2008a).

4.9a. EXP1

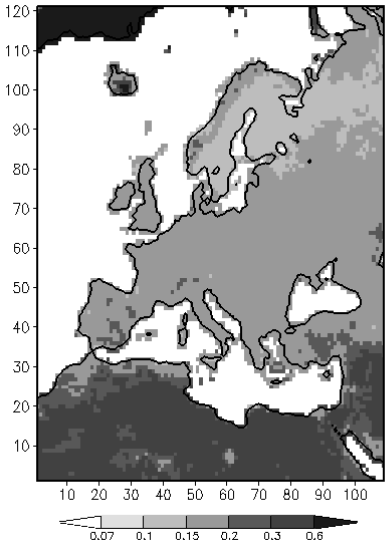

4.9b. EXP1-CONT

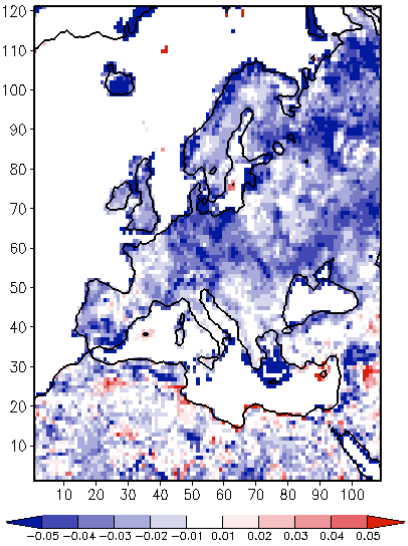

4.9c. DJF, EXP2-EXP1

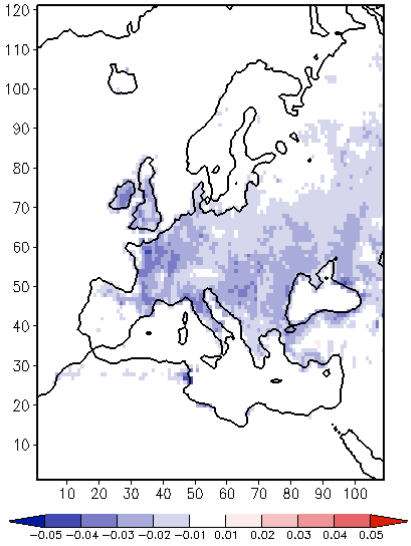

4.9d. JJA, EXP2-EXP1

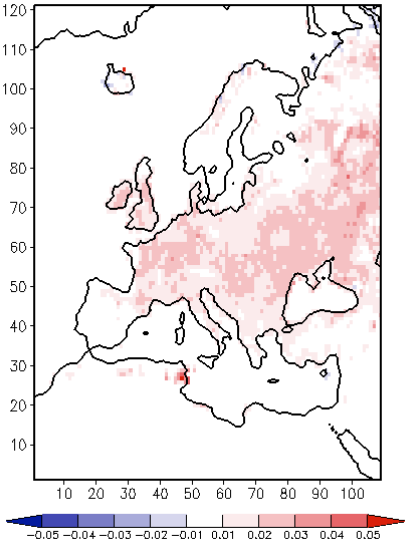

Figure 4.9: New annual mean background albedo of EXP1 (4.9a) compared to the old annual mean EXP1-CONT (4.9b) and seasonal differences for DJF (4.9c) and JJA (4.9d) of temporal varying background albedo compared to the new annual mean EXP2-EXP 1979-1993

4. 4. 2. 2 Total surface albedo

The differences of the simulated total surface albedo caused by the new background albedo parameterization show the same patterns as for the background albedo itself, except for the northern part of Europe, where the background is covered by snow during the winter season without changes (not shown).

4. 4. 2. 3 Mean sea level pressure

In contrast to the global simulation results the regional experiments show no significant changes in mean sea level pressure (not shown) and the circulation patterns are not modified. The external forcing prescribes the large-scale boundary conditions; only local effects of the new albedo parameterization are expected.

4. 4. 2. 4 Net surface solar radiation

4.10a. JJA, EXP1-CONT 4.10b. JJA, EXP2-EXP1

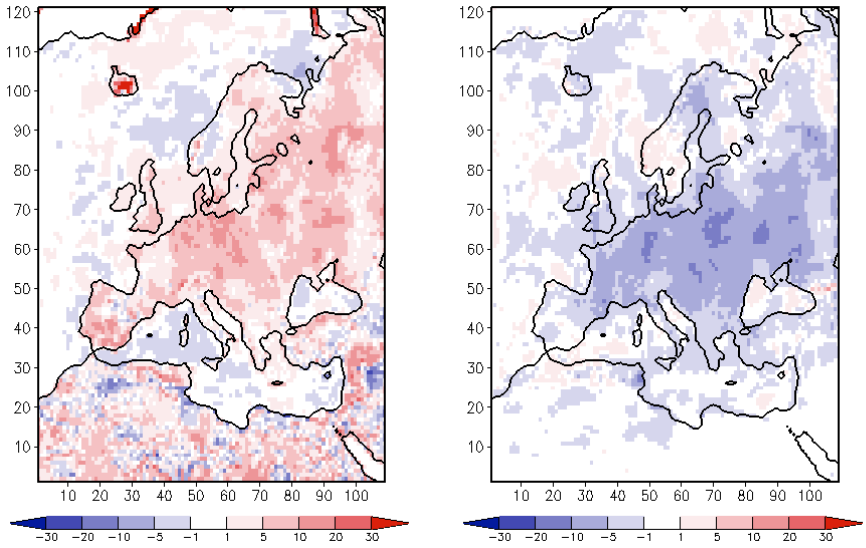

Figure 4.10: Differences of net surface solar radiation [W/m^2] due to the new annual mean background albedo EXP1-CONT (4.10a) and due to temporal varying background surface albedo EXP2-EXP1 (4.10b) for JJA 1979-1993

During the winter season the new albedo parameterization has almost no effect on the simulated net surface solar radiation (not shown). Only in southern Europe the solar radiation input to the earth surface is slightly increased. But the total solar radiation input during DJF is relatively low due to high cloud cover and shorter length of the days, so that radiation fluxes at the surface are quite low compared to the conditions during the summer season. In JJA the lower mean background albedo leads to higher solar radiation input to the surface, especially on the Iberian Peninsula and Iceland (figure 4.10a). Over Iceland the new albedo scheme replaced the old albedo mean of constant ice cover with more realistic lower albedo values during the summer season. In figure 4.10b the higher background albedo during summer caused by the seasonal variability of the albedo cycle directly translates into lower net surface solar radiation up to -30Wm^{-2}. In many regions the radiation effects of the new albedo mean and the seasonal varying albedo compared to the control run compensate each other.

4. 4. 2. 5 Surface temperature

The seasonal background albedo cycle has no effect on surface temperature during the winter season (not shown) as it caused no changes on the net surface solar radiation (compare section 4.4.2.4). Also the influence of the new albedo mean is negligible as snow cover is dominating the surface properties during DJF. But during the summer season, the higher solar radiation input to the surface due to the lower mean background albedo (EXP1-CONT) lead to higher temperatures up to +1.5K in eastern Europe during JJA (figure 4.11a). For the comparison of EXP2-EXP1 in figure 4.11b the lower solar radiation input to the land surface due to higher background albedo values in JJA causes lower surface temperatures up to -1.5K. Together, as for the net surface radiation the effects of the new albedo mean and the seasonal varying albedo on surface temperatures compensate each other in most regions.

4.11a. JJA, EXP1-CONT 4.11b. JJA, EXP2-EXP1

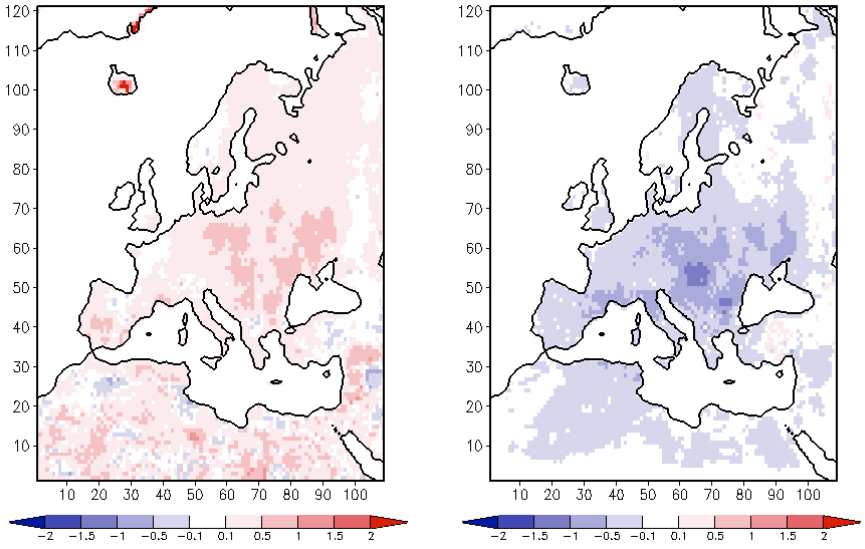

Figure 4.11: Differences of surface temperature [K] due to the new annual mean background albedo EXP1-CONT (4.11a) and due to temporal varying background surface albedo EXP2-EXP1 (4.11b) for JJA 1979-1993

4. 4. 2. 6 Precipitation

As for the net surface solar radiation and the surface temperatures, the seasonal background albedo cycle and the new albedo mean have almost no effect on precipitation during the winter season, either (not shown). During JJA stronger effects on precipitation occur (figure 4.12a and 4.12b). In many regions the precipitation changes do not show systematic patterns and probably result from the high sensitivity of the precipitation parameter to model experiments. Systematic differences seem to occur over the Alps and over South-West-Scandinavia with higher precipitation up to +30 mm/month in EXP1 compared to CONT and lower precipitation up to -20 mm/month in EXP2 compared to EXP1. But these absolute

differences are not significant compared to the high total amount of precipitation in both regions. They might indicate some smaller changes in the circulation patterns within the regional model domain, but which is much less pronounced than in the global model experiments.

4.12a. JJA, EXP1-CONT 4.12b. JJA, EXP2-EXP1

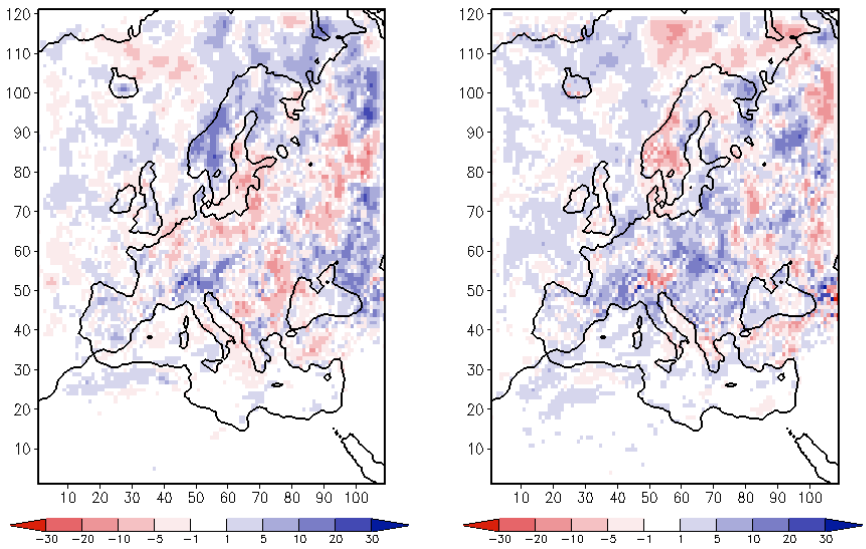

Figure 4.12: Differences of precipitation [mm/month] due to the new annual mean background albedo EXP1-CONT (4.12a) and due to temporal varying background surface albedo EXP2-EXP1 (4.12b) for JJA 1979-1993

4. 5 Comparison of the global and regional sensitivity studies

4. 5. 1 Temperature

In the following the results from the global and the regional sensitivity studies are compared against each other. For this purpose the results of the global climate model are prepared for the same region and time period as available for the regional model results. In figure 4.13 the seasonal differences of 2m-temperatures caused by the temporal varying background surface albedo (EXP2-EXP1) are displayed for the global and regional experiments over Europe. The global and regional studies show different results. Whereas in REMO during DJF no significant changes occur, in the global experiment the temperature decreases especially in the northeast of Europe up to -2K. For the summer season the global results show a slight increase in temperature up to +1K over central and eastern Europe. In contrast, in the regional simulation the temperature decreases in this region during JJA up to -1.5K. In the regional model, this is a clear local reaction of temperature on the seasonal background albedo variability with higher albedo during JJA and lower solar radiation input to the surface compared to the annual constant mean. In the global simulation, the local processes are superposed by the changed large-scale conditions. In figure 4.14 the differences of the mean annual cycles of 2m-temperatures between EXP2-EXP1, EXP2-CONT and EXP1-CONT are

compared for the global (dashed lines) and the regional simulations (solid lines) for selected sub-areas. Except for eastern Europe, in the other European regions, the global results show higher sensitivity to the changed albedo parameterization.

ECHAM: DJF, EXP2-EXP1 REMO: DJF, EXP2-EXP1

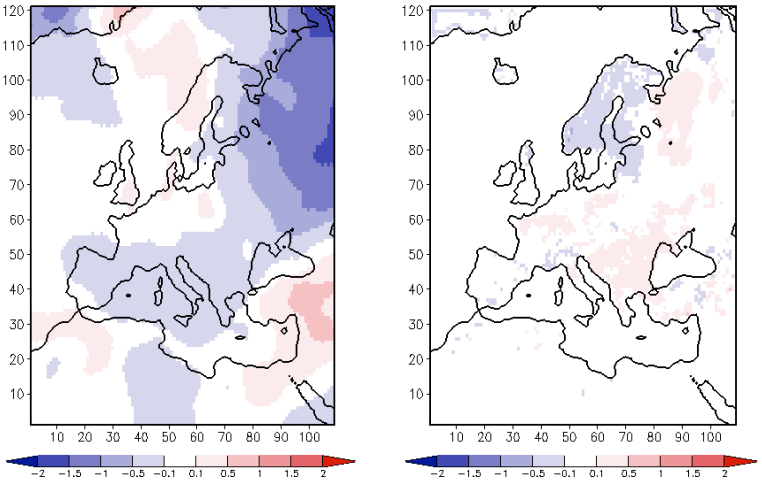

ECHAM: JJA, EXP2-EXP1 REMO: JJA, EXP2-EXP1

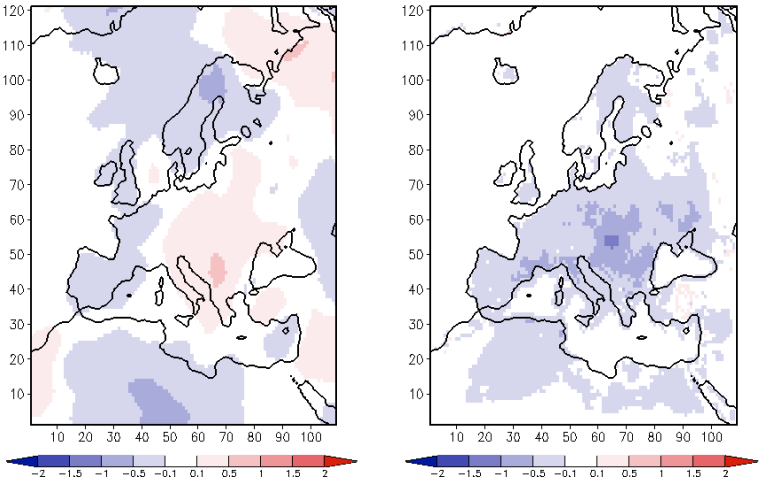

Figure 4.13: Seasonal differences of 2m-temperature [K] due to temporal varying background surface albedo (EXP2-EXP1) 1979-1993 in the global and regional experiments

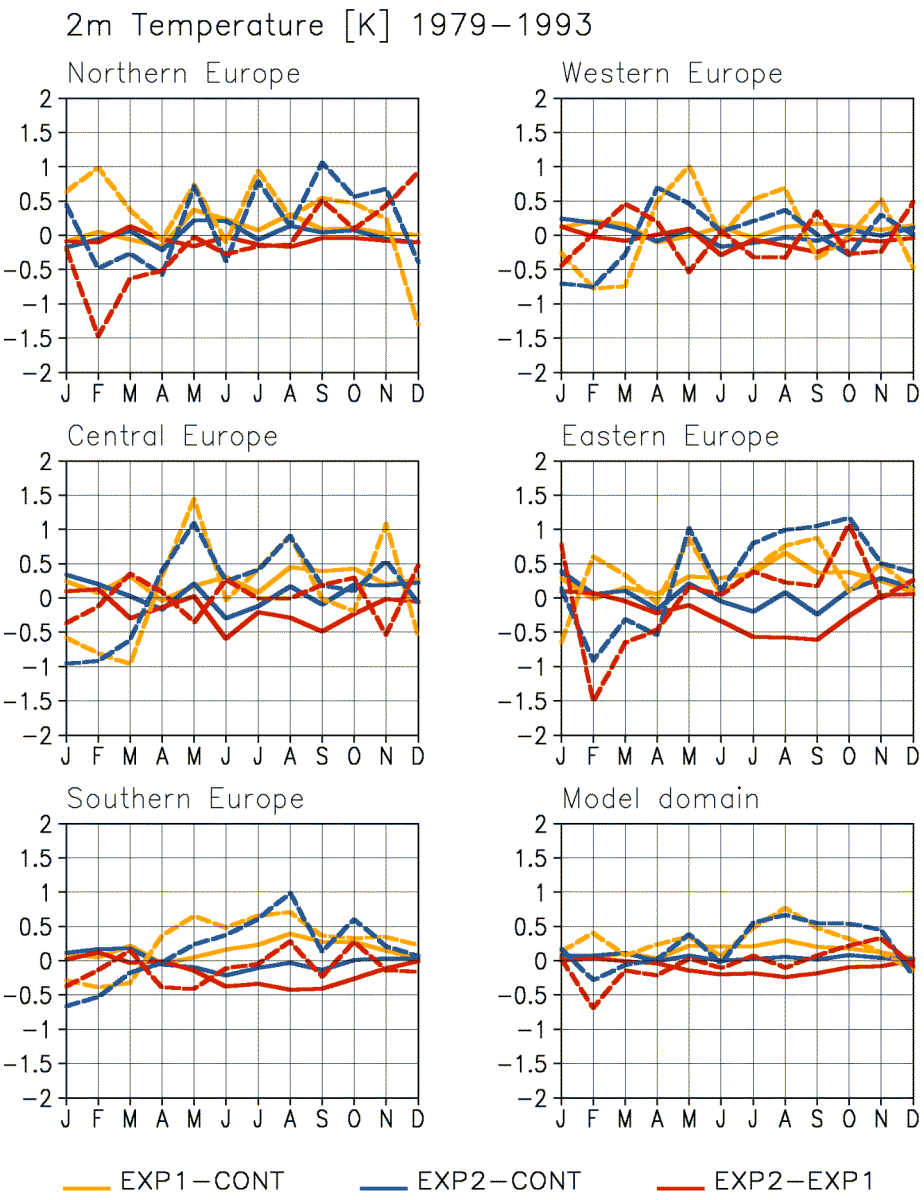

Figure 4.14: Annual cycles of 2m temperature differences [K] 1979-1993 between EXP1-CONT, EXP2-CONT and EXP2-EXP1 for the global simulations (dashed lines) and for the regional results (solid lines)

4. 5. 2 Precipitation

In figure 4.15 the seasonal differences of precipitation caused by the temporal varying background surface albedo (EXP2-EXP1) are presented for the global and regional experiments over Europe. Again, the global and regional studies show different results. Whereas in REMO during DJF no remarkable changes occur, in the global experiment the precipitation decreases in western and central Europe up to -30mm/month. This precipitation decrease is significant on the 95% level estimated by the one-sided t-test. The lower precipitation values result possibly from weakened westerlies caused by the changed pressure regime with lower NAO index as discussed in section 4.3.2.3. In contrast to the global simulation, where the large-scale conditions are changed by the new albedo parameterization, in the regional simulations the circulation patterns within the model domain are not

influenced. Here, the external forcing via the lateral boundaries of the regional model domain suppresses changes in the large-scale circulation that might occur without the external forcing. In JJA the global and regional patterns also look different. Whereas in the global study the summer precipitation slightly decreases up to -20mm/month over central and eastern Europe, in the regional simulation the precipitation slightly increases up to 20mm/month in this area except for the eastern Alpine region. Also for southern Scandinavia, the global and regional simulations show contrary results with increased values in ECHAM5 and decreased values in REMO. Together, due to the higher resolution of the regional simulations more horizontal details can be seen. In figure 4.16 the differences of the mean annual cycles of precipitation between EXP2-EXP1, EXP2-CONT and EXP1-CONT are presented for the global (dashed lines) and the regional simulations (solid lines). Here again, in all selected European regions, the global results show a slightly higher sensitivity to the changed albedo parameterization.

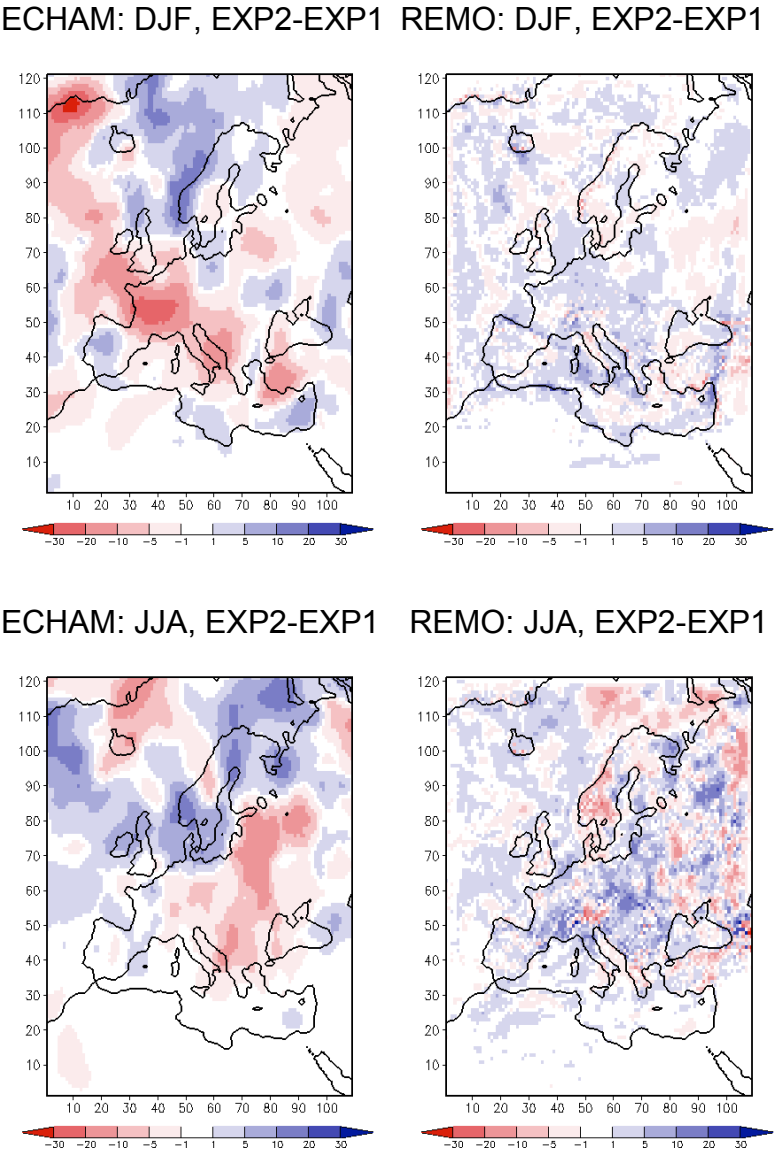

Figure 4.15: Seasonal differences of precipitation [mm/month] due to temporal varying background surface albedo (EXP2-EXP1) 1979-1993 in the global and regional experiments

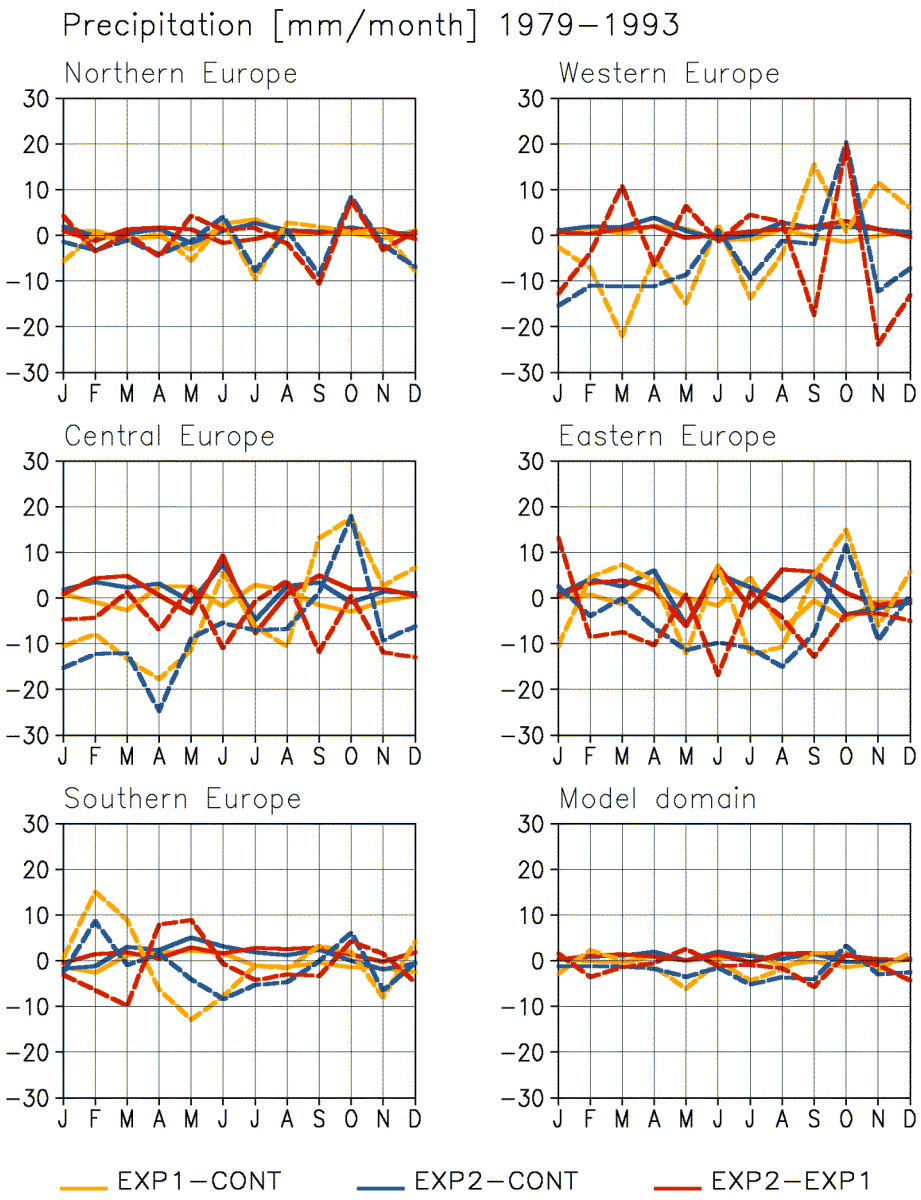

Figure 4.16: Annual cycles of precipitation differences [mm/month] 1979-1993 between EXP1-CONT, EXP2-CONT and EXP2-EXP1 for the global simulations (dashed lines) and for the regional results (solid lines)

From the comparison of the regional and global model simulation we conclude that studies on land use changes and their influence on the regional climate should be done on the global as well as on the regional scale. The consistent global simulation can be used to drive the regional simulation on the lateral boundaries to consider the influence of changed land surface properties on the large scale circulation patterns. The regional simulation then is able to resolve local effects of changed land surface properties which are often superposed by large-scale effects in the global simulations.

4. 5. 3 Comparison to observational data sets

Observational datasets are extracted from the Climate Research Unit analyses version 2.0 (CRU, MITCHELL et al., 2004, NEW et al. 2000) and the Global Precipitation Climatology Project version 2.0 (GPCP, HUFFMANN et al., 1997). The CRU dataset provides global 2m-temperature and precipitation fields as time series of monthly means for the time period 1901–2000 at 0.5 degree horizontal resolution for the land surface area. The temperature and precipitation fields are based on gauge measurements. The GPCP precipitation dataset is globally gridded data at 2.5 degree resolution based on gauge measurements over land and satellite data over sea. The GPCP precipitation values are corrected for undercatch of gauge stations. Time series of monthly means are available for 1979–2000. By using area averages we expect to reduce uncertainties in the observations that are caused by location, exposure and altitude of the stations.

In figure 4.17 the simulated mean annual cycles of 2m-temperatures are presented as differences to CRU observations (zeroline) area-averaged over the selected European regions for the regional (solid lines) and the global (dashed lines) simulations. In the regional simulations, except for northern Europe, in all regions the temperatures during summer and autumn are overestimated up to +2.5K in southern Europe. In northern Europe the winter temperatures are overestimated up to +2K. The seasonal variability of background surface albedo compensates the slightly worsened overestimation of summer temperatures caused by the lower mean background albedo of experiment 1 compared to the control run. In the global simulations the summer and autumn temperatures are in better agreement with the observed values. In contrast to the regional results, the winter and spring temperatures in northern Europe are underestimated. Together, the temperature differences to the observations are larger than the differences between the three model simulations.

In figure 4.18 the mean annual cycles of the simulated precipitation are presented in comparison to observational data from CRU and GPCP. The regional results are in better agreement with the observations than the global results. Here, the higher resolution of the regional model simulation shows its advantage in resolving orographical effects on precipitation. Especially in western, central and eastern Europe the regional simulated precipitation cycles fit very well to the observations. In northern Europe the model simulations overestimate precipitation from October to May, especially in comparison to the CRU data. In southern Europe the simulated precipitation is underestimated during late summer and autumn and in the global simulation already during spring. Between the three regional model experiments almost no differences exist. In contrast, the global simulation studies show larger differences to each other, but together the differences to the observations are larger than the differences between the model simulations. Thus, the sensitivity of the simulated temperature and precipitation to the changed albedo parameterization lies within the uncertainty range of the simulated model results compared to the observation data set used in this study. So, it is not possible to say if the new albedo parameterization improves the model simulations with regard to temperature and precipitation.

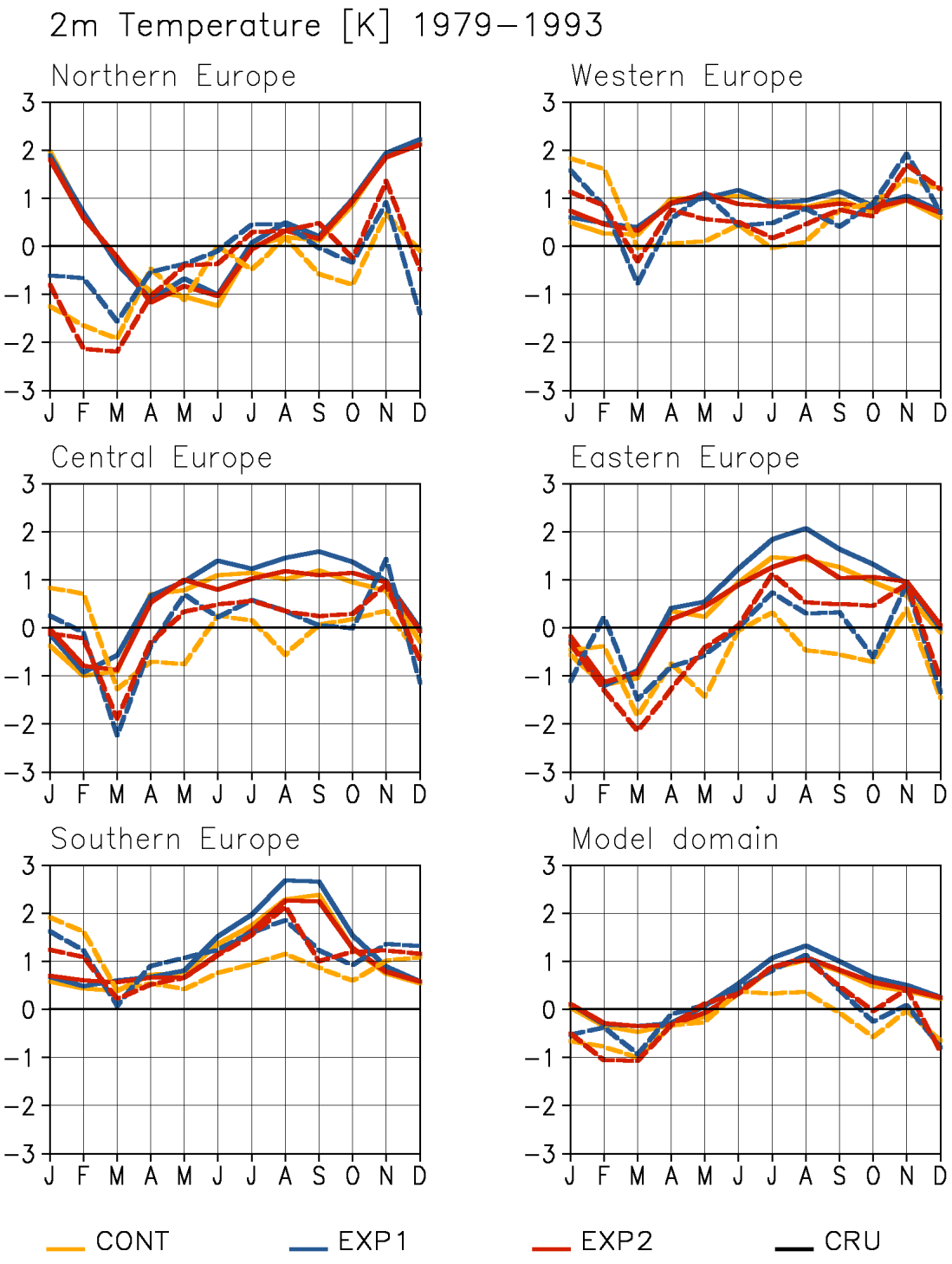

Figure 4.17: Annual cycles of 2m temperature differences [K] 1979-1993 of the three model simulations compared to CRU observations (zeroline) for the global (dashed lines) and the regional (solid lines) sensitivity studies

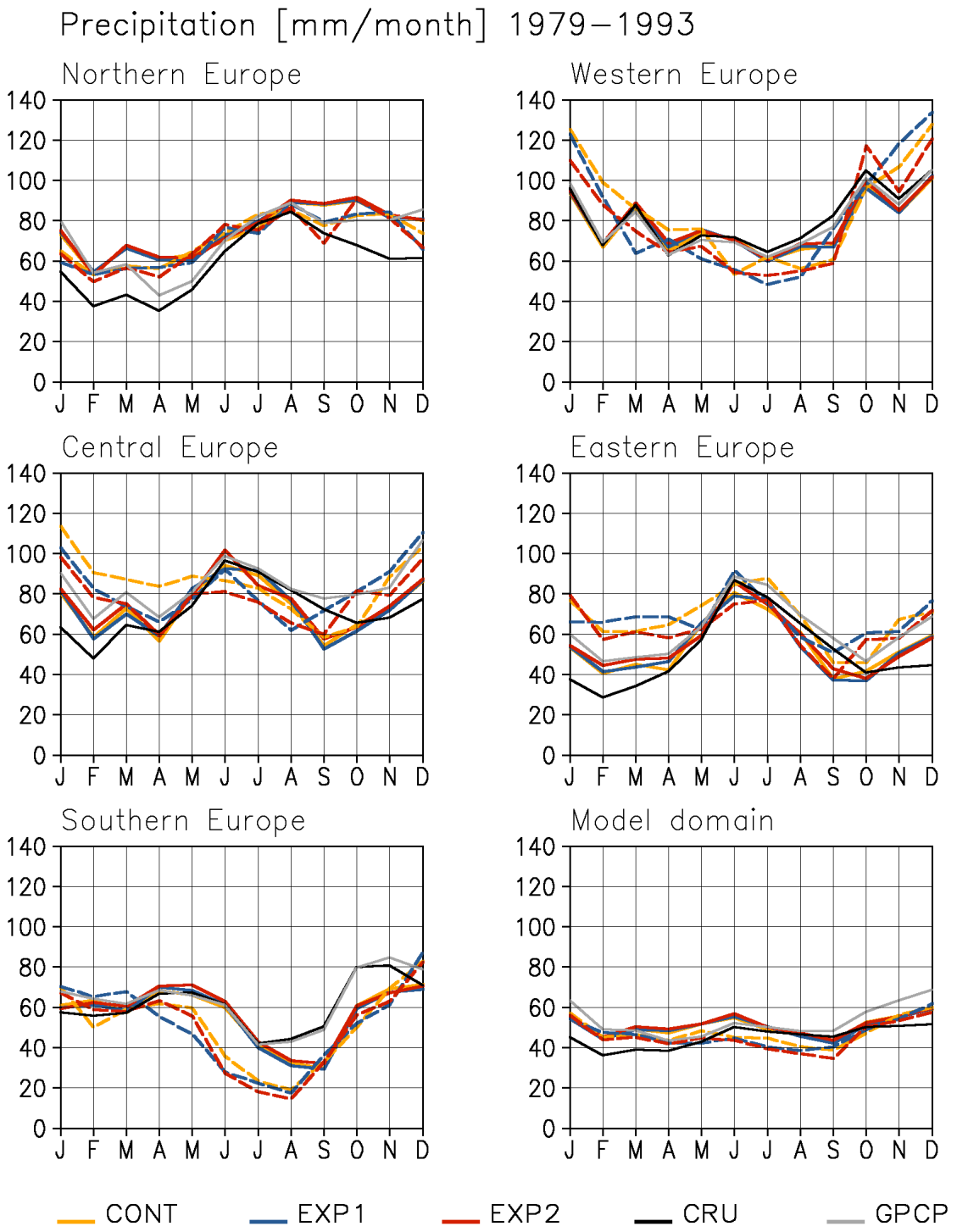

Figure 4.18: Annual precipitation cycles [mm/month] 1979-1993 of the three simulations for the global (dashed lines) and the regional (solid lines) sensitivity studies and of observations from CRU and GPCP

4. 6 Conclusions and outlook

An advanced parameterization of the snow-free land surface albedo describing the monthly variation of surface albedo as a function of vegetation phenology derived from MODIS data was integrated into the land surface schemes of the global climate model ECHAM5 and the regional climate model REMO. Three model simulations were performed, respectively, to study the sensitivity of the simulated climate to the seasonal background albedo variability. The analysis of the simulation results demonstrates the influence of the new albedo parameterization on the model simulations. The effect of the new mean background albedo superposes partly the effect of the seasonal albedo variability, which became evident while evaluating both effects separately. Strong effects occur over Europe, so it was an appropriate model domain for the regional simulation studies. In this region the regional and the global model simulations respond differently to the new albedo parameterization. In contrast to the global simulation, where the large-scale atmospheric conditions are changed by the new albedo parameterization, in the regional simulations the circulation patterns within the model domain are not influenced. Here, the external forcing via the lateral boundaries of the regional model domain suppresses changes in the large-scale circulation that might occur without the external forcing. In the regional model simulations mainly local effects occur during the summer season, when the vertical energy exchange at the land surface is enhanced compared to the winter season with snow cover dominating the surface properties. In the global ECHAM5 simulations, the moderate albedo forcing during DJF causes strong changes in the analysed near-surface climate parameters. The effects on the simulated climate are not restricted to regions where land surface albedo is changed, but also occur in remote regions through atmospheric teleconnections. These remote climate impacts of the changed land surface albedo can only be explained by the modification of the planetary-scale atmospheric circulation. We did some first attempts to reveal changes in the atmospheric circulation patterns, but it would be very interesting to analyse those atmospheric teleconnections with more detail in further studies, especially with regard to land cover change studies.

The comparison between the regional and global studies for the selected European regions yielded that the global results show higher sensitivity of the annual temperature and precipitation cycles to the changed albedo parameterization. In the global simulations the summer and autumn temperatures are in better agreement to the observations compared to the regional simulation results. For both the regional and the global study the temperature differences to the observations are larger than the differences between the three model simulations. For precipitation, the regional results are in better agreement with the observations than the global results. Here, the higher resolution of the regional model simulation shows its advantage resolving more horizontal details considering orographical effects on precipitation.

It is not possible to say if there is an improvement of the climate model simulations with regard to near surface temperature and precipitation compared to the observations on the continental scale investigated in this study. It could be investigated in further studies if the simulated model parameters show higher sensitivity to the changed land surface albedo scheme on smaller scales. Nevertheless, we can recommend the implementation of the new parameterization scheme for the background surface albedo in climate models. The consideration of the seasonal surface albedo variations in climate simulations is more realistic for the representation of land surface processes and the new albedo scheme only marginally extends the computation time of the climate models. Moreover, the dynamic formulation of the background surface albedo as a function of the leaf area index is a first step on the way to

a dynamic vegetation phenology scheme. The extension of the introduced albedo scheme to spatial vegetation changes will also enable advanced impact studies of land use change, deforestation and desertification.

For the regional model REMO Rechid & Jacob (2006) investigated the influence of vegetation phenology on the simulated climate in Europe. Compared to the results of this study, the sensitivity of the regional climate to the monthly varying leaf area index was larger than to the new albedo parameterization, especially for precipitation. At this time a dynamic vegetation phenology scheme for the leaf area index as a function of the model's climate is in preparation to represent the inter-annual variability of vegetation phenology and its feedback to the simulated climate. The new albedo parameterization introduced in this study will also be applied to this phenology scheme.

Chapter 5

Dynamic interactions between plant phenology and climate variability simulated by the regional climate model REMO over Europe[4]

Abstract

To study the dynamic interactions between plant phenology and climate variability over Europe, the vegetation phenology scheme PHENO was developed and fully coupled to the regional climate model REMO. PHENO relates the species-averaged parameter LAI to simulated climate parameters of near surface heat and moisture conditions. The simulation results of PHENO in offline mode show the interannual variability and temporal trends in vegetation phenology caused by climate variability. The timing of leaf expansion in spring is varying from year to year in dependence on the surface temperatures. The leaf senescence in fall is varying in dependence on surface temperatures and surface moisture contents. Especially in warm and dry years the LAI decreases earlier in late summer and autumn due to water limiting conditions. The observed long-term trends in plant phenology are captured by the PHENO simulations. The onset of spring phenology becomes 5.9 days earlier and the growing season becomes 4.1 day longer during the simulated period from 1958 to 2003. Substantial changes in vegetation phenology appear under future climate warming conditions, which were simulated by a regional climate projection from 2071 to 2100. In northern, eastern and central Europe, the growing season is lengthened by up to 2 months due to higher temperatures. In western Europe, the length of the vegetation period is no longer limited by low temperatures. In southern Europe, the water limitation of plant growth increases during summer and autumn due to enhanced hot and dry weather conditions. To account for the interannual variability and long-term trends in vegetation phenology in the regional climate simulation, PHENO was run fully coupled to the REMO model for the same time period from 1958 to 2003. The results of the online simulation show the feedback of the interannual variability of plant phenology on the simulated climate and the vegetation itself. The positive feedback on drought conditions during warm and dry summer and autumn seasons intensifies the effect of water limitation in the coupled model simulation, which leads to another decrease in LAI. Thus, the interannual variability of the LAI is enhanced by the interaction between plant phenology and the simulated climate. The use of the PHENO scheme leads to an improved representation of vegetation in REMO, that may become especially important in climate change simulations.

---

[4] *Rechid D, Jacob D (2008) Dynamic interactions between plant phenology and climate variability simulated by the regional climate model REMO over Europe. Submitted to Climate Dynamics.*

5. 1 Introduction

Vegetation cover determines the earth surface characteristics and strongly influences the vertical exchange of water, energy and momentum between biosphere and atmosphere at the land surface. The interactions between terrestrial ecosystems and atmosphere impact weather and climate at all spatial and temporal scales (for an overview see the review of Pielke et al. 1998). Over the last decades, lots of climate modelling studies have shown the sensitivity of the simulated climate to land surface conditions, and point out the need for their accurate representation (e.g. Shukla & Mintz 1982, Mintz 1984, Sud et al. 1988, Sud et al. 1990, Bonan et al. 1992, Collins & Avissar 1994, Chase et al. 1996). On the other hand, spatial and temporal variability of vegetation is determined by the climate, e.g. through temperature and water availability (e.g. Woodward 1987, Woodward & McKee 1991, Neilson & Marks 1994, Chapin & Starfield 1997). Vegetation variability again affects climate (e.g. Avissar & Liu 1996, Lu & Shuttleworth 2002, Lawrence & Slingo 2004a, 2004b, Koster & Suarez 2004). To include those complex biosphere-atmosphere feedbacks into climate models a two-way coupling of vegetation and climate is needed, especially for future climate projections. Levis et al. (1999), e.g., use a fully coupled climate-vegetation model to show potential vegetation feedbacks to climate change.

Strong interactions between vegetation and climate can be observed in plant phenology. Phenology comprises the study of "life cycle phases or activities of plants and animals in their temporal occurrence throughout the year" (Lieth 1974) in relation to climate (Schnelle 1955). With phenology being an integral bio-indicator for climate change the interest in plant phenological observations substantially increased, while recognising its value in the area of climate change research (Menzel 2002). Phenological networks were established, extended and standardised. They collected considerable data archives, such as the German Weatherservice (Bruns 2007) and the International Phenological Gardens (IPG) in Europe (Chmielewski 1996). Many studies analyse those phenological observations to determine spatial variations, interannual variability and temporal trends in plant phenology in relation to climate data (Ahas 1999, Menzel & Fabian 1999, Jaagus & Ahas 2000, Menzel 2000, Rötzer et al. 2000, Chmielewski & Rötzer 2001, Defila & Clot 2001, Menzel et al. 2001, Ahas et al. 2002, Chmielewski & Rötzer 2002, Scheifinger et al. 2002, Sparks & Menzel 2002, Menzel 2003, Menzel et al. 2003, Studer et al. 2005, Menzel et al. 2006). For detecting regional trends of phenological phases and finding their relation to climate changes, Rötzer & Chmielewski (2001) computed phenological maps of Europe. They showed long-term means, trends and annual timings of phenological phases. In high and mid-latitudes, phenological phases were found to depend strongly on temperature conditions. As a consequence of climate change, many studies showed evidence of a shift in plant development towards an earlier onset of spring and a lengthening of the growing season in Europe (Menzel 2000, Defila & Clot 2001, Menzel et al. 2001, Ahas et al. 2002, Menzel et al. 2003, Menzel et al. 2006); and in Northern America (Beaubien & Freeland 2000, Schwartz & Reiter 2000, Cayan et al. 2001). Menzel et al. (2006) found an average advance of spring phases of 2.5 days per decade for 21 European countries from 1971-2000. Changes in autumn are not so easily to detect, as the factors causing changes in autumn phases are not clear (Menzel et al. 2001, Sparks & Menzel 2002) and the signal is ambiguous (Menzel et al. 2006). Spring and summer phenological phases, such as leaf unfolding and flowering, strongly correlate with temperature of the preceding months (e. g. Chmielewski & Rötzer 2001, Ahas et al. 2002, Menzel 2003,). The spring phenological anomalies also correlate with the Northern Atlantic Oscillation Index (NAO) of January to March (e. g. Scheifinger et al. 2002, Menzel 2003).

Whereas ground observations of plant phenology are often site- and/or species-specific, satellite data can provide spatially and species-averaged information on the start and end of the growing season, as the Normalised difference vegetation index (NDVI) or derived leaf area index (LAI) data (Myneni et al. 1997, Tucker et al. 2001, Zhou et al. 2001, Schwartz et al. 2002, Zhang 2003). Chen et al. (2000) analysed the relation between ground phenology observations and remote sensing derived measures of greeness to determine the growing season of land vegetation on the regional scale.

During the last decades, consistently processed satellite-derived NDVI and LAI data became available. 'They provide spatially averaged information of land surface vegetation on a regional and a global scale for the consideration of current plant phenology variations within climate modelling. While using satellite-derived LAI data in the land surface schemes of climate models, Buermann et al. (2001) studied the impact of interannual variability of phenology on climate. Bonan et al. (2002) studied the impact of spatial variability of phenology on climate simulations. Lawrence and Slingo (2004a, 2004b) prescribed an annual vegetation cycle on the basis of satellite-estimated LAI to a global climate simulation. They found a reduction in surface temperatures in extratropical regions during both the summer and winter season. Where the magnitude of LAI values is enhanced, precipitation increases. In the study of Lu & Shuttleworth (2002), vegetation phenology was assimilated into the climate version of a regional atmospheric modelling system using estimated LAI values. They concluded that the effect of enhanced heterogeneity dominates over the effect of an reduced magnitude in LAI fields.

The sensitivity of the simulated climate by the regional climate model REMO (REgional MOdel, Jacob et al. 1997, Jacob et al. 2001) to seasonal vegetation changes was investigated in the study of Rechid & Jacob (2006). The results showed a significant influence of monthly varying vegetation properties on the simulated European climate. The vertical surface fluxes, temperature and precipitation are strongly affected. The near-surface climate becomes cooler and wetter during the growing season, especially in eastern Europe and regions with predominating continental climate. But so far, the seasonal variability of vegetation was prescribed as a mean annual vegetation cycle, which does not account for interannual variability and temporal trends of plant phenology caused by climate variability. To consider the interannual variability of vegetation and its feedback on the simulated climate, a dynamic phenology scheme was developed and fully coupled to the regional climate model REMO, which will be introduced in this study.

Phenology modelling approaches vary from statistical analyses (e. g. Galan et al. 1998, Dose & Menzel 2006) to more mechanistic models with plant physiologically based approaches (e. g. Hänningen 1990, Chuine et al. 2003, Schaber & Badeck 2003). Several phenological bud burst models of forest tree species have been published (Hänninen 1994, Kramer 1994, 1995, Rötzer et al. 2004), which are, however, limited to single species and/or geographic areas. For trees, the onset of greeness has been successfully modelled while using a simple cumulative thermal summation (e. g. Murray et al. 1989, Hari & Häkkinen 1991, Hänningen et al. 1993). White et al. (1997) developed predictive phenology models on the continental scale. Their their application revealed extensive interannual variability in the timing of the onset and the offset of greening in the United States. To quantify the effects of climate change on forest growth, different phenological models for the growth of boreal, temperate and Mediterranean forest ecosystems were developed and coupled to a forest model by Kramer et al. (2000). Chmielewski et al. (2005) investigated the possible impacts of future climate change on natural vegetation in Saxony using simple phenological models in relation to regional climate

scenarios, but still only driven by temperature. Relatively little research has been performed on the relation between water availability and phenology (Loustau et al. 1992, 1996, Kramer et al. 2000). But climate changes can lead to more frequent droughts in summer with decreasing soil water content, which limits the growth conditions for plants. Most climate scenarios for the mid-latitudes predict decreasing precipitation in southern and central Europe during summer (IPCC 2007, Jacob et al. 2007). The extreme European summer heatwave, as experienced in 2003, demonstrated the impact of extremely limited soil moisture on vegetation and climate (Fischer et al. 2007). Seneviratne et al. (2006) emphasise the importance of soil-moisture-climate feedbacks in influencing summer climate variability in Europe. Soil moisture strongly links vegetation phenology and climate variability, which should be accounted for in climate modelling.

In most dynamic global vegetation models (DGVMs) phenology is already included (Cramer et al. 2001), but often run uncoupled from general circulation models (GCMs). During recent years, work focused on executing DGVMs coupled to GCMs (Foley 1998, Levis 1999, Krinner 2005); Foley et al. (2000) gave a review about coupling techniques. The Jena Scheme for Biosphere-Atmosphere Coupling in Hamburg (JSBACH) developed at MPI-BGC in Jena and MPI-M in Hamburg is a dynamic land-vegetation model that incorporates model components of BETHY (Knorr 2000) and LPJ (Sitch et al. 2003). It also includes a prognostic phenology scheme for plant functional types, which are used in this model framework to classify vegetation. It was coupled to the general atmospheric circulation model ECHAM5 to simulate biogeophysical and biogeochemical interactions between vegetation and atmosphere at the global scale. But it is still not common to run DGVM-GCMs routinely, especially because of the high demand on computational efforts. Most studies are done on coarse horizontal resolutions. Another problem arises if there are large differences between the land surface schemes of the GCM and the DGVM. To overcome such inconsistencies the approach of Bonan et al. (2003) is noticeable which added dynamic vegetation processes from a DGVM directly to the land component of a climate model.

In the current study, we present a dynamic vegetation phenology scheme, that was developed for the land surface scheme of the regional climate model REMO. We refine our scheme to the physical effects of the interaction between the vegetation phenological cycle and the simulated climate. No complex vegetation model is needed to drive the phenology scheme, as no biogeochemical cycles are considered. It relates basic phenological phases, such as the onset and end of the vegetation growing season, directly to the simulated climate. The near surface climate conditions drive the phenology scheme on a daily basis. Hereby, we also consider the effect of water availability on vegetation phenology. The temporal vegetation variability caused by the climate variability influences the physical properties of the land surface, which feeds back to the climate. Our intention is to present the developed dynamic phenology scheme PHENO and to investigate the interactions between climate variability and vegetation phenology.

The paper is organised as follows: In section 5.2 the parameterisation of vegetation in the regional climate model REMO is described. In section 5.3 we present the dynamic phenology scheme which was developed for REMO. To investigate the relations between the simulated climate and vegetation phenology the results of the offline phenology scheme driven by simulated climate parameters are examined in section 5.4. In section 5.5 the feedback of vegetation phenology on climate is analysed. In section 5.6 we give conclusions and a short outlook.

5. 2 Vegetation parameterisation in REMO

In the regional climate model REMO (REgional MOdel, Jacob et al. 1997, Jacob et al. 2001) land surface processes are influenced by physiological vegetation properties. The vegetation cover is represented by parameter values for the leaf area index (LAI, ratio of one-sided leaf area to ground area), fraction of green vegetation cover, background surface albedo (albedo over snow-free land surfaces), surface roughness length due to vegetation, fractional forest cover (used as a constant stem index) and water holding capacity (depending on plant rooting depths). The horizontal vegetation distribution is based on a global dataset of major ecosystem types (Global Land Cover Characteristics Database; GLCCD) according to a classification list of Olson (1994a, 1994b). The Olson ecosystem types were derived from Advanced Very High Resolution Radiometer AVHRR data at 1 km resolution, which were supplied by the International Geosphere-Biosphere Program (Eidenshink & Faundeen 1994) and constructed by the U.S. Geological Survey (1997, 2002). For each land cover type the parameter values for the vegetation properties are allocated. This information is aggregated to the model grid scale averaging the vegetation parameters of all land cover types, which are located in one model grid cell.

The seasonal variability of vegetation is represented by monthly varying fields of LAI and fractional green vegetation cover (Rechid & Jacob 2006). These temporal varying vegetation fields are taken from the global dataset of land surface parameters LSP2 designed by Hagemann (2002). The seasonal variation of the LAI between minimum and maximum values is estimated by a global data field of the monthly growth factor, which is defined by climatologies of 2m temperature and FPAR (Hagemann 2002). This dataset is prescribed to the climate model simulations as a mean annual vegetation cycle without interannual variability. In the study of Rechid et al. (2008a), an advanced parameterisation of the snow-free land surface albedo was developed, which describes the seasonal variation of surface albedo as a function of monthly varying LAI on the basis of data products derived from the Moderate-Resolution Imaging Spectroradiometer (MODIS). The seasonal variation of land surface albedo was integrated into the land surface scheme of REMO (Rechid et al. 2008b) and provides a good basis for the treatment of land surface albedo within a dynamic phenology scheme.

The vegetation parameter values are prescribed to the model simulations as lower boundary conditions and influence the vertical exchange of water and energy at the land surface between atmosphere and the underlying soil. The surface albedo determines the short-wave radiation budget at the earth surface. The vegetation density represented by the LAI and green vegetation cover controls evaporation via interception of water on the skin of the canopy and transpiration by leaf stomatal conductance (for details see Rechid & Jacob 2006). Evapotranspiration determines the partitioning of the vertical turbulent heat fluxes into latent and sensible heat. Latent and sensible heat fluxes are the main mechanisms to return energy from the surface into the atmosphere and influence convective processes and the boundary layer structure. These surface processes controlled by vegetation properties impact the near surface atmospheric conditions such as the near surface temperature, the near surface humidity and the low level cloudiness. They provide the appropriate feedback mechanisms to other physical processes in the atmosphere. Land surface processes also influence conditions in the soil like soil temperature and soil moisture content. Vice versa, conditions in the atmosphere and the soil determine the plant growing. But so far, the changed conditions in atmosphere and soil do not feedback to the vegetation.

5. 3 Dynamic phenology scheme

The dynamic phenology scheme PHENO was developed to consider the interannual variability of vegetation phenology due to climate variability and its feedback to the simulated climate. It relates basic phenological phases, such as the start and the end of the vegetation growing season, directly to the simulated climate. The model is designed and tested especially for Europe, the standard model domain of the regional climate model REMO. The annual vegetation cycle with minimum vegetation cover during the dormancy season and maximum vegetation cover during the growing season is described as a function of near surface heat and moisture conditions simulated by the regional climate model. Running 10-day means of surface temperature, soil wetness and precipitation are given to the phenology model PHENO once a day, which, in turn, computes daily values of leaf area index LAI, fractional green vegetation cover and background land surface albedo. These values are returned to the climate model once a day and can give a feedback to the near surface climate conditions.

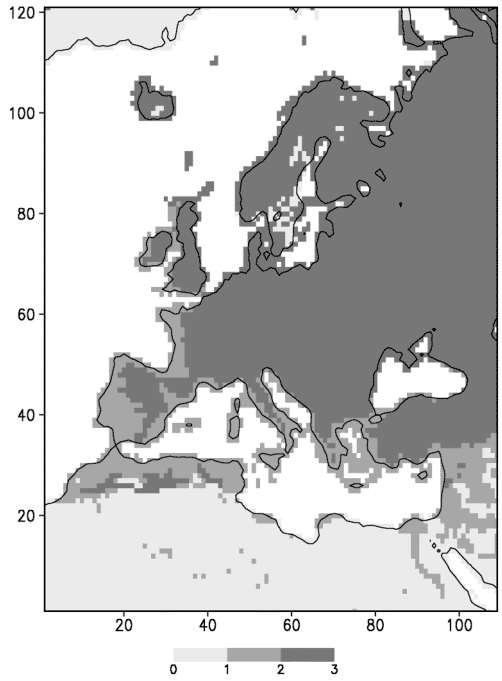

Figure 5.1: Distribution of phenology types over the REMO model domain (1958-1987). 0: 100% water, 1: evergreen and bare soil, 2: water-limited, 3: temperature-limited

The spatial distribution of minimum and maximum LAI values is taken from the LSP2 dataset (Hagemann 2002). The seasonal variation between the minimum and maximum LAI is computed by the phenology model PHENO. Main types of plant phenology are defined and arranged within the following classes: 1. evergreen vegetation and bare soil, 2. water-limited vegetation and 3. temperature-limited vegetation. Evergreen vegetation and bare soil are located, where the minimum and maximum LAI do not differ. To identify the locations of temperature-limited and water-limited vegetation, the surface temperature simulated by REMO from 1958-1983 was analysed. The mean daily surface temperature averaged over the 30 years was calculated. In regions where the surface temperature is only at 10 days or less below 278.15 K, vegetation is not limited by temperature but only by water availability; and

belongs to class 2 of phenology types within the PHENO scheme. Where the surface temperature is below 278.15 K at more than 10 days, vegetation is mainly limited by temperature, but can also be limited by water availability; and belongs to class 3. The resulting horizontal distribution of the phenology types in the REMO model domain used in this study is presented in figure 5.1. In most parts of Europe, temperature is the dominant limitation factor of plant growth. Only in some parts of southern Europe and in small parts along the western coasts, the plant growth is not limited by temperature but only by water availability. During a model simulation, the 30-year climatology of the daily surface temperature is updated at the end of each simulation year, so that it represents always the climatological values of the past 30 model years. According to this, the distribution of the phenology types are updated at the end of each simulation year. This means, that a spatial shift of vegetation phenology types is possible within the PHENO scheme.

To quantify the limitation of plant growth by temperature and water, growth factors are computed. The temperature-limited growth factor gf_T is calculated after Dickinson (1993):

$$gf_T = \begin{cases} 0 & T < T_{\min} \\ 1 - ((T_{opt} - T)/(T_{opt} - T_{\min}))^2 & T_{\min} \le T < T_{opt} \\ 1 & T \ge T_{opt} \end{cases} \qquad (5.1)$$

T_{min} is 278.15 K, the minimum temperature limit at which the plant growth starts. T_{opt} is 288.15 K, the optimum temperature for plant growth. T is the running 10-day mean of the surface temperature. In REMO, the simulated surface temperature is the temperature of the most upper soil layer at 3.25 cm below the earth surface. As displayed in figure 5.2a, the daily mean of the simulated surface temperature area-averaged over Germany from 1958 to 1962 shows strong fluctuations. To avoid unrealistic short-term fluctuations of the LAI, the running 10-day mean of the surface temperature is chosen (figure 5.2b) for the calculation of gf_T.

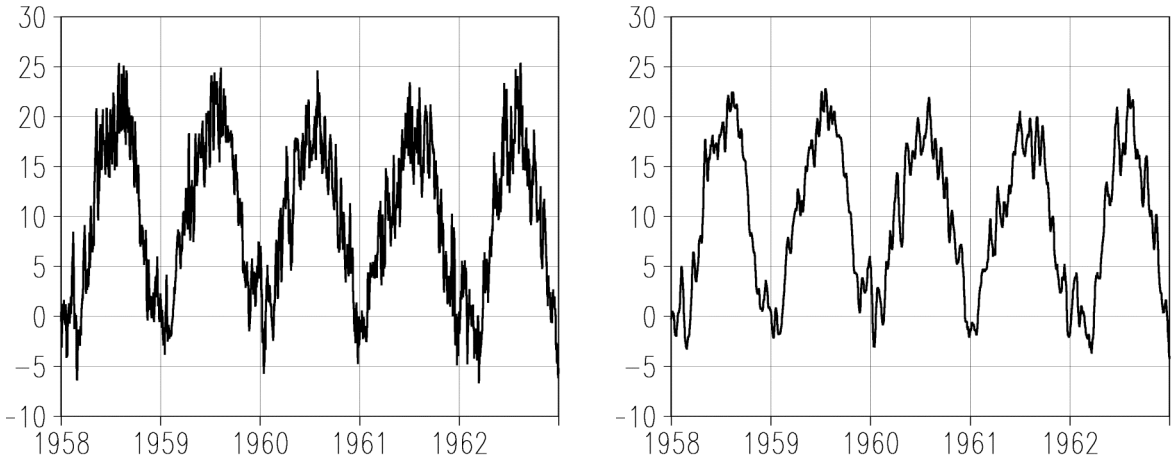

Figure 5.2: Simulated surface temperature by REMO-50km area-averaged over Germany 1958-1962: Daily means (left pannel), Running 10-day means (right pannel)

The water-limited growth factor gf_W depends on the soil wetness and the precipitation, it is calculated after equation (5.2):

$$gf_W = \begin{cases} 0 & W_{soil} \le W_{pwp} \wedge P < P_{crit} \\ gf_{W_{-1}} & W_{soil} \le W_{pwp} \wedge P \ge P_{crit} \\ (W_{soil} - W_{pwp})/(W_{crit} - W_{pwp}) & W_{pwp} < W_{soil} < W_{crit} \\ 1 & W_{soil} \ge W_{crit} \end{cases} \qquad (5.2)$$

W_{soil} is the running 10-day mean of the soil wetness. The simulated soil wetness is the soil water amount in mm per 1 m soil column. P is the running 10-day mean of the total amount of precipitation. P_{crit} is set to 0.1 mm per day. W_{crit} is a critical value of soil wetness, below which the plant growth is limited by water stress. It is set to 50 % of the field capacity of the soil. The field capacity of soil is the maximum amount of water, that can be hold by the soil against the force of gravity. In REMO, the applied dataset of the soil field capacity accounts for soil texture types and plant rooting depths (Hagemann et al 1999). W_{pwp} is the permanent wilting point of plants. Its value is also taken from the REMO model with 35 % of the soil field capacity. If the soil wetness is lower than W_{pwp} and the precipitation is lower than P_{crit}, the water limiting growth factor is zero and no plant growth happens. If the soil wetness is lower than W_{pwp} and precipitation is at least 0.1mm per day, gf_W is the same value as the day before ($gf_{W_{-1}}$). If the soil wetness is between W_{pwp} and W_{crit}, water stress is limiting the plant growth. If the soil wetness is above the critical values W_{crit}, plant growth is not limited by water and gf_W is 1. The total growth factor gf is the minimum value of gf_T and gf_W:

$$gf = \min(gf_T, gf_W) \qquad (5.3)$$

The vegetation density represented by the leaf area index is varying between the minimum and maximum LAI as a function of the growth factor:

$$LAI = LAI_{\min} + gf \cdot (LAI_{\max} - LAI_{\min}) \qquad (5.4)$$

A maximum growth rate of 10 % per day is assumed. There are still short-term fluctuations in the 10-day means of surface temperature (figure 5.2b) and soil wetness (not shown) and thus in the growth factor. To avoid unrealistic fluctuations of the LAI, different periods of growth (gp) are defined. During the dormancy period (gp=0), the LAI is at its minimum. During the vegetation period, a growth phase (gp=1) with a monotonic increasing LAI, and a degeneration phase (gp=2) with a monotonic decreasing LAI are distinguished. The LAI of the actual day (t) is compared to the LAI of the day before (t-1), respectively:

$$LAI(t) = \begin{cases} LAI_{\min} & gp = 0 \\ \max(LAI(t-1), LAI_{\min} + gf\,(LAI_{\max} - LAI_{\min})) & gp = 1 \\ \min(LAI(t-1), LAI_{\min} + gf\,(LAI_{\max} - LAI_{\min})) & gp = 2 \end{cases} \qquad (5.5)$$

In regions with temperature-limited vegetation phenology, the growth phase starts, if on 5 consecutive days the surface temperature T is higher than 5°C. The degeneration phase starts, if the total growth factor gf decreases on 5 consecutive days. As the total growth factor depends on heat and moisture conditions, the plant degeneration can be caused by temperature and/or water limitation. To avoid plant growth during the dormancy season, a 30-year mean climatology of the daily leaf area index LAI_{clim} is analysed . LAI_{clim} is computed from the simulated 30-year climatologies of the daily surface temperature T_{clim}, the daily soil wetness W_{clim} and the daily precipitation P_{clim}. The day of the year, when LAI_{clim} starts to increase, is called day_{start}. The day of the year, when the vegetation period is terminated, is called day_{end}. These numbers contain information about the climatological mean dates of the beginning and end of the vegetation period. The time period, in which the growing season of the actual year can start, is limited to day_{start} +/- 30 days. The time period, in which the growing season of the actual year ends, is defined by day_{end} +/- 30 days. In regions with temperature-limited phenology types, the analysis of the surface temperature climatology T_{clim} also gives day_{max}, the day of the year with the maximum temperature. From this day forth, the plant growth phase can change into the plant degeneration phase. The first value of LAI_{clim} also gives the initialisation value for the LAI at the beginning of the simulation.

During the model simulation with the dynamic phenology scheme PHENO, LAI_{clim} is updated with the actual LAI of each day, so that at the end of each year, LAI_{clim} always presents the climatological values of the past 30 years. The 30-year climatology of the daily surface temperature T_{clim} is also updated once a day with the actual surface temperature simulated by REMO. At the end of each year, the completely updated climatologies of LAI_{clim} and the surface temperature T_{clim} are used to derive the climatological values for day_{start}, day_{max} and day_{end} for the next simulation year and also the updated spatial distribution of the phenology types. This means, that long-term trends of plant phenology and the spatial shift of phenology types can be considered by the PHENO scheme.

In regions, where only water is the limiting factor, the occurrence and the length of the vegetation period depend on precipitation and the water storage in the soil. There can be several local minima and maxima of the plant growth during the year. The 30-year climatology of LAI_{clim} is used n these regions to analyse how the plant growth occurs in the long-term mean. The LAI of the actual year is geared to the mean LAI_{clim} distribution. If LAI_{clim} decreases, the minimum function of the actual LAI is applied, and if LAI_{clim} increases, the maximum function of the actual LAI is applied according to equation (5.5), respectively.

The fraction of green vegetation cover fveg is computed analogue to the LAI:

$$fveg = fveg_{\min} + gf \cdot (fveg_{\max} - fveg_{\min}) \qquad (5.6)$$

The snow-free land surface albedo is varying with the plant cover density and is computed as a function of the LAI (Rechid et al. 2008a):

$$a = a_{soil} \cdot e^{-0.5 \cdot LAI} + a_{canopy} \cdot (1 - e^{-0.5 \cdot LAI}) \qquad (5.7)$$

a_{soil} is the pure soil albedo and a_{canopy} is the pure vegetation albedo, which were derived as global maps from remotely sensed data.

5. 4 Phenology scheme offline driven by REMO

5. 4. 1 Model simulations

To study the performance of the new phenology scheme, it was driven offline by the results of a regional model simulation for today's climate. The REMO simulation was done at 0.44 degree horizontal resolution (**REMO-50km**) with 31 vertical levels for the time period from 1958-2003 driven by lateral boundary conditions and sea surface temperatures from the European Centre for Medium-Range Weather Forecasts (ECMWF) Reanalysis Project (ERA40, Uppala et al. 2005). The model domain is focused on Europe as shown in figure 5.3. It presents the model orography superposed by European sub-regions, which are used for evaluations. To test the phenology scheme at higher horizontal resolution it was also driven by a REMO simulation at 0.088 degree (**REMO-10km**), which was performed for the German Federal Environment Agency (Jacob et al. 2008). The simulation was done for the time period from 1979 to 2003 driven by the lateral boundary conditions and sea surface temperatures from the ECMWF Reanalysis Project (ERA15, Gibson et al. 1997) and ECMWF operational analyses. The model domain is focused on Germany, Switzerland and Austria (not shown).

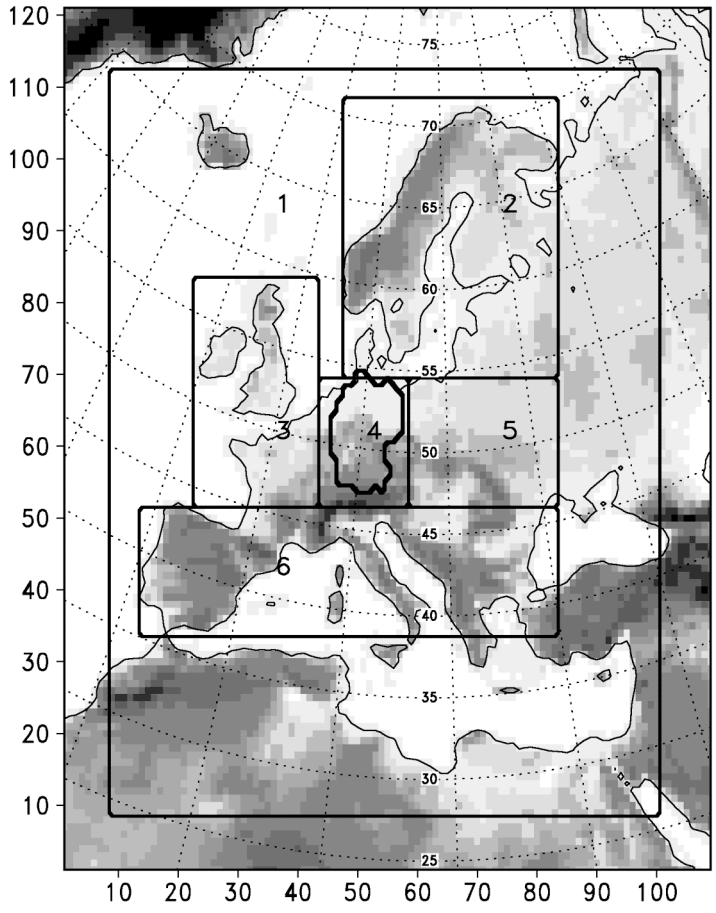

Figure 5.3: REMO model orography [m] at 0.44 degree horizontal resolution with European subregions: 1 model domain area without the 8 boundary grid boxes, 2 northern Europe, 3 western Europe, 4 central Europe and Germany, 5 eastern Europe, 6 southern Europe.

5. 4. 2 Interannual variability and long-term mean of LAI

The LAI, which was offline simulated by the phenology model PHENO and driven by REMO-50km area-averaged over Germany from 1958 to 1962, is presented in figure 5.4. It is compared to the mean LAI of the LSP2 dataset (which is applied in REMO by default) to visualise the interannual variability of the LAI as a function of the simulated model climate. Additionally, the lower lines between 0 and 1 in figure 5.4 show the growth factors. The simulated annual LAI distributions look realistic and similar to the LSP2 data. But they differ from year to year in the beginning and the end of the growing season and also the duration of the optimum plant growth period. In 1959, 1960 and 1961 the growing season simulated by PHENO starts earlier than in LSP2. In 1962, the plant growth starts later due to lower spring temperatures. The main factor limiting the plant growth over Germany is the temperature. But during late summer, when the soil water reservoirs are exhausted and precipitation is low water can become the limiting factor as it is the case in the first year and especially during the summer in 1959. This can also be found in the LAI distribution which shows an earlier decrease in summer due to plant wilting. During the other years no water limitation occurs.

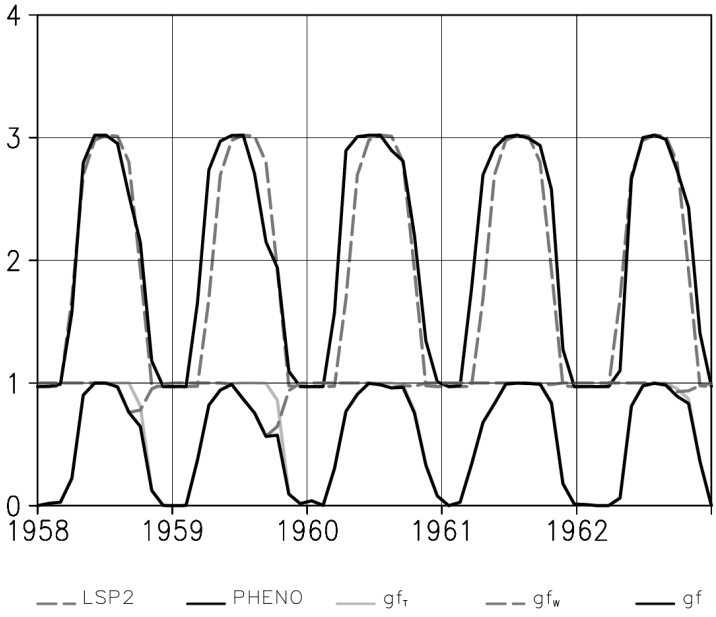

Figure 5.4: Offline simulated LAI (PHENO) area-averaged over Germany 1958-1962 compared to the LAI climatology of LSP2 and growth factors (lower lines): gf_T: temperature limited growth factor, gf_W: water limited growth factor, gf: total growth factor.

In figure 5.5 the long-term mean LAI from 1958 to 2003 area-averaged over the European subregions is presented in comparison to the LAI of the LSP2 data. The lower lines between 0 and 1 represent the mean growth factors. The simulated long-term mean annual cycles of LAI over Europe differ from the mean LAI of LSP2, as PHENO takes account for the water availability at the surface. In most parts of Europe temperature is the dominant limiting plant growth factor. However, in eastern Europe and especially in southern Europe, water is becoming the dominant limitation factor of plant growth during summer and autumn. Here, the new phenology scheme PHENO simulates a stronger LAI decrease during summer and autumn corresponding to the reduced growth factor, which seems to be more realistic than in

the LSP2 data. The earlier decrease in the annual LAI is more pronounced during summer seasons with hot and dry weather conditions (not shown). In western and central Europe a longer mean length of the vegetation period becomes evident compared to the LSP2 data.

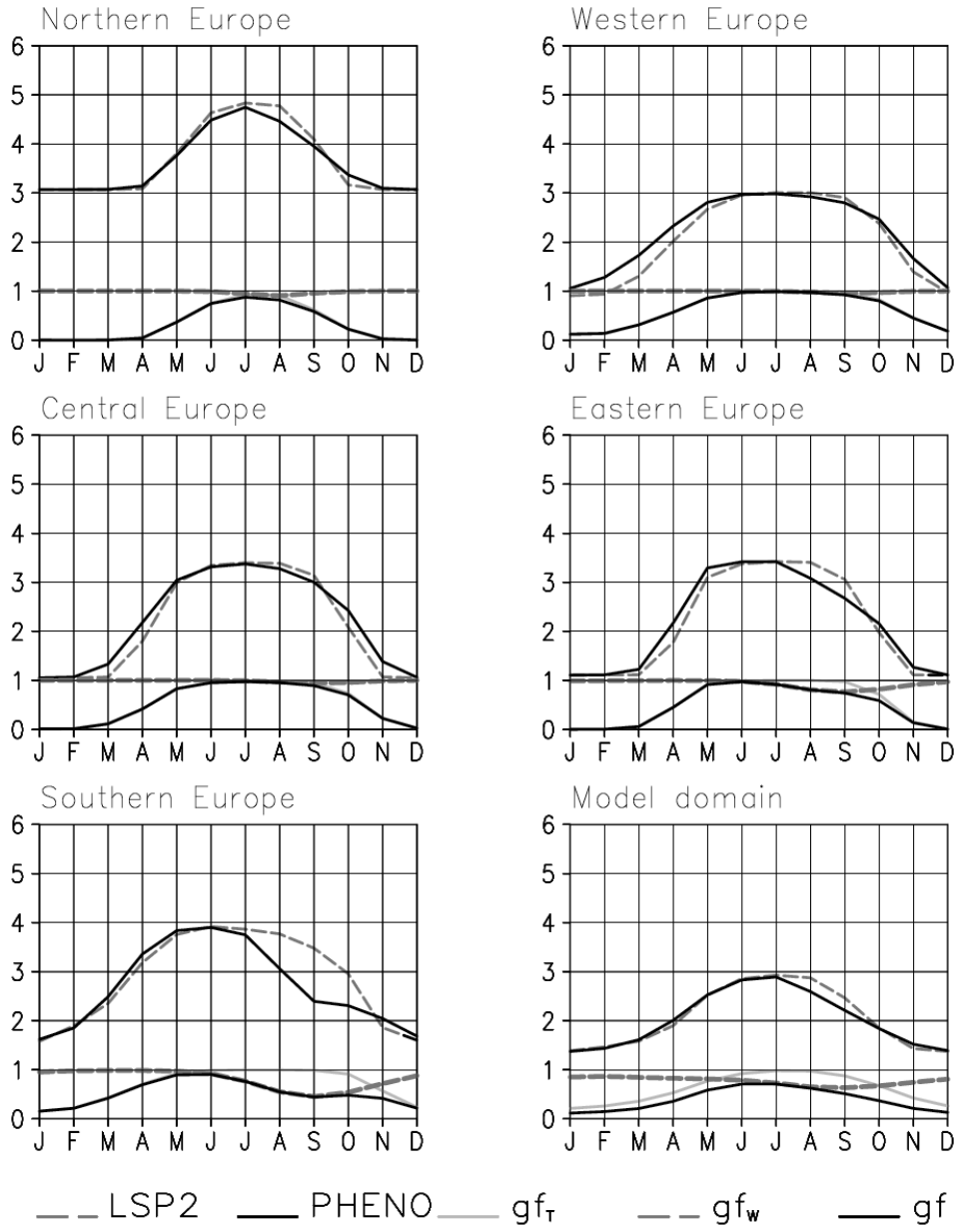

Figure 5.5: Offline simulated long-term mean LAI (PHENO) 1958-2003 area-averaged over European subregions compared to the LAI climatology of LSP2 and mean growth factors (lower lines): gf_T: temperature limited growth factor, gf_W: water limited growth factor, gf: total growth factor.

5. 4. 3 Comparison to remotely-sensed data

Evaluating the LAI simulated by the new phenology scheme PHENO, the question about the reliability of the simulation results raises. To get a first impression, some selected results are compared to remotely-sensed data retrieved from MODIS and VEGETATION instruments.

The LAI level 4 MODIS land product MOD15A2 (Myneni et al. 2002) is composited over an 8-day period at 1 km spatial resolution projected on a sinusoidal grid. The data are distributed by the EROS Data Center, a detailed description is available at http://cybele.bu.edu/modismisr/products/modis/-userguide.pdf. To compare the MODIS LAI to the LAI simulated by PHENO, the data was re-projected to a regular longitude/latitude grid. The LAI estimates from VEGETATION sensors are produced within the CYCLOPES project (Baret et al. 2007) at 10 days temporal sampling interval under a regular latitude/longitude projection at 1/112° spatial resolution. The CYCLOPES products and associated detailed documentation are available at http://postel.mediasfrance.org. Moreover, the simulated results of the snow-free land surface albedo are compared to MODIS broadband albedo level 4 product MOD43C1 (Gao et al. 2005, Schaaf et al. 2002), which is composited over a 16 day period and aggregated to a regular geographic latitude/longitude grid at 0.05 degree spatial resolution. These albedo values are based on spatial averages of the underlying 1-km albedo data. The products are provided to the user community by the Earth Resources Observation System (EROS) Data Center. The MOD43 User's Guide is available at http://geography.bu.edu/brdf/userguide. The accompanying information about snow cover is used to mask out snow pixels.

The LAI simulated offline by PHENO is compared to the MODIS and the CYCLOPES LAI data area-averaged over Northern and Southern Germany for 2002 and 2003 (figure 5.6). The simulated LAI distributions are much smoother than the LAI distributions of the data retrieved from satellites. Especially the MODIS LAI distributions show strong fluctuations. The strong peak of the MODIS LAI at the end of the year is unrealistic. The CYCLOPES LAI data seems to be better processed. In southern Germany, the satellite LAI data differ strongly, the CYCLOPES LAI is lower than the MODIS LAI during the optimum plant growth period. This shows that LAI data retrieved from satellites are still associated with uncertainties. The LAI model results are similar to the remotely sensed LAI data but show a longer optimum plant growth period. The MODIS and CYCLOPES LAI is decreasing earlier after the maximum plant growth. The effects of the unusual hot and dry summer of 2003 can be seen in the LAI of both the model results and the satellite data. The LAI is decreasing earlier during the summer in 2003 than in 2002 due to the strong water limitation. However, in the PHENO LAI simulation driven by the higher resolution climate data this effect of water limitation is much more pronounced than in the LAI simulation driven by REMO-50km. The climate data simulated by REMO-10km shows more geographical detail, especially of precipitation and soil moisture (not shown). Thus, it better represents the local hydrological cycle at the surface. As the near-surface moisture conditions strongly link vegetation and atmosphere, this may be the reason for the better results of PHENO driven by REMO-10km. This shows that the reliability of the PHENO results depends on the quality of the simulated climate data from the regional model and points at the importance of the high resolution of climate model simulations.

How do the simulated LAI data agree with the satellite retrieved data over Europe? In figure 5.7 the model results driven by REMO-50km are compared to MODIS and CYCLOPES LAI for 2002 to 2003 in 8 day periods area-averaged over the European subregions. In central, western and eastern Europe the data agree quite well, in eastern Europe the LAI is somewhat overestimated by PHENO compared to MODIS and CYCLOPES. Here again, the effect of the water limitation during the hot and dry weather conditions during the summer 2003 can be seen. In northern and southern Europe the simulated LAI values are strongly overestimated compared to the remotely sensed LAI values. These differences are caused by the higher minimum and maximum LAI values that are assumed by the LSP2 data, which are also used

in the PHENO scheme. Over large regions of Scandinavia the LSP2 dataset assumes conifer forests with LAI values of 6 throughout the year which is not the case in the satellite retrieved data. During the dark winter season, however, observations from satellites are not possible. The truth may lie in-between. In southern Europe, the simulated LAI slightly increases again in autumn, when again more water is available for plants. This is not the case in the LAI data retrieved from the satellites. Here, ground observations would be helpful to validate the simulated LAI.

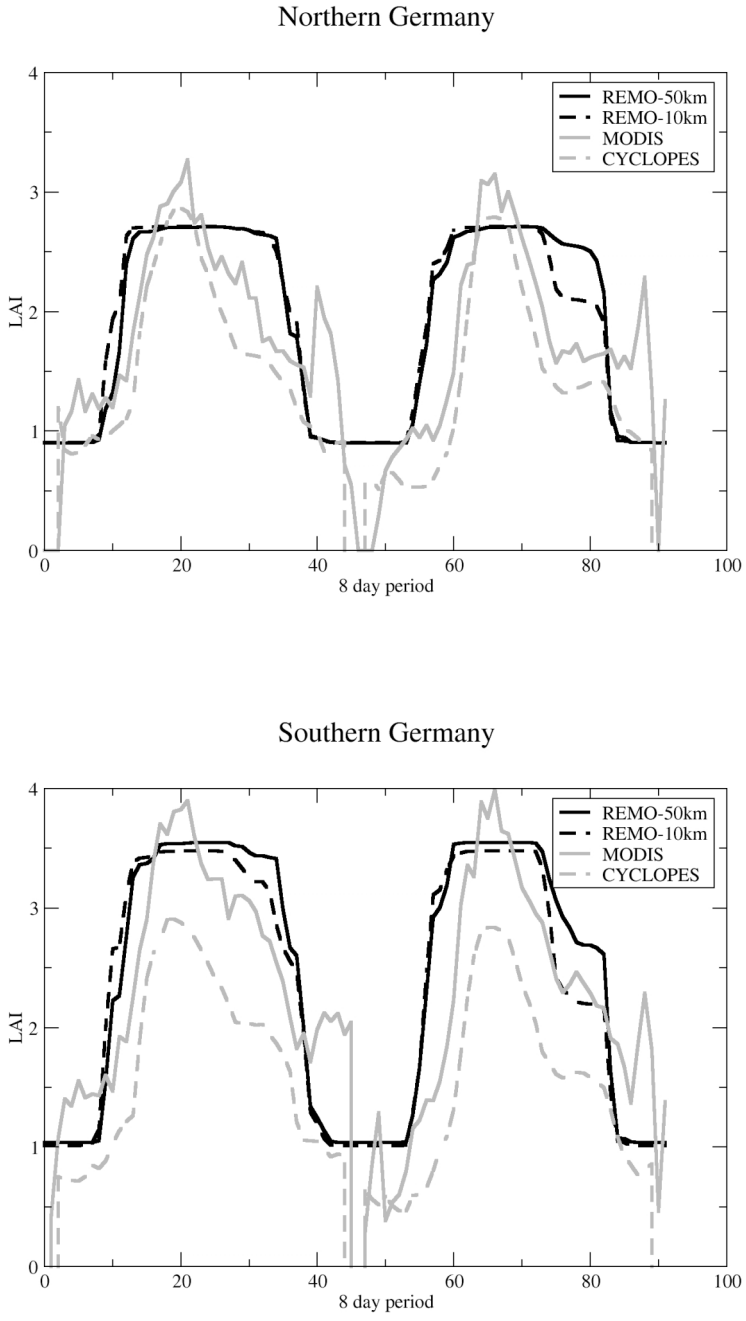

Figure 5.6: Offline simulated LAI 2002-2003 driven by REMO-50km and REMO-10km area-averaged over Northern and Southern Germany compared to MODIS and CYCLOPES LAI data.

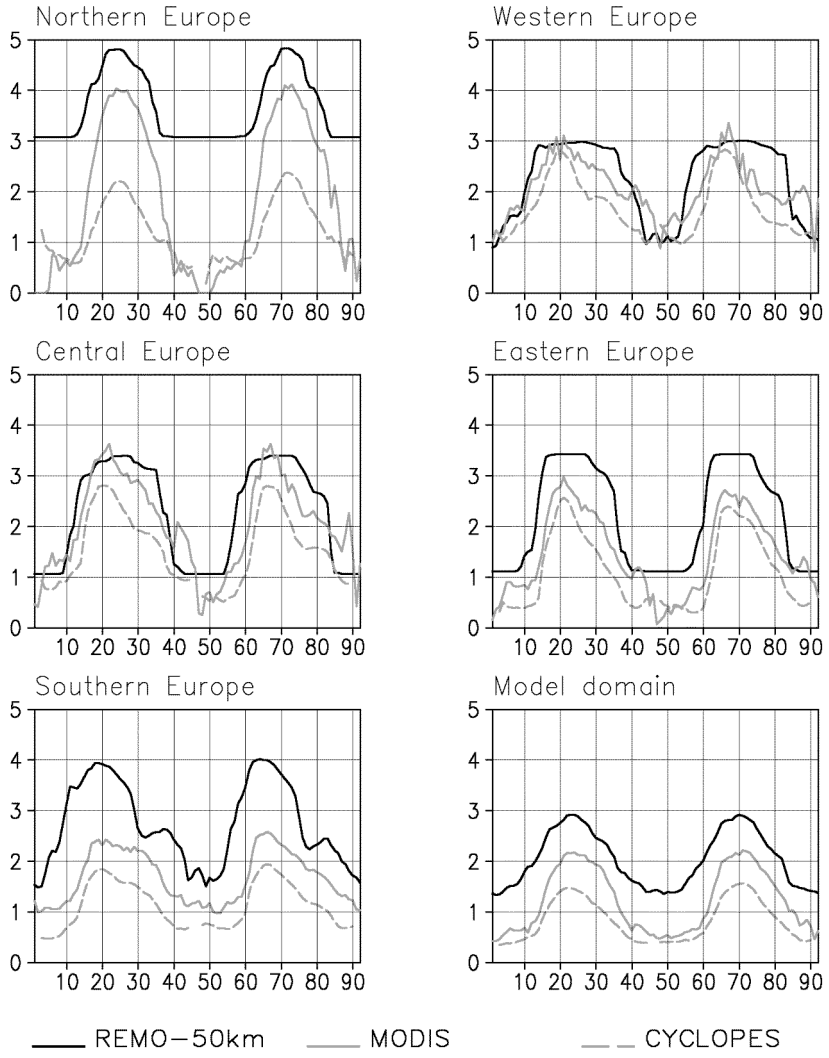

Figure 5.7: Offline simulated LAI in 8day-periods 2002-2003 driven by REMO-50km area-averaged over European subregions compared to MODIS and CYCLOPES LAI data.

The snow-free land surface albedo simulated by PHENO is compared to MODIS albedo data in figure 5.8. The results are again area-averaged over northern and southern Germany for the time period from 2001 to 2003 in 16 day periods. The simulated albedo captures the distribution of the remotely sensed data quite well. During 2001 and 2002 the simulated albedo values decrease later than MODIS albedo due to the longer optimum plant growth period in the PHENO simulation. The hot and dry weather conditions during the summer in 2003 appear also in the land surface albedo, which is lower compared to the values during the first two years. The LAI decreases earlier due to water limitation in summer 2003, the darker soil surface becomes more visible, which reduces the land surface albedo. This effect is again captured better by the PHENO simulation driven by REMO-10km.

The comparison of the simulated land surface albedo to satellite retrieved albedo values over Europe (figure 5.9) shows good agreement of the data in all evaluated regions. However, the simulated albedo again decreases later than the MODIS albedo due to the longer optimum

plant growth period in PHENO with maximum LAI values. The fluctuations and peaks of the MODIS albedo in northern Europe obviously result from undetected cloud and/or snow cover. In southern Europe the simulated albedo cycle is less variable than in the data retrieved from satellites. The comparison of the albedo data averaged over the whole model domain again shows the peaks of undetected cloud and/or snow cover during the winter season; during the summer season, the simulated and observed data agree. Note, that the comparison for albedo data averaged over large areas is difficult, anyway, and gives only a rough estimation.

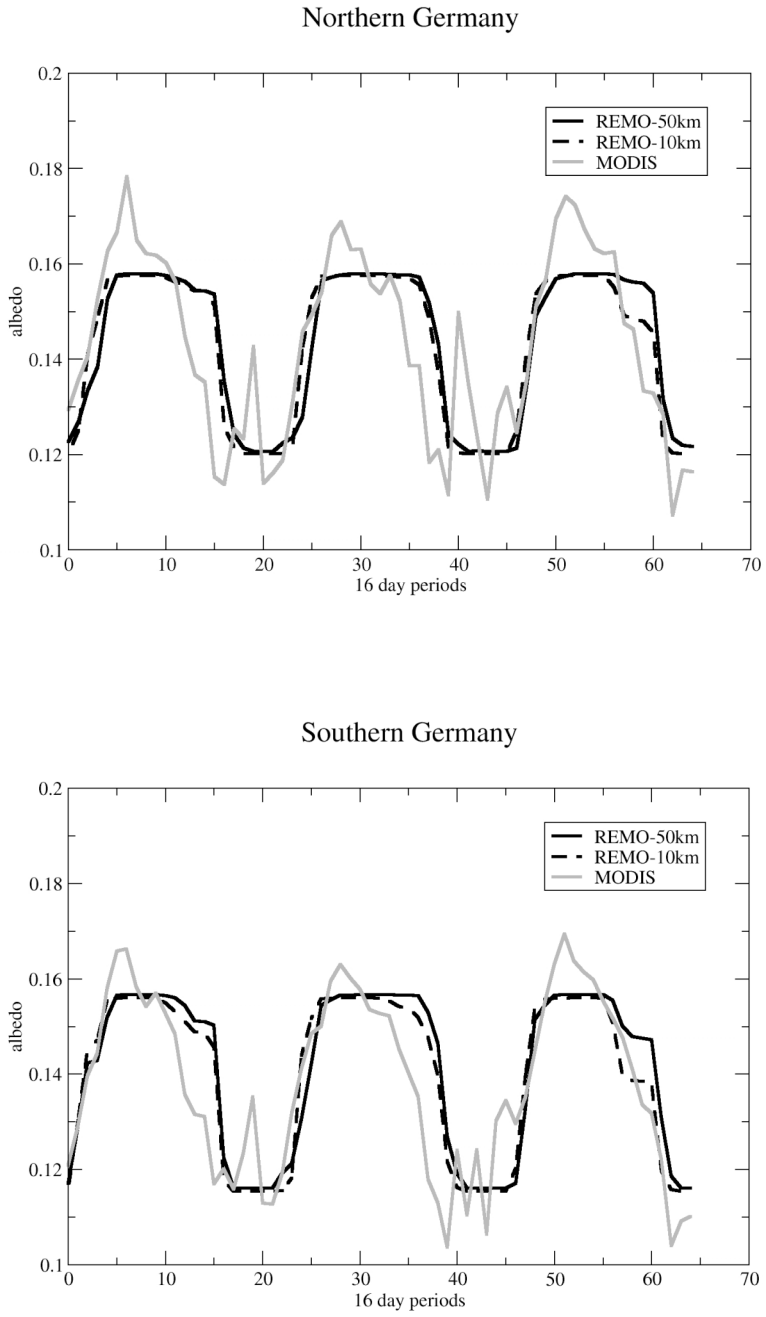

Figure 5.8: Offline simulated snow-free land surface albedo 2001-2003 driven by REMO-50km and REMO-10km area-averaged over Northern and Southern Germany compared to MODIS snow-free land surface albedo data.

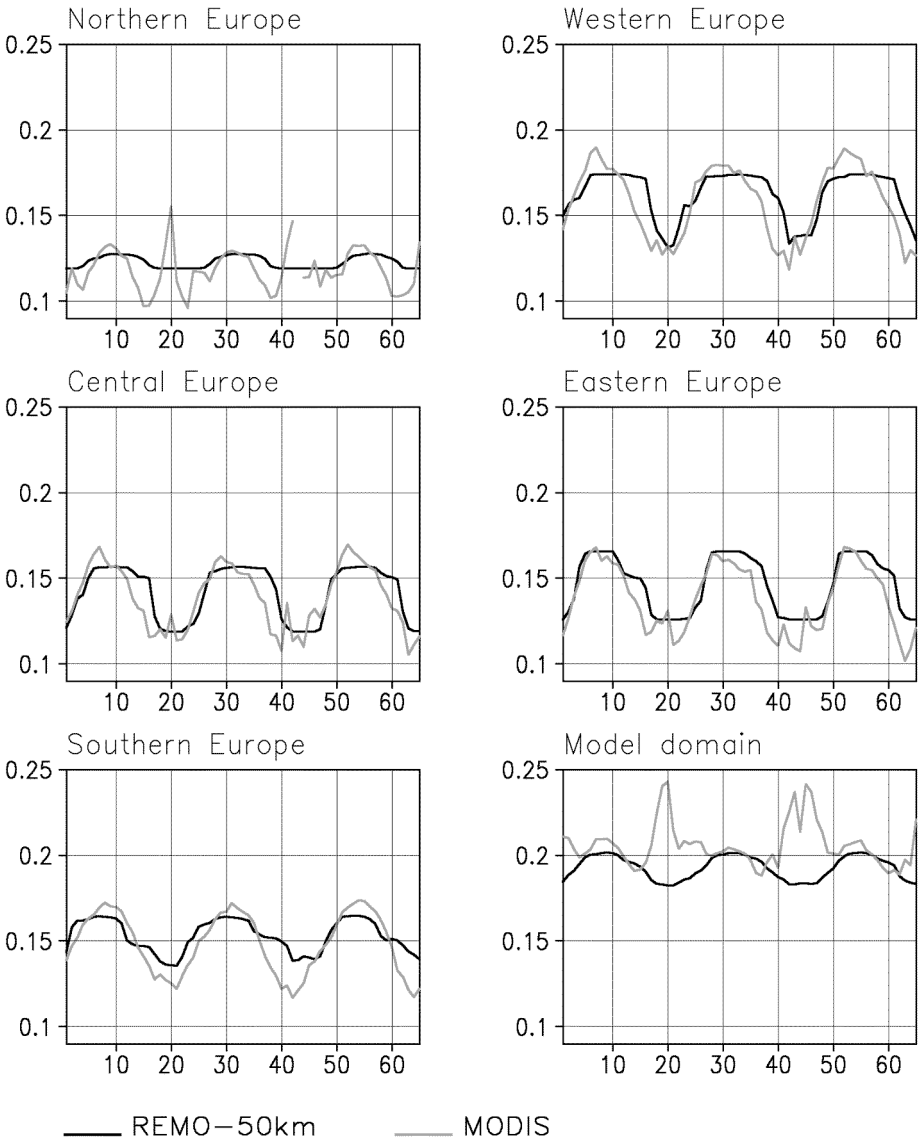

Figure 5.9: Offline simulated snow-free land surface albedo in 16day-periods 2001-2003 driven by REMO-50km area-averaged over European subregions compared to MODIS snow-free land surface albedo data.

5. 4. 4 Long-term trends

The computation of the LAI as a function of the model climate not only considers the interannual variability but also long-term trends of the plant phenology. As a consequence of climate change many studies show evidence of a shift in plant development towards an earlier onset of spring phenology in Europe (Menzel 2000, Defila & Clot 2001, Menzel et al. 2001, Ahas et al. 2002, Menzel et al. 2003, Menzel et al. 2006) – compare also section 5.1. Spring phenological phases, such as leaf unfolding and flowering, strongly correlate with temperature of the preceding months (e. g. Chmielewski & Rötzer 2001, Ahas et al. 2002, Menzel 2003). Does the regional climate model simulation capture these trends in temperature and plant phenology?

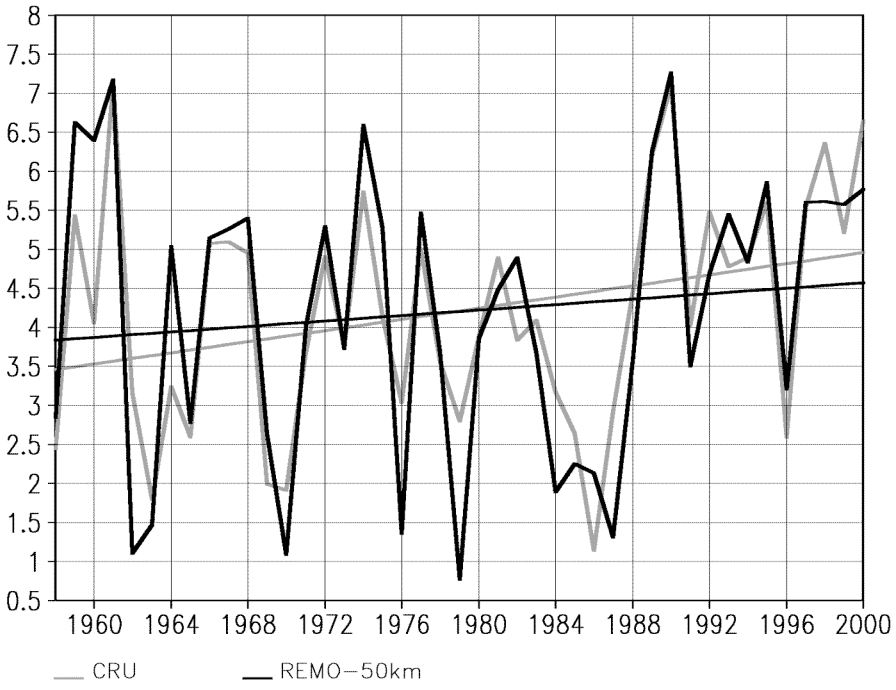

Figure 5.10: Mean 2m temperature February-March-April 1958-2000 and trend in Germany simulated by REMO-50km (black lines) in comparison to CRU (grey lines)

The onset of spring phenology in central Europe is mostly determined by the temperatures in February-March-April (FMA). In figure 5.10 the simulated trend of the 2m temperature during FMA area-averaged over Germany from 1958 to 2000 is shown in comparison to the observed warming trend extracted from the Climate Research Unit analyses version 2.0 (CRU, MITCHELL et al., 2004, NEW et al. 2000). The CRU dataset provides global 2m-temperature and precipitation fields as time series of monthly means for the time period 1901–2000 at 0.5 degree horizontal resolution for the land surface area. The observed warming trend in CRU data is 0.36 K per decade and 1.54 K from 1958 to 2000. The simulated warming trend in spring from 1958 to 2000 is +0.18 K per decade with a total temperature increase of 0.75 K during the 43 years. The analysis of the simulated warming trend for the period 1958 to 2003 yields a stronger trend with 0.28 K per decade, which means a total temperature increase during the 46 years of about 1.29 K (not shown). The simulated trend of the temperatures during FMA is stronger than the warming trend of the annual means (not shown), which is important for the onset of plant growth in spring. Altogether, the regional model captures the warming trend during the last decades. What is the effect on the simulated plant phenology?

To address this question, the simulated onset, length and end of the growing season in Germany from 1958 to 2003 is analysed in figure 5.11. Here, the interannual variability of plant phenology appears with clear trends in the onset and length of the growing season. The decreasing trend in the growing season beginning is -1.28 days per decade and the increasing trend in the growing season length is +0.90 days per decade. So, the onset of spring phenology is 5.9 days earlier and the growing season becomes 4.1 day longer during the

period 1958 to 2003. The end of the growing season is 1.8 days earlier with an decreasing trend of 0.39 days per decade from 1958 to 2003. Similar trends are found in the observations from the International Phenological Gardens (IPG). Chmielewski & Rötzer (2001) analysed trends in plant phenology from IPG observations for the period of 1969 to 1998. Over Germany, they found an earlier onset of spring phenology of 5 days per decade for the Northern lowlands (3.5 days simulated by PHENO over Northern Germany) and 3.1 days per decade for the Northern Alpine foreland (3.2 days simulated by PHENO over Southern Germany). The lengthening of the growing season for the same regions is 5.9 (2.1) and 3.5 (2.7) days per decade, respectively. The later end of the growing season in the IPG data, however, is not significant. Changes in autumn are not easily to detect as the factors causing changes in autumn phases are not clear (Menzel et al. 2001, Sparks & Menzel 2002) and the signal is ambiguous (Menzel et al. 2006).

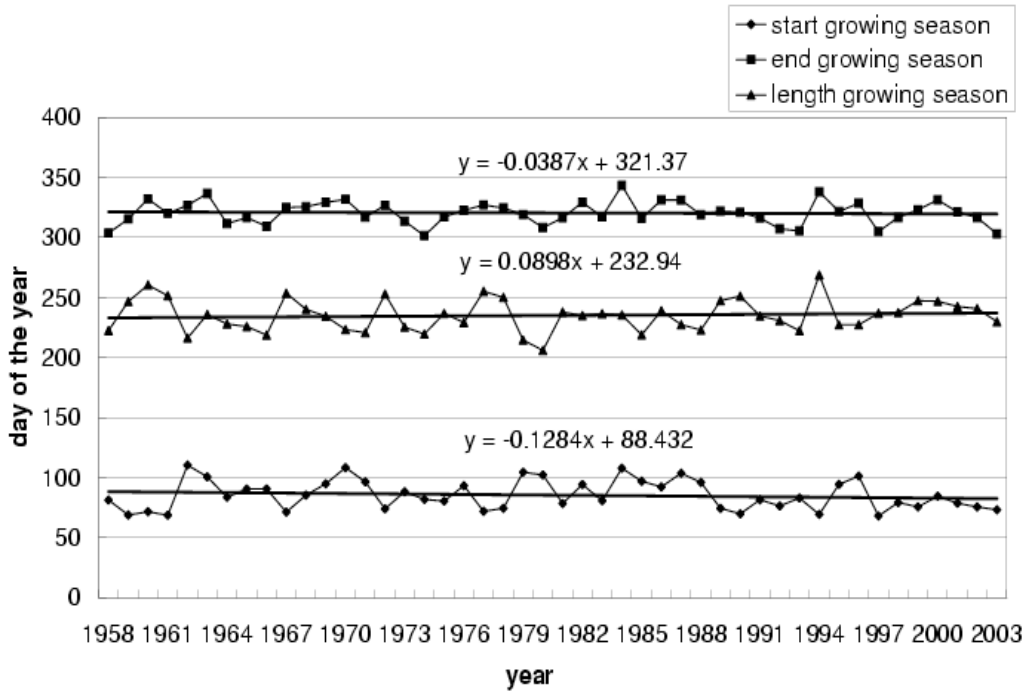

Figure 5.11: Start and end of the growing season [day of the year] and length of the growing season [days] in Germany from 1958-2003 offline simulated by PHENO driven by REMO-50km

5. 4. 5 Future scenario

To study the effects of future climate trends on plant phenology, the PHENO scheme was driven by a regional climate change simulation of REMO (REMO-scenario). The regional climate scenario was done at 0.44 degree horizontal resolution with 31 vertical levels for the time period from 2071-2100 assuming the greenhouse gas concentrations of the IPCC SRES A1B scenario (Nakicenovic et al. 2000). The regional model domain focusing on Europe is the same as used for the simulation of today's climate (REMO-50km) presented in figure 5.3. The climate projection indicates an increase of the annual mean 2m temperature by up to +4 K for most parts of Europe for 2071-2100 compared to the control period 1961-1990 (not

shown). In southern Europe, the temperature even changes by up to +5 K in parts. The projected annual mean precipitation changes show an increase in the northern parts of Europe by up to 20%, and a decrease in the southern parts of Europe by up to 30%, especially during the summer months by up to 50% less precipitation in some regions in southern Europe (not shown). This projected climate change will certainly strongly affect the phenology of plants.

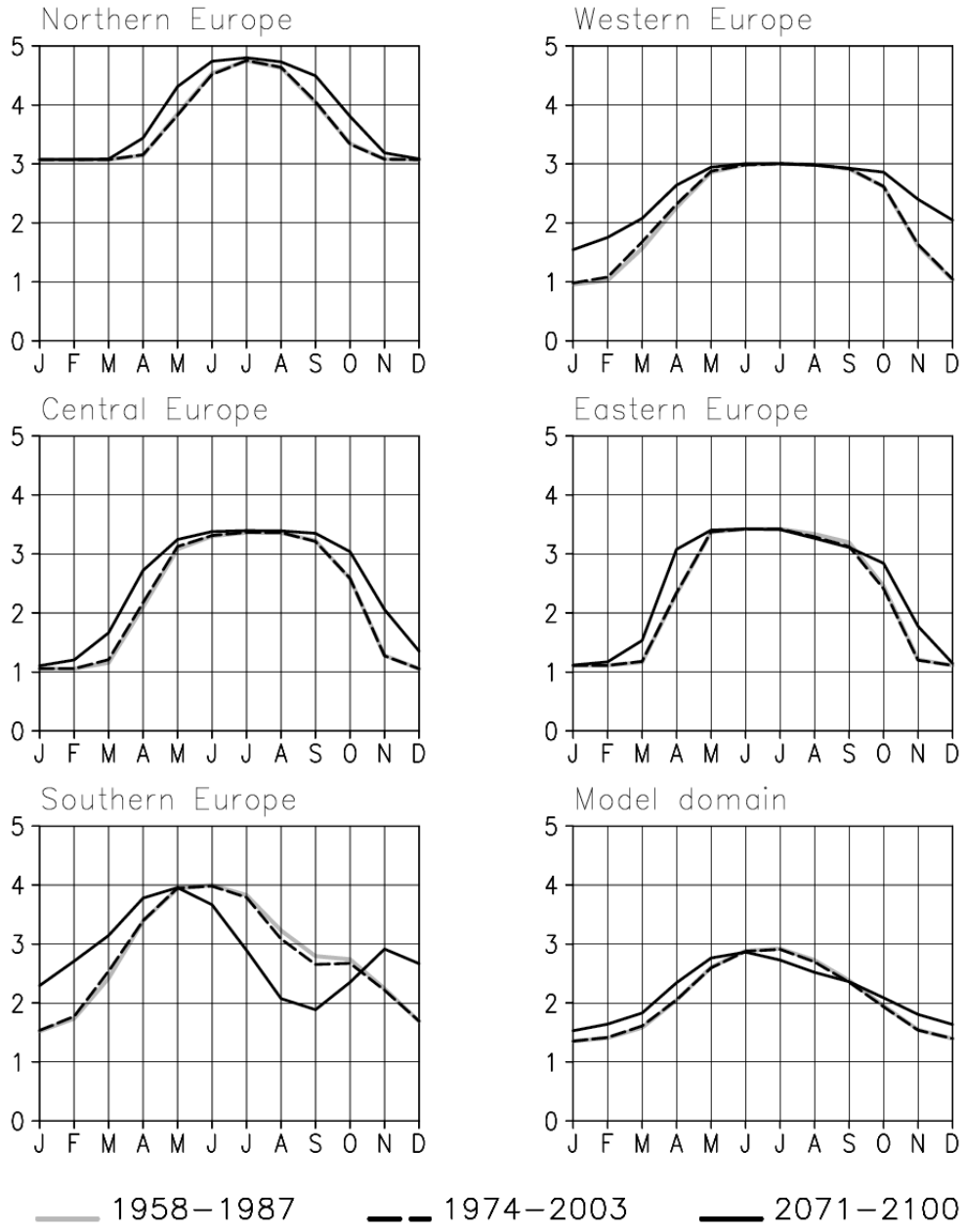

Figure 5.12: 30-year LAI climatologies offline simulated by PHENO driven by REMO-50km for 1958-1987 (solid grey line) and 1974-2003 (dashed black line) and driven by REMO-scenario for 2071-2100 (solid black line) area-averaged over European subregions

The simulated 30-year mean annual LAI cycle for the future time period from 2071 to 2100 is compared to the period from 1958-1987 in figure 5.12. Substantial changes in plant

phenology appear. In northern, eastern and central Europe the growing season is lengthened by up to 2 month due to higher temperatures. In many parts of western Europe the length of the vegetation period is no longer limited by temperature, which reveals the horizontal distribution of the plant phenology types under the projected climate change conditions (not shown). A strong shift of the vegetation phenology types occurs with an extension of the water-limited vegetation phenology type in all parts of southern Europe and into many parts of western Europe. In southern Europe the water limitation of plant growth increases especially during summer and autumn due to hot and dry weather conditions. The results reveal a strong impact of the future climate warming on plant phenology, which again would affect the simulated climate change. The future climate conditions will also change the minimum and maximum LAI due to spatial changes of vegetation type distributions. These long-term effects of climate change are not considered in the phenology scheme PHENO. In figure 5.12, the LAI climatology is also presented for the time period from 1974-2003. In contrast to the future LAI climatology, it hardly changes during the model simulation under today's climate conditions.

5. 5 Online phenology scheme: feedback simulations

5. 5. 1 Model simulation

In order to study the dynamic interactions between vegetation phenology and climate variability, the phenology scheme PHENO was fully coupled to the regional climate model REMO. The vegetation phenology is simulated once a day using the daily means of the surface temperature, soil wetness and precipitation. The resulting LAI, fractional vegetation cover and background surface albedo are used in the simulation of the atmospheric dynamics during the following day. At the end of each simulation year, PHENO updates the distribution of the plant phenology types and re-computes the plant growth phases from the updated 30-year climatologies of the daily surface temperature T_{clim} and of the leaf area index LAI_{clim}.

The regional climate simulation for today's climate was repeated (see section 5.4.2) with the fully coupled phenology scheme (**REMO-online**). However, the PHENO scheme was integrated into the latest version of the regional climate model in order to consider the latest model developments and also to avoid double programming work. To be able to analyse the feedback effects of plant phenology on the simulated climate, a new reference simulation had to be performed. Consequently, the REMO-50km simulation was repeated with the latest REMO model version and its results were used to drive the offline version of the PHENO scheme (**REMO-offline**). Thus, the results of REMO-offline can somewhat differ from the PHENO results driven by REMO-50km presented in section 5.4.

5. 5. 2 Feedback effect on the simulated climate

To detect the feedback of the interannual variability of vegetation phenology on the simulated climate, several simulated climate parameters are investigated. The long-term mean climate from 1958-2003 in Europe is not affected by the online simulated vegetation phenology (not

shown). There is also no feedback effect on the long-term trends of the simulated climate in Europe. The analysis of time-series of monthly mean climate parameters indicate feedback effects during several years. In the following the time period from 1958 to 1962 is exemplarily analysed, the simulation results are area-averaged over Germany. We always compare the results of REMO-online against the results of REMO-offline to show the effects of the interannual variability of vegetation phenology. The land surface temperature in Germany is affected especially in 1960 with an increase by 2K during summer (figure 5.13). The same is the case for the summer in 1959, but to a smaller extent.

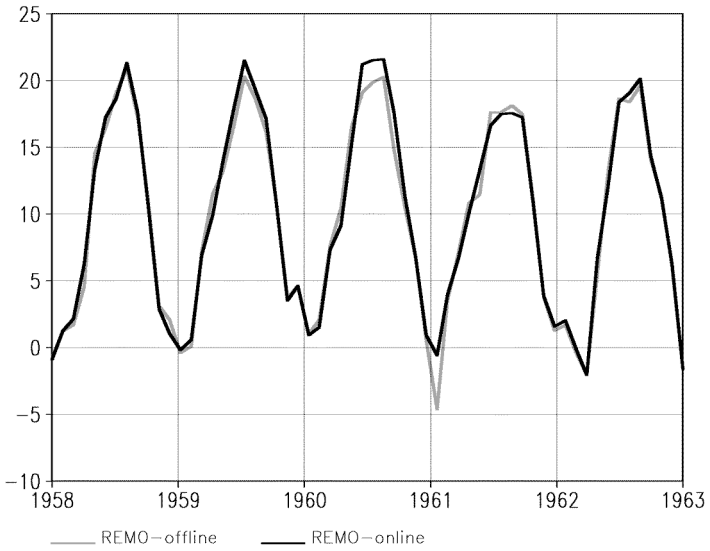

Figure 5.13: Feedback of the online simulated vegetation phenology on the soil surface temperature [°C] area-averaged over Germany 1958-1962

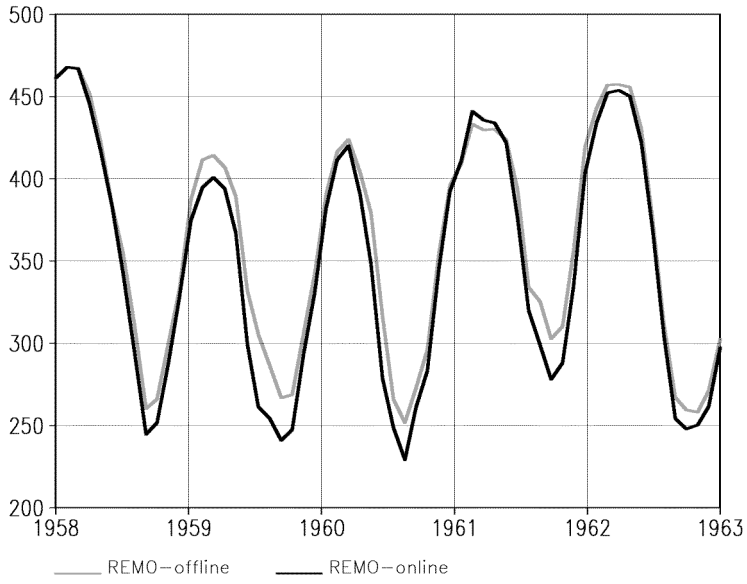

Figure 5.14: Feedback of the online simulated vegetation phenology on the soil surface wetness [mm] area-averaged over Germany 1958-1962

The evapotranspiration is reduced in both summer seasons of 1959 and 1960 by up to 20mm/month (not shown). The soil wetness is also reduced (figure 5.14). In addition, precipitation is somewhat reduced (figure 5.15). But what is cause and what is effect? During the summer in 1960 the LAI simulated by PHENO is lower than the LAI of LSP2, which is used in the reference simulation REMO-offline (will be presented in figure 5.19 in section 5.5.3). The LAI is reduced due to the degeneration of plants caused by water stress, which is considered by the PHENO scheme. The lower LAI reduces the evapotranspiration and therefore the latent heat flux, which leads to a warming of the land surface (figure 5.13). During the summer in 1960 the land surface albedo is reduced by up to -0.02 due to the reduced LAI (not shown). Thus, more energy remains at the land surface which additionally raises the surface temperature.

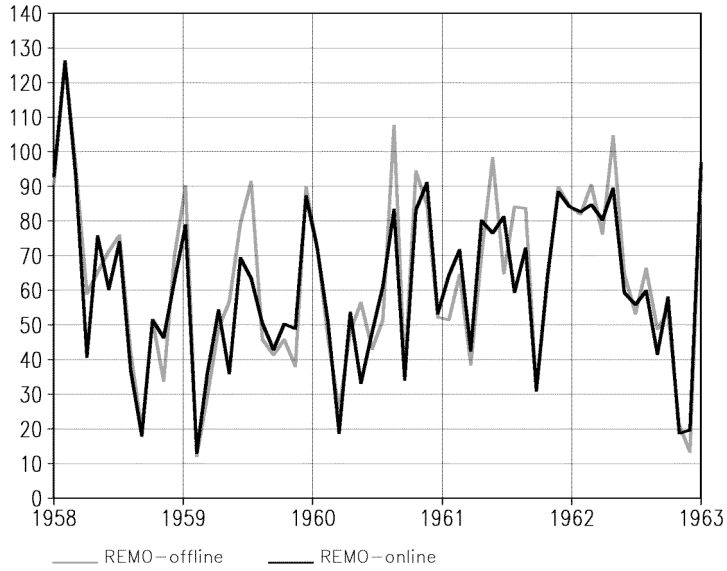

Figure 5.15: Feedback of the online simulated vegetation phenology on precipitation [mm/month] area-averaged over Germany 1958-1962

But why is the soil wetness also reduced in spite of less evaporation of water from the soil? The lower precipitation might be the reason for that. The analysis of the precipitation change reveals that the convective part of the total precipitation is reduced (not shown), which indicates less initiating of summer convection due to decreased LAI values. Thus, the water input to the soil is lower and soil wetness is reduced. The warm and dry weather conditions are intensified. This positive feedback of the interannual variability of vegetation phenology on drought conditions can be observed in most warm and dry summer and autumn seasons during the whole simulation period (not shown). The local cycle of water is reduced, however, it is not completely understood, why there is less water available. Some changes in atmospheric circulations might be the reason. They are not investigated in the current study. Altogether, the climate feedback of the interannual variability of vegetation is small under today's climate conditions. This might change under future climate conditions. If the climate feedback of vegetation phenology increases under climate warming, the coherences between vertical and horizontal atmospheric dynamics should be investigated with more detail to solve the open question.

Averaged over the whole simulation period from 1958 to 2003, the mean soil surface temperature in Germany is not affected by the interannual variability of vegetation phenology (figure 5.16). To analyse the effect on the interannual variability of climate, the surface temperature of the months with the minimum and the maximum temperature value of the whole simulation period and the standard deviation of all months compared to the mean temperature is additionally presented in figure 5.16. The effects on the minimum and the maximum temperature values are negligible and the standard deviation is also not affected; there is no effect on the interannual variability of temperature.

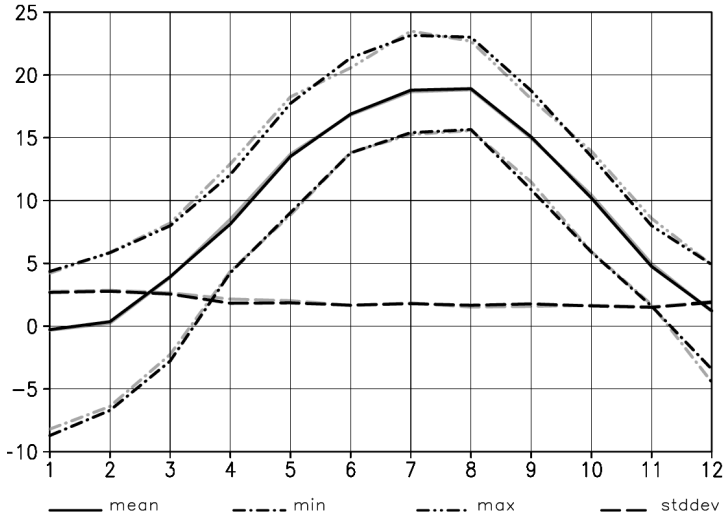

Figure 5.16: Feedback of the online simulated vegetation phenology on the soil surface temperature T [°C] area-averaged over Germany and time average for 1958-2003; online simulation: black lines, offline simulations: grey lines; mean: mean T, min: minimum T; max: maximum T, stddev: standard deviation of T

The mean soil wetness is somewhat reduced from May to December (figure 5.17), which confirms the results presented above, that interannual variability of phenology has a positive feedback on drought conditions. The minimum soil wetness values of the whole simulation period are clearly reduced from May to August by up to 30 mm. The maximum soil wetness values are also somewhat reduced. The standard deviation is only slightly enhanced during these months. there is only a minor increase in the interannual variability of soil wetness conditions.

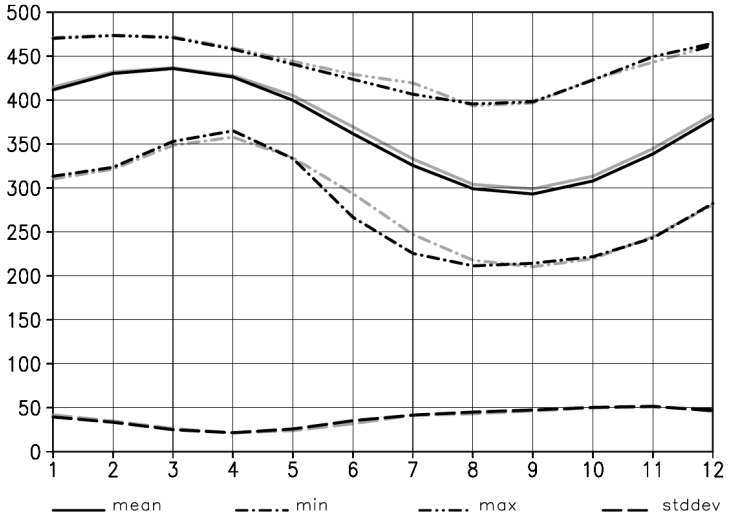

Figure 5.17: Feedback of the online simulated vegetation phenology on the soil wetness W [mm] area-averaged over Germany and time average for 1958-2003; online simulation: black lines, offline simulations: grey lines; mean: mean W, min: minimum W, max: maximum W, stddev: standard deviation of W

For precipitation, the maximum values of the whole simulation period are clearly reduced from April to July area-averaged over Germany (figure 5.18). This is in line with the reduced soil wetness during this period. The minimum values are also reduced, but to a smaller extent. Thus, the interannual variability of precipitation expressed by the standard deviation is slightly reduced during summer.

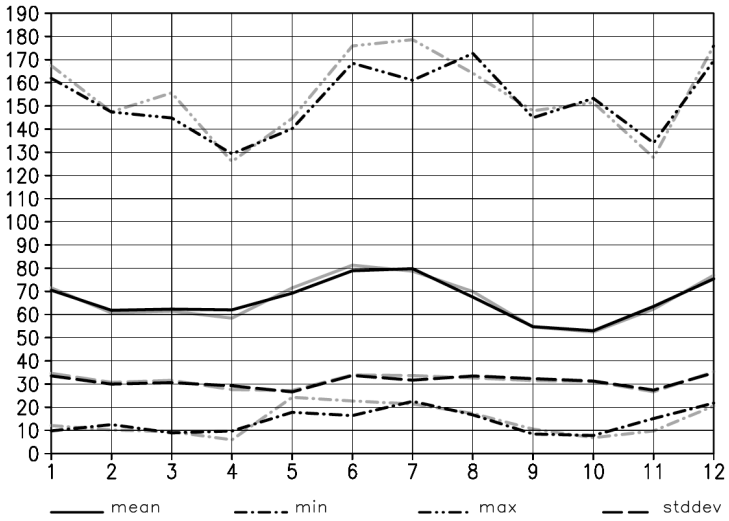

Figure 5.18: Feedback of the online simulated vegetation phenology on the precipitation P [mm/month] area-averaged over Germany and time average for 1958-2003; online simulation: black lines, offline simulations: grey lines; mean: mean P, min: minimum P, max: maximum P, stddev: standard deviation of P

5. 5. 3 Feedback effect on vegetation

The effects of the interannual variability of vegetation phenology on climate can again feedback to vegetation. To detect possible vegetation feedbacks, the online simulated LAI is compared to the offline simulated LAI. The long-term mean annual LAI cycles for the European subregions averaged over the whole simulation period from 1958 to 2003 show no differences compared to the offline simulated LAI cycles (not shown). There is also no feedback effect on the long-term trends of the growing season. As for the climate feedback of vegetation phenology, the effects occur during individual years.

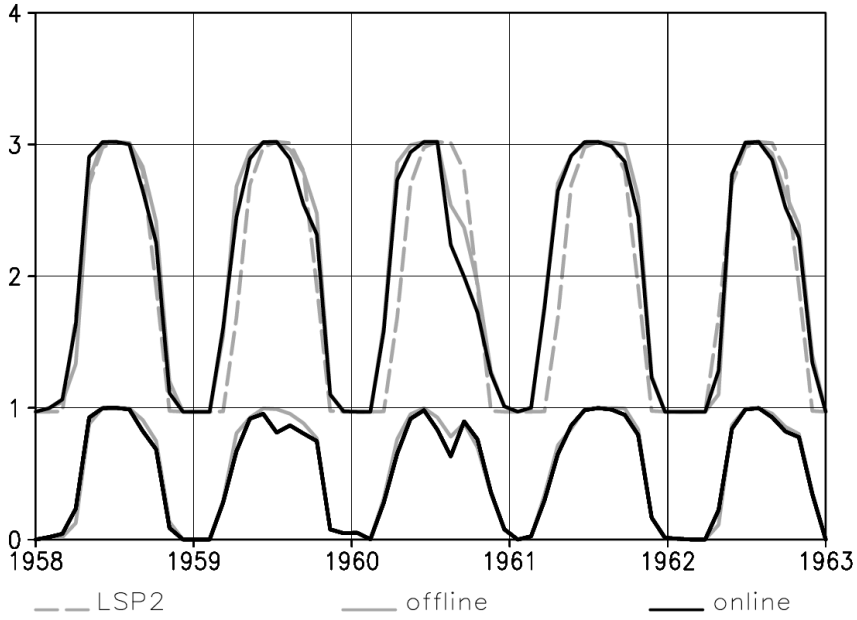

Figure 5.19: Online simulated LAI (black solid line) area-averaged over Germany 1958-1962 compared to the offline simulated LAI (grey solid line) and to the LAI climatology of LSP2 (grey dashed line); lower lines: total growth factors of PHENO-offline (grey solid lines) and PHENO-online (black solid lines)

In figure 5.19 the online simulated LAI is compared to the offline simulated LAI exemplarily for the time period from 1958 to 1962 area-averaged over Germany. In addition, the constant annual LAI cycle of LSP2 is displayed, which was used in the REMO reference simulation (REMO-offline) as lower boundary condition. In 1958, 1961 and 1962, the online simulated LAI is very similar to the LAI offline simulated by PHENO. Main differences again occur in 1960 during late summer, when the offline simulated LAI is lower compared to LSP2 due to water limiting conditions in the soil. Due to the positive feedback of the interannual variability of vegetation phenology on drought conditions, as discussed in section 5.5.2, this effect of water limitation is even enhanced in the online simulation leading to another decrease in LAI. The online simulated total growth factor (lower lines between 0 and 1) is lower than the offline simulated growth factor, which also indicates warmer and dryer weather conditions in the online simulation during that time. The same effect appears during late summer in 1959, but to a smaller extent.

During the whole simulation period from 1958 to 2003 the feedback of the online simulated phenology on the LAI itself is low in most years (not shown). But one systematic effect occurs during warm and dry summer seasons, when the LAI stronger decreases during the drought periods. This is also the case during the hot and dry summer in 2003, which converges the simulated LAI closer to the LAI values retrieved from satellite data (figure 5.20). The positive feedback on drought conditions during warm and dry summer/autumn seasons intensifies the effect of water limitation in the coupled model simulation leading to another decrease in LAI, which increases the interannual variability of vegetation phenology.

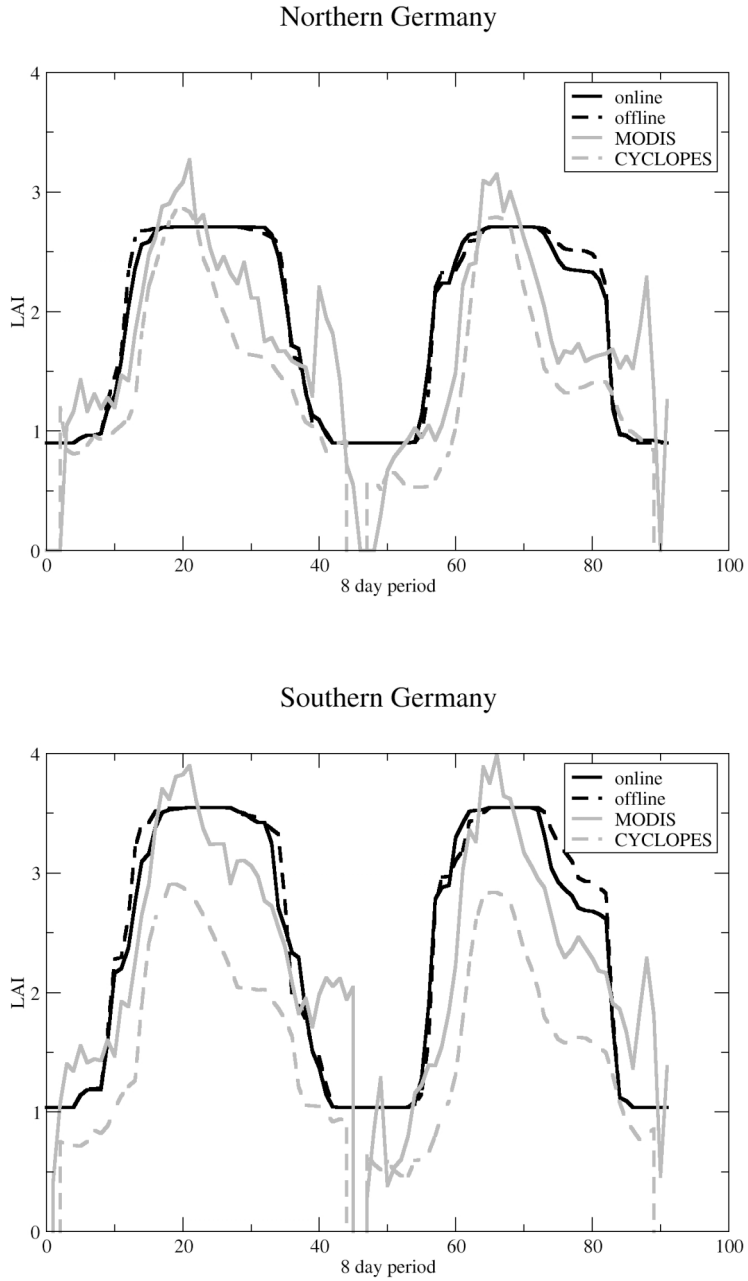

Figure 5.20: Online and offline simulated LAI 2002-2003 area-averaged over Northern and Southern Germany compared to MODIS and CYCLOPES LAI data.

5. 6 Conclusions and outlook

To study the dynamic interactions between plant phenology and climate variability over Europe, the vegetation phenology model PHENO was developed and fully coupled to the regional climate model REMO. PHENO relates the species-averaged parameter LAI directly to simulated climate parameters of near-surface heat and moisture conditions. The simulation results in offline mode show the interannual variability and temporal trends in vegetation phenology caused by climate variability. In Germany, the timing of leaf expansion in spring is varying from year to year in dependence on the surface temperatures. The leaf senescence in fall is varying in dependence on surface temperatures and surface moisture content. Especially in warm and dry years, the LAI decreases earlier in late summer/autumn due to water limiting conditions. This could be approved by the comparison of the simulated LAI to the LAI retrieved from satellite data for the years 2002 and 2003. During the extremely hot and dry summer 2003, plants were wilting and tree leaves were shrinking due to water stress, which is reflected by the earlier decrease in LAI values compared to 2002. Here, the PHENO simulation driven by the higher resoluted climate data yields better results.

Over Europe, the simulated long-term mean annual cycles of LAI differ from the mean LAI of the LSP2 dataset (which is applied in REMO simulations by default), as PHENO accounts for the water availability at the surface. In most parts of Europe, temperature is the dominant limiting plant growth factor. However, in eastern Europe and especially in southern Europe, water is becoming the dominant limitation factor of plant growth during summer and autumn. The earlier decrease of the simulated LAI compared to the mean LAI cycle is more pronounced during summer seasons with hot and dry weather conditions.

The observed long-term trends in plant phenology, that are investigated in many ecological studies, are captured by the PHENO simulations. The onset of spring phenology is 5.9 days earlier and the growing season becomes 4.1 day longer during the simulated period from 1958 to 2003. This means, that in warm and dry years the earlier start of the growing season is compensated by limited growth conditions during summer and autumn by only shifting or even shortening the vegetation period.

In the simulated 30-year climatology of LAI, that is updated at the end of each year, there are only minor changes in the period from 1974 to 2003 compared to the period from 1958 to 1987. But compared to the LAI climatology from 2071 to 2100, which was simulated by PHENO driven by the results of a regional climate projection, substantial changes in vegetation phenology appear. In northern, eastern and central Europe, the growing season is lengthened by up to 2 month due to higher temperatures. In western Europe, the length of the vegetation period is no longer limited by low temperatures. In southern Europe, the water limitation of plant growth increases during summer and autumn due to hot and dry weather conditions. The results reveal a strong impact of the future climate warming on plant phenology. Vice versa, the changed vegetation phenology will certainly impact the simulated future climate.

For today's climate the feedback of the interannual variability of plant phenology on the simulated climate as well as on vegetation itself is investigated by the PHENO simulation coupled to REMO. The evaluations for Germany showed reduced LAI values in warm and dry summer and autumn seasons in the online simulation compared to the offline simulation. The lower LAI reduces evapotranspiration and convective precipitation processes. Thus, the water input to the soil is lower and soil wetness is reduced. Moreover, the land surface albedo

is reduced due to the lower LAI values. Thus, more energy remains at the land surface raising the surface temperature. The warm climate conditions are enhanced and the hydrological cycle is less intensive in the online simulation. The positive feedback on drought conditions during warm and dry summer and autumn seasons intensifies the effect of water limitation in the coupled model simulation, which leads to another decrease in LAI. Thus, the interannual variability of the LAI is enhanced by the interaction between plant phenology and the simulated climate. However, it is not completely understood, why the local cycle of water is reduced, why there is less water available. Some changes in atmospheric circulations might be the reason. They are not investigated in the current study. Altogether, the climate feedback of the interannual variability of vegetation is small under today's climate conditions. This might change under future climate conditions. If the climate feedback of vegetation phenology increases under climate warming, the coherences between vertical and horizontal atmospheric dynamics should be investigated with more detail to solve these open questions.

The introduced dynamic phenology scheme PHENO relates basic phenological phases, such as the onset and end of the vegetation growing season, directly to climate parameters simulated by REMO. Our research was on the biogeophysical interactions between vegetation phenology and climate variability, with focus on the hydrological cycle. Hereby, we also consider the effect of water availability on vegetation phenology. It does not account for biogeochemical cycles. Thus, no complex vegetation model is needed to drive the phenology scheme. However, in the case that carbon and other nutrients become dominant factors for the plant growth, the model is not applicable. As the PHENO model needs no additional input data and simulates no complex vegetation processes, the computational efforts on processing power, working memory and storage space are low. It can be used in climate simulations fully coupled to the regional model by default. The use of the PHENO scheme leads to an improved representation of vegetation in REMO, that may become especially important in climate change simulations.

The results reveal a strong impact of the future climate warming on plant phenology, which again would affect the simulated climate change. Within further studies it will be quite interesting to perform another regional climate projection for the period 2071 to 2100 with the regional climate model fully coupled to the PHENO scheme. Will the changes in vegetation phenology lead to positive feedbacks on the climate warming? Will the effects of interannual variability of vegetation phenology on the simulated climate increase under climate change conditions projected for the end of the century?

The long-term climate trends and land use changes will certainly also modify the spatial distribution of vegetation types. For the phenology scheme, this would mean changes in the spatial distribution of minimum and maximum LAI values. As these changes occur on longer time scales than plant phenological cycles, variable minimum and maximum LAI values computed by a complex vegetation model could be annual input to the PHENO scheme. To account for land use changes, the spatial vegetation variability retrieved from satellite data could be applied for today's climate. The results of a land use change scenario could be used as input data for future climate projections.

Chapter 6

Overall conclusions and outlook

The biogeophysical interactions between vegetation phenology and the regional climate were investigated by model simulation studies using the regional climate model REMO. The seasonal vegetation variability was successfully integrated into REMO by the following 3 steps:

1. The seasonal vegetation cycle was implemented into the regional climate model REMO, and its impact on the simulated climate over Europe was investigated.

2. An advanced parameterisation of the snow-free land surface albedo was developed for climate modelling, which describes the seasonal variation of albedo as a function of vegetation phenology. Global maps of separated soil and vegetation albedo were derived from MODIS data, and applied to compute the annual albedo cycle from monthly values of the leaf area index. The seasonal background albedo cycle was integrated into the land surface scheme of REMO in order to study the sensitivity of the climate model to the advanced albedo parameterisation. In addition, the advanced albedo parameterisation was implemented into the global climate model ECHAM5, and the influence on the simulated global climate was investigated.

3. A plant phenology scheme, which relates the species-averaged vegetation parameter LAI directly to the simulated climate parameters, was developed. It was fully coupled to the regional climate model REMO in order to study the dynamic interactions between the vegetation phenology and the climate.

Each advancement was extensively tested, and the impact on the simulated climate was investigated, respectively. The evaluations were done with focus on the questions verbalised in chapter 1. 3 and shall be answered as follows:

How is the near-surface climate affected by seasonal vegetation variability? What are the impacts on vertical surface fluxes, near-surface temperature and precipitation?

Seasonal vegetation variability strongly affects the water and energy fluxes at the land surface. During the summer season, the increase of the LAI and of the fractional green vegetation cover considerably enhances the evapotranspiration and the latent heat flux, whereas the sensible heat flux decreases. These changes lead to lower surface temperatures and increased precipitation during the summer season. The results are in line with many other studies on the impact of vegetation on the climate (e. g. Bounoua et al. 2000, Crucifix et al. 2005, Sánchez et al. 2007).

Is the effect of vegetation phenology on climate varying with regard to different regions of Europe and with regard to the different seasons?

The effect of seasonal vegetation variability on the simulated climate over Europe clearly varies from one subregion to antoher. The most significant effects occur over eastern and central Europe. In these regions, land-atmosphere interactions play a dominant role due to the long distance to the sea with the influence of the Atlantic climate decreasing and the continental climate conditions increasing. In contrast, the simulated climate in the western European regions close to the sea are less affected by the modified vegetation parameterisation due to dominant large scale weather conditions. In these regions, the westerlies suppress the influence of vegetation-atmosphere interactions on climate.

All over Europe, the vegetation effect mainly occurs in the summer season. The exchange processes of mass and energy at the land surface are most intensive due to the high solar radiation input and the enhanced convective activity during this season. These processes are strongly controlled by land surface properties. The simulated climate for the winter season is only slightly affected. This is mainly due to the snow cover which disconnects vegetation from the atmosphere.

Does the vegetation effect on climate simulations depend on the spatial horizontal resolution of the climate modelling grid?

The sensitivity of REMO to a mean annual vegetation cycle was examined at 0.5 degree and 0.l6 degree horizontal resolution. The comparison of the model simulations showed no influence of the different horizontal resolutions on the effects of the modified vegetation treatment on the mean climate in Europe. The horizontal distribution of the results with higher resolution shows more geographical detail.

The studies with the new PHENO scheme, however, show the importance of the resolution of the climate model data. The LAI values simulated by PHENO and driven by REMO-50km and by REMO-10km, respectively, were compared to remotely sensed data from MODIDS and CYCLOPES. The PHENO results driven by the climate data with the higher resolution are in better agreement with the observations. The LAI decreases earlier during the summer of 2003 than of 2002 due to the strong water limitation. In the PHENO LAI simulation driven by REMO-10km, the effect of water limitation is much more pronounced than in the LAI simulation driven by REMO-50km. The climate data at higher horizontal resolution show more geographical detail, especially of precipitation and soil moisture. Thus, it better represents the local hydrological cycle at the surface. As the near-surface moisture conditions strongly link the vegetation to the atmosphere, this may be the reason for the better results of the PHENO version which was driven by the higher resoluted climate data.

Do the advanced vegetation treatments improve the climate model simulation results with regard to observations?

The implementation of an annual vegetation cycle into the REMO model improves the simulation of the near-surface temperature in comparison to the observations of CRU. The

overestimation of the 2m-temperature during the summer season is significantly reduced by the vegetation effect, except for the Iberian peninsula. There, the mean absolute deviation between the simulation and the observation increases, because the winter 2m-temperatures are underestimated. With regard to precipitation, the deviations from the observations of CRU and GPCP increase in the Baltic and the Mediterranean area. Central and eastern Europe including the Hungarian lowlands show improved results.

The implementation of an advanced land surface albedo scheme into the regional climate model REMO and the global climate model ECHAM yields no significant improvement of the regional nor the global simulation results with regard to the near-surface temperature and the precipitation. For both, the regional and the global study, the temperature differences to the observations are larger than the differences between the three model simulations. Thus, the sensitivity of the simulated temperature and precipitation to the changed albedo parameterisation lies within the uncertainty range of the simulated model results compared to the observational data sets used in this study.

How strong is the effect of seasonal albedo variations caused by vegetation phenology on the simulated near-surface climate? Do the global and the regional climate model simulations respond differently to the advanced albedo parameterisation?

The effect of the seasonal albedo variations is superposed by the effect of the new background albedo mean, which is significantly reduced by the new albedo parameterisation. In the global climate simulations, the lower mean albedo directly translates into higher net surface solar radiation in the mid-latitudes over the continents, especially during the summer season when the solar input is high. The higher net solar radiation input to the land surface leads to higher surface temperatures. In contrast, the effects caused by the seasonal variability in background albedo during the summer season are quite low. But in winter an interesting effect occurs over central Siberia and in the northwest of Alaska. The surface temperatures there decrease by more than 2K over a large area. In this region, the background albedo did not change at all. Even snow cover or snow albedo make no differences. The significant temperature decrease is a remote effect of the seasonal land surface albedo variability and can only be explained by the modification of the planetary-scale atmospheric circulation. Also the precipitation changes are remote effects of the lower mean surface albedo and the seasonal surface albedo variability, occurring in most cases over the ocean.

In the regional climate simulations, the lower mean albedo also leads to higher net surface solar radiation input to the surface, as such raising the near-surface temperature during the summer season. In these simulations, the seasonal albedo variability also affects the near-surface climate. In most of the regions of Europe, plant phenology increases the surface albedo during summer, because the underlying soils are darker than the vegetation cover there. The higher surface albedo reduces the solar radiation input to the surface and decreases the temperatures. Thus, the effects of the new albedo mean and the seasonally varying albedo on surface temperatures compensate each other in most regions in summer. During the winter season, the seasonal albedo variability has no effects on the temperatures. With regard to precipitation, systematic differences seem to occur over the Alps and over South-West-Scandinavia in summer with the lower albedo mean leading to higher precipitation and the higher summer albedo (compared to the mean albedo) leading to lower precipitations. But these differences are not significant compared to the high total amount of precipitation in both

regions. They might indicate some smaller changes in the circulation patterns within the regional model domain. But these changes are much less pronounced than in the global model experiments.

In both, the global and the regional simulations, clear effects occur over Europe, but, in most cases, with contrary responses to the new land surface albedo scheme. In contrast to the global simulation, where the large-scale atmospheric conditions are changed by the new albedo parameterisation, in the regional simulations, the circulation patterns within the model domain are not influenced. The external forcing via the lateral boundaries of the regional model domain suppresses changes in the large-scale circulation that might occur without the external forcing. In the regional model simulations, local effects mainly occur during the summer season. In summer, the vertical energy exchange at the land surface is enhanced compared to the winter season, when snow cover dominates the surface properties. In the global model simulations, the effects on the simulated climate are not restricted to regions where land surface albedo is changed, but also occur in remote regions through atmospheric teleconnections. The comparison between the regional and the global studies for the selected European regions yielded that the global results showed higher sensitivity of the annual temperature and the precipitation cycles to the changed albedo parameterisation.

Is a simple phenology model capable of representing the interannual variability and temporal trends in vegetation phenology caused by climate variability?

The simple phenology model PHENO is capable of representing the interannual variability and the temporal trends in vegetation phenology caused by climate variability. In Germany, the timing of the leaf expansion in spring is varying from year to year in dependence on the surface temperatures. The leaf senescence in fall is varying in subject to the surface temperatures and the soil moisture content. Especially in warm and dry years, the LAI decreases earlier in late summer/autumn due to water limiting conditions. This can be proved by the comparison of the simulated LAI to the LAI retrieved from satellite data for the years 2002 and 2003. During the extremely hot and dry summer of 2003, plants were wilting and tree leaves were shrinking due to water stress. This is also captured by the model results, which show an earlier decrease in LAI values compared to the summer of 2002. In most parts of Europe, temperature is the dominant limiting plant growth factor. However, in eastern Europe and especially in southern Europe, water is becoming the dominant limitation factor of plant growing during summer and autumn. The earlier decrease in the annual LAI compared to the mean LAI cycle is more pronounced during summer seasons with hot and dry weather conditions. The observed long-term trends in plant phenology, which have been investigated in many ecological studies, are captured by the PHENO simulations. The onset of spring phenology is 5.9 days earlier and the growing season becomes 4.1 days longer during the simulated period from 1958 to 2003. This means that in warm and dry years the earlier start of the growing season is compensated by limited growing conditions during summer and autumn. As a consequence, the vegetation period is only shifted or even shortened.

How is vegetation phenology affected by climate warming conditions simulated by a future climate projection for the end of the century?

The PHENO model was driven by the results of a regional climate projection for the time period from 2071 to 2100. The simulated 30-year LAI mean was compared to the LAI climatology from 1958 to 1987. The evaluations indicate substantial changes in the vegetation phenology under climate warming conditions. In northern, eastern and central Europe, the growing season is lengthened by up to 2 months due to higher temperatures. In western Europe, the length of the vegetation period is even no longer limited by low temperatures. In southern Europe, the water limitation for the plant growing increases during summer and autumn due to hot and dry weather conditions.

What is the feedback effect of interannual variability of vegetation phenology on the simulated regional climate and vegetation itself?

For today's climate, the feedback of the interannual variability of the plant phenology on the simulated climate as well as on the vegetation itself was investigated by the PHENO online simulation fully coupled to REMO. The evaluations for Germany show reduced LAI values in warm and dry summer and autumn seasons in the online simulation compared to the offline simulation. The lower LAI reduces the evapotranspiration as well as convective precipitation processes. Thus, the water supply to the soil is lower, and the soil wetness is reduced. Moreover, the land surface albedo is reduced due to the lower LAI values. Therefore, more energy remains at the land surface, which leads to a raise of the surface temperature. The warm climate conditions are enhanced, and the hydrological cycle is less intensive in the online simulation. However, it remains unclear, why there is less water available. Some changes in the atmospheric circulations might be the reason. They, however, are not investigated in the current study. Altogether, the climate feedback of the interannual variability of vegetation is small under today's climate conditions. This might change under future climate conditions. If the climate feedback of vegetation phenology increases under climate warming, the coherences between vertical and horizontal atmospheric dynamics need to be investigated in more detail to answer the open questions.

The positive feedback on drought conditions during warm and dry summer and autumn seasons intensifies the effect of water limitation in the coupled model simulation leading to another decrease in LAI. Thus, the interannual variability of the LAI is enhanced by the interaction between the plant phenology and the simulated climate. The effect of the interannual variability of vegetation phenology on the climate variability with regard to temperature and moisture conditions is marginal. There is no feedback effect on the long-term means and trends of the simulated climate.

To conclude: the analyses of this thesis demonstrate strong interactions between vegetation phenology and climate variability over Europe. The interactions differ from region to region and from season to season. In all experiments of this thesis, the main effects occur in eastern Europe where land-atmosphere interactions play an important role due to the dominating

continental climate conditions. With regard to temporal scales, main effects occur during the summer season, when exchange processes of mass and energy at the land surface are most intensive and strongly controlled by the land surface properties. To compare the effect of the seasonal albedo variations to the effect of seasonal LAI variations simulated by REMO, the experiment from the first study of this thesis was rerun by performing another model simulation with the same setup as in study three of this thesis, but with constant vegetation cover over the year. The results reveal that the influence of the seasonal LAI variability on the near-surface climate is much stronger than the influence of seasonal albedo variability (not shown). Compared to the effects of the mean annual vegetation cycle, the interannual variability of the vegetation phenology has only minor effects on the simulated present-day climate over Europe.

In this thesis, only the temporal vegetation variability is considered. The long-term climate trends will certainly modify the spatial distribution of vegetation types as well. For the phenology scheme, this would mean changes in the spatial distribution of minimum and maximum LAI values. As these changes occur on longer time scales than plant phenological cycles, the variable minimum and maximum LAI values could be first simulated by a complex vegetation model and then used as annual input to the PHENO model. To account for land use changes in the present or past, the spatial vegetation variability retrieved from satellite data could be applied for today's climate. For future climate projections, the spatial distribution of vegetation types could be taken from vegetation model simulations assuming a certain land use change scenario. This would allow for many further investigations on the vegetation effect on the climate. How strong is the impact of spatial vegetation variability on the regional climate? How will the combined effects of temporal and spatial variability of vegetation influence the simulated climate?

The effects of vegetation on the simulated regional climate can be superposed by uncertainties due to deficiencies in other model parameterisations as, for example, in aerosol processes or in the treatment of convective clouds. The thesis of Pfeifer (2006) revealed the strong impacts of advanced cloud parameterisations on the simulated regional climate. An advanced representation of aerosol processes in REMO is being worked on, and its impacts on the regional climate in South America is being investigated by Class Teichmann (personal communication). Other possible human impacts such as land use changes or water management should also be accounted for. Studies on the land use and water availability in the Aral sea region are currently done by Eva Starke (personal communication). Investigations on the influence of small-scale local land use (<10 km) on the local to the regional climate are being prepared by Swantje Preuschmann (personal communication). With the recent development of a new dynamical core for the REMO model by Holger Goettel (personal communication), climate model simulations on horizontal resolutions of less than 10 km have become possible. A model grid size of 1 km will facilitate the explicit representation of single land cover types in REMO, which are available from the land use data of LSPII, that were retrieved from satellite data at 1 km horizontal resolution. This will allow for substantial advancements of the vegetation processes in the REMO model.

To emphasise an interesting result which brings up new questions for ongoing research activities: The investigations on the dynamic interactions between vegetation phenology and climate indicate that soil moisture is a relevant factor in land-atmosphere coupling. It strongly links vegetation phenology to climate variability. Soil-moisture-atmosphere-feedbacks were investigated in several recent studies, which confirm the strong influence of soil moisture on climate variability. Seneviratne et al. (2006) emphasise the importance of soil-moisture-

climate-feedbacks as processes which influence the summer climate variability in Europe. The study of Fischer et al. (2007) showed that soil moisture is an important parameter influencing the formation of European summer heatwaves as experienced in 2003. The lack of soil moisture due to a large precipitation deficit together with early vegetation green-up and strong positive radiative anomalies in the months preceding the extreme summer event strongly reduced latent cooling, and thereby, amplified the surface temperature anomalies. Moreover, they found that drought conditions influence the tropospheric circulation by producing a surface heat low and an enhanced ridging in the mid-troposphere. This suggests a positive feedback mechanism between soil moisture, continental-scale circulation and temperature. With the new PHENO model, dynamic vegetation phenology processes are now considered in the regional climate model simulations, and the feedbacks between vegetation phenology, soil moisture and atmosphere can be investigated. Some of the first evaluations on this topic are dealt with in this thesis. The dynamic interactions between vegetation phenology, soil moisture and atmosphere lead to a positive feedback on drought conditions during warm and dry summer and autumn seasons. This intensifies the effect of water limitation in the coupled model simulation leading to another decrease in vegetation cover. But why is the local cycle of water reduced, why is there less water available? Might changes in the regional atmospheric circulation be the reason? The coherences between vertical and horizontal atmospheric dynamics need to be investigated in detail to answer the open questions.

What is the benefit of the advanced vegetation parameterisations developed within this work? First, the influence of the temporal vegetation variability on the simulated mean climate over Europe could be investigated. Second, the implementation of an annual vegetation cycle improves the regional climate model simulations with regard to the simulated annual mean near-surface temperature cycles over Europe. In reference to precipitation, the regions with dominant vertical land-atmosphere interactions under continental climate conditions in central and eastern Europe show improved results. Third, the advanced albedo scheme allows for new studies on land use changes. For instance, what are the consequences of the extensive planting of rape on the regional and global climate? Rape will considerably lighten the land surface during bloom. What are the climate impacts of the increased land surface albedo? The results of this thesis indicate the strong influence of land albedo changes on the simulated climate. The global climate experiments also demonstrate remote effects of relatively small albedo changes through atmospheric teleconnections. This means that extensive planting of canola in the USA can influence the climate in Europe. Land conversion effects are quite complex and a big challenge for ongoing research activities. Research on the interactions between land use change and climate are of high socio-political interest and are important for decisions on adaptation strategies.

Finally, the new PHENO scheme couples for the first time the vegetation and the atmosphere within the regional climate model REMO. The vegetation is no longer only a constant boundary condition to the regional climate simulations. Now, feedbacks from the atmosphere to the vegetation can occur. The dynamic interactions between vegetation phenology and climate variability can now be investigated. The land-climate coupling will be especially important for model simulations of the future climate as no vegetation input from observations is available. Will future climate warming and the potential increase in climate variability enhance the importance of vegetation phenology in land-atmosphere-feedbacks? The results of the last study of this thesis revealed a strong impact of the future climate warming on plant phenology. This was investigated by a PHENO simulation in offline mode, driven by the results of a regional climate projection. In this connection, feedback effects

were not considered. But the strong changes of plant phenology will certainly affect the simulated climate change. Within further studies, it will be quite interesting to perform another regional climate projection for the period 2071 to 2100 with the regional climate model fully coupled to the PHENO scheme. Will the changes in vegetation phenology lead to positive feedbacks on the climate warming? What will be the importance of soil moisture in land-atmosphere-feedbacks under future climate conditions? Will the effects of interannual variability of vegetation phenology on the simulated climate increase under climate change conditions projected for the end of the century? Altogether, the advanced representation of vegetation in the regional climate model facilitates many new investigations on the interactions between vegetation and climate, and will give more answers to open questions.

Bibliography

Ahas R, Aasa A, Menzel A, Fedotova G, Scheifinger H (2002) Changes in European spring phenology. Int J Climatol, 22, 1727-1738

Ahas R (1999) Long-term phyto-, ornitho- and ichthyophenological time-series analysis in Estonia. Int J Biometeorol, 42, 119-123

Avissar R, Liu Y (1996) Three-dimensional numerical study of shallow convective clouds and precipitation induced by land surface forcing. J Geophys Res, 101, 7499-7518

Avissar R, Verstraete MM (1990) The representation of continental surface processes in atmospheric models. Rev Geophys, 28, 35-52

Baret, F, O Hagolle, B Geiger, P Bicheron, B Miras, M Huc, B Berthelot, f Nino, M Weiss, O Samain, JL Roujean, and M Leroy, LAI, FAPAR, and FCover CYCLOPES global products derived from Vegetation. Part 1 : principles of the algorithm, Remote Sensing of Environment, 110:305-316, 2007

Beaubien EG, Freeland HJ (2000) Spring phenology trends in Alberta, Canada: Links to ocean temperature. Int J Biometeorol, 44, 53-59

Berbet MLC, Costa MH (2003) Climate change after tropical deforestation: Seasonal variability of surface albedo and its effects on precipitation change. J Clim, 116, 2099-2104

Betts RA (2001) Biogeophysical impacts of land use on present-day climate: Near-surface temperature change and radiative forcing. Atmos Sci Lett, 2, doi: 10.1006/asle.2000.0023.

Bonan GB, Levis S, Sitch S, Vertenstein M, Oleson KW (2003) A dynamic global vegetation model for use with climate models: concepts and description of simulated vegetation dynamics. Glob Chang Biol, 9, 1543-1566

Bonan GB, Levis S, Kergoat L, Oleson KW (2002) Landscapes as patches of plant functional types: an integration concept for climate and ecosystem models. Glob Biogeochem Cycles, 16, 5.1-5.25

Bonan GB, Oleson KW, Vertenstein M, Levis S, Zeng X, Dai Y, Dickinson RE, Yang ZL (2002) The land surface climatology of the Community Land Model coupled to the NCAR Community Climate Model. J Clim, 15, 3123–3149

Bonan GB (1997) Effects of land use on the climate of the United States. Clim Chang, 37, 449-486

Bonan GB, Pollard D, Thompson SL (1992) Effects of boreal forest vegetation on global climate. Nature, 359, 716-718

Bougeault P, 1983: A non-reactive upper boundary condition for limited-height hydrostatic models. Mon Weather Rev, 111, 420-429

Bounoua L, Collatz GJ, Los SO, Sellers PJ, Dazlich DA, Tucker CJ, Randall DA (2000) Sensitivity of climate to changes in NDVI. J Clim, 13, 2277-2292

Bremicker M (1998) Aufbau eines Wasserhaushaltmodells für das Weser- und Ostsee-Einzugsgebiet als Baustein eines Atmosphären-Hydrologie-Modells. Dissertation an der Geowissenschaftlichen Fakultär der Albert-Ludwigs-Universität Freiburg, 36 pp

Bruns E (2007) Phänologische Beobachtungsnetze heute und gestern. Promet, 33, 2-6

Buermann W, Dong J, Zeng X, Myneni RB, Dickinson RE (2001) Evaluation of the utility of satellite-based vegetation leaf area index data for climate simulations. J Clim, 14, 3536-3550

Burke EJ, Shuttleworth WJ, Yang ZL, Mullen SL, Arain, MA (2000) The impact of the parameterization of heterogeneous vegetation on the modeled large-scale circulation in CCM3-BATS. Geophys Res Let, 27, 397-400

Cayan DR, Kammerdiener SA, Dettinger MD, Caprio JM, Peterson DH (2001) Changes in the onset of spring in the western united states. Bull Am Meteorol Soc 82, 399-415

Charney JG (1975) Dynamics of deserts and drought in Sahel. QJR Met Soc, 101,193-202

Chase TN, Pielke RA, Kittel TGF, Zhao M, Pitman AJ, Nemani RR, Running SW (2002) Relative climatic effects of landcover change and elevated carbon dioxide combined with aerosols: a comparison of model results and observations. J Geophys Res, 106, 31685-31691

Chase TN, Pielke RA, Kittel TGF, Nemani R, Running SW (2000) Simulated impacts of historical land cover changes on global climate in northern winter. Clim Dyn, 16, 93-105

Chase TN, Pielke RA, Kittel TGF, Nemani R, Running SR (1996) The sensitivity of a general circulation model to global changes in leaf area index. J Geophys Res, 101, 7393-7408

Chapin FS, Starfield AM (1997) Time lags and novel ecosystems in response to transient climatic change in arctiv Alaska. Clim Chang, 35, 449-461

Chen X, Zhongjun T, Schwartz MD, Xu C (2000) Determining the growing season of land vegetation on the basis of plant phenology and satellite data in Northern China. Int J Biometeorol, 44, 97-101

Chen JM, Rich PM, Gower ST, Norman JM, Plummer S (1997) Leaf area index of boreal forests: Theory, techniques, and measurements. J Geophys Res, 102, 29429-29444, 10.1029/97JD01107

Chmielewski FM, Müller A, Küchler W (2005) Possible impacts of climate change on natural vegetation in Saxony (Germany). Int J Biometeorol, 50, 96-104

Chmielewski FM, Rötzer T (2002) Annual and spatial variability of the beginning of growing season in Europe in relation to air temperature changes. Clim Res, 19, 257-264

Chmielewski FM, Rötzer T (2001) Response of tree phenology to climate change across Europe. Agric For Meteorol, 108, 101-112

Chmielewski FM, Rötzer T (2000) Phenological trends in Europe in relation to climatic changes. Agrarmeteorologische Schrift 07 der Humboldt Universität Berlin

Chmielewski FM (1996) The international phenological gardens across Europe. Present state and perspectives. Phenol Season, 1, 19-23

Chuine I, Kramer K, Hänninen H (2003) Plant development models. In: Schwartz MD (ed) Phenology: an integrative environmental science. Kluwer, 217-235

Collins DC, Avissar R (1994) An evaluation with the Fourier Amplitude Sensitivity Test (FAST) of which land surface parameters are of greatest importance in atmospheric modelling. J Clim, 7, 681

Cox PM, Betts RA, Bunton CB, Essery RLH, PR Rowntree, Smith J (1999) The impact of new land surface physics on the GCM sensitivity of climate and climate sensitivity. Clim Dyn, 15, 183-203

Cramer W, Bondeau A,Woodward FI, Prentice IC, Betts RA, Brovkin V, Cox J, Fisher V, Foley JA, Friend AD, Kucharik C, Lomas MR, Ramankutty N, Sitch S, Smith B, White A, Molling YC (2001) Global response of terrestrial ecosystem structure and function to CO_2 and climate change: results from six dynamic global vegetation models. Glob Chang Biol, 7, 357-373

Crucifix M, Betts RA, Cox PM (2005) Vegetation and climate variability: a GCM modelling study. Clim Dyn, 24, 457-467

Dai Y, Zeng X, Dickinson RE, Baker I, Bonan GB, Bosilovich MG, Denning AS, Dirmeyer PA, Houser PR, Niu G, Oleson KW, Schlosser CA, Yang ZL (2003) The Common Land Model, Bull Am Meteorol Soc, 84, 1013–1023

Davies HC (1976) A lateral boundary formulation for multi-level prediction models. Q J R Meteorol Soc, 102, 405-418

Defila C, Clot B (2001) Phytophenological trends in Switzerland. Int J Biometeorol, 45, 203-207

Dickinson RE, Henderson-Sellers A and Kennedy P (1993) Biosphere-atmosphere transfer scheme (BATS) version 1e as coupled to the NCAR community climate model. NCAR Technical Note TN-387+STR, National Center for Atmospheric Research, Boulder, Colorado

Dickinson RE, Hanson B (1984) Vegetation-albedo feedbacks, in Climate Processes and Climate Sensitivity, Geophys Monogr Ser, 29, edited by Hanson JE and Takahashi T, pp 180-186, AGU, Washington, DC

Dirmeyer PA, Shukla, J (1994) Albedo as a modulator of climate response to tropical deforestation. J Geophys Res, 99, 20,863-20,877.

DKRZ (1993) Deutsches Klimarechenzentrum: The ECHAM-3 general circulation model. DKRZ Technical Report, No. 6, Hamburg

Dose V, Menzel A (2006) Bayesian correlation between temperature and blossom onset data. Glob Chang Biol, 12, 1451-1459

Dümenil L, Todini E (1992) A rainfall-runoff scheme for use in the Hamburg climate model. In: Advances in Theoretical Hydrology, A Tribute to James Dooge (Ed. J.P. O'Kane). European Geophysical Society Series on Hydrological Sciences, 1, Elsevier Press Amsterdam, 129-157

Eidenshink JC, Faundeen JL (1994) The 1 km AVHRR global land dataset: First stages in implementation. Int J Remote Sens, 15, 3443-3462

Fischer EM, Seneviratne SI, Vidale PL, Lüthi D, Schär C (2007) Soil moisture–atmosphere interactions during the 2003 European summer heat wave. J Clim, 20, 5081–5099.

Foley JA, Levis S, Costa MH, Cramer W, Pollard D (2000) Incorporating dynamic vegetation cover within global climate models. Ecol Appl, 10, 1620–1632

Foley JA, Levis S, Prentice IC, Pollard D, Thompson SL (1998) Coupling dynamic models of climate and vegetation. Glob Chang Biol, 4, 561–579

Foley JA, Kutzbach JE, Coe MT, Levis S (1994) Feedbacks between climate and boreal forests during the Holocene epoch. Nature, 371, 52-54

Fraedrich K, Kleidon A, Lunkeit F (1999) A Green Planet versus a Desert World: Estimating the Effect of Vegetation Extremes on the Atmosphere. J Clim, 12, 3156-3163

Galán C, Fuillerat JM, Comtois P, Dominguez-Vilches E (1998) Bioclimatic factors affecting daily Cupressaceae flowering in southwest Spain. Int J Biometeorol, 41, 95-100

Gao F, Schaaf CB, Strahler AH, Roesch A, Lucht W, Dickinson R (2005) MODIS bidirectional reflectance distribution function and albedo Climate Modeling Grid products and the variability of albedo for major global vegetation types. J Geophys Res, 110, D01104, doi: 10.1029/2004JD005190

Garratt J (1993): Sensitivity of climate simulations to land-surface and atmospheric boundary-layer treatments-A review. J Clim, 6, 419–448

Gibbard S, Caldeira K, Bala G, Phillips TJ, Wickett M (2005) Climate effects of global land cover change. Geophys Res Lett, 32, L23705, doi:10.1029/2005GL024550

Gibson JK, Kållberg P, Uppala S, Hernandez A, Nomura A, Serrano E (1997) Era description. ECMWF Re-Anal Proj Rep Ser 1, Reading, UK

Goirgi F, Bi X (2000) A study of internal variability of a regional climate model. J Geophys Res, 105, 29503-29521

Gower ST, Kucharik CJ, Norman JM (1999) Direct and indirect estimation of leaf area index, fAPAR and net primary production of terrestrial ecosystems. Remote Sens Environ, 70, 29–51

Göttel H, Alexander J, Rechid D, Wolf A, Jacob D (2008) Influence of changed vegetation fields on regional climate simulations in the Barents Sea Region. Clim Change, 87, 35-50

Häninnen H (1994) Effects of climatic change on trees from cool and temperate regions: an ecophysiological approach to modeling of bud burst phenology. Can J Bot, 73, 183-199

Häninnen H, Kellomäki S, Laitinen K, Pajari B, Repo T (1993) Effect of increased winter temperature on the onset of height growth of Scots pine: A field test of a phenological model. Silva Fenn, 27, 251-257

Häninnen H (1990) Modelling bud dormancy release in trees from cool and temperate regions. Acta Forestalia Fenn, 231, 47

Hagemann S (2002) An improved land surface parameter dataset for global and regional climate models. Report 336, Max-Planck-Institute for Meteorology, Hamburg

Hagemann S, Botzet M, Machenhauer B (2001) The summer drying problem over south-eastern Europe: Sensitivity of the limited area model HIRHAM4 to improvements in physical parameterizations and resolution. Phys Chem Earth B, 26, 391-396

Hagemann S, Botzet M, Dümenil L, Machenhauer M (1999) Derivation of global GCM boundary conditions from 1 km land use satellite data. Report 289, Max-Planck-Institute for Meteorology, Hamburg

Hari P, Häkkinen R (1991) The utilization of old phenological time series of budburst to compare models describing annual cycles of plants. Tree Physiol, 8, 281-287, 1991

Henderson-Sellers A (1993) A factorial assessment of the sensitivity of the BATS land-surface parameterization scheme. J Clim, 6, 227-247

Henderson-Sellers A, Yang ZL, Dickinson RE (1993) The Project for Intercomparison of Land-surface Parameterization Schemes, Bull Am Meteorol Soc, 74, 1335-1349

Houghton JT, Ding Y, Griggs DJ, Noguer M, van der Linden PJ, Xiaosu D (2001) Climate change 2001. The scientific basis. Contribution of Working Group I to the Third Assessment Report of the Intergovernmental Panel on Climate Change

Huffman GJ, Adler RF, Arkin A, Chang A, Ferraro R, Gruber A, Janowiak J, Joyce RJ, McNab A, Rudolf B, Schneider U, Xie, P (1997) The Global Precipitation Climatology Project (GPCP) combined precipitation data set. Bull Am Meteorol Soc, 78, 5-20

Humbolt, A von (1807) Ideen zu einer Geographie der Pflanzen. Tübingen

IPCC 2007: The Physical Science Basis. Contribution of Working Group I to the Fourth Assessment Report of the Intergovernmental Panel on Climate Change [Solomon, S, D Qin, M Manning, Z Chen, M Marquis, KB Averyt, M Tignor and HL Miller (eds)], Cambridge UniversityPress, Cambridge, United Kingdom and New York, NY, USA

Jaagus J, Ahas R (2000) Space-time variations of climatic seasons and their correlation with the phenological development of nature in Estonia. Clim Res, 15, 207-219

Jacob D, Göttel H, Kotlarski S, Lorenz P, Sieck K (2008): Klimaauswirkungen und Anpassung in Deutschland: Erstellung regionaler Klimaszenarien für Deutschland mit dem Klimamodell REMO. Forschungsbericht 204 41 138 Teil 2, i.A. des UBA Dessau

Jacob D, Barring L, Christensen OB, Christensen JH, de Castro M, Deque M, Giorgi F, Hagemann S, Lenderink G, Rockel B, Sanchez E, Schar C, Seneviratne SI, Somot S, van Ulden A, van den Hurk B (2007): An inter-comparison of regional climate models for Europe: model performance in present-day climate, Clim Change, 81, 31-52

Jacob D, Andrae U, Elgered G, Fortelius C, Graham PL, Jackson SD, Karstens U, Koepken C, Lindau R, Podzun R, Rockel B, Rubel F, Sass HB, Smith RND, Van den Hurk BJJM, Yang X (2001) A comprehensive model inter-comparison study investigating the water budget during the BALTEX-PIDCAP period. Meteorol Atmos Phys, 77, 19-43

Jacob D (2001) A note to the simulation of the annual and interannual variability of the water budget over the Baltic Sea drainage basin. Meteorol Atmos Phys, 77, 61-73

Jacob D, Podzun R (1997) Sensitivity studies with the regional climate model REMO. Meteorol Atmos Phys, 63, 119-129

Jarvis PG, Leverez JW (1983) Productivity of temperate deciduous and evergreen forests. In: Ecosystem process: Mineral cycling, productivity and man's influence. Physiological plant ecology, New series, Vol. 12D, eds Lange, OL, Nobel PS, Osmond CB, Ziegler H, Springer Verlag, New York, 233-280 pp

Jin Y, Schaaf CB, Gao F, Li X, Strahler AH, Lucht W, Liang S (2003a) Consistency of MODIS surface bidirectional reflectance distribution function and albedo retrievals: 1. Algorithm performance. J Geophys Res, 108(D5), 4158, doi:10.1029/2002JD002803

Jin Y, Schaaf CB, Woodcock CE, Gao F, Li X, Strahler AH, Lucht W, Liang S (2003b) Consistency of MODIS surface bidirectional reflectance distribution function and albedo retrievals: 2. Validation, J Geophys Res, 108(D5), 4159, doi:10.1029/2002JD002804.002804

Kleidon A, Fraedrich K, Heimann M (2000) A green planet versus a desert world: Estimating the maximum effect of vegetation on the land surface climate. Clim Chang, 44, 471-493

Knorr W (2000) Annual and interannual CO_2 exchanges of the terrestrial biosphere: process based simulations and uncertainties. Glob Ecol and Biogeogr, 9, 225-252

Köppen W (1936) Das geographische System der Klimate. In: Köppen W, Geiger R (1936) Handbuch der Klimatologie, Borntraeger, Berlin, 46 pp

Koster RD, Suarez MJ (2004) Suggestion in the observational record of land-atmopshere feedback operating at seasonal time scales. J Hydrometeor, 5, 567-572

Kramer K, Leinonen I, Loustau D (2000) The importance of phenology for the evaluation of impact of climate change on growth of boreal, temperate and Mediterranean forests eccosystems: an overview. Int J Biometeorol, 44, 67-75

Kramer K (1995) Modelling comparison to evaluate the importance of phenology and spring frost damage for the effects of climate change on growth of mixed temperate-zone decidious forests. Clim Res, 7, 31-41

Kramer K (1994) Selecting a model to predict the onset of growth of Fagus sylvatica. J Appl Ecol, 31, 172-181

Krinner G, Viovy N, Noblet-Ducoudré N de, Ogée J, Polcher J, Friedlingstein P, Ciais P, Sitch S, Prentice IC (2005) A dynamic global vegetation model for studies of the coupled atmosphere-biosphere system. Glob Biogeochem Cycles, 19, GB1015, doi:10.1029/2003GB002199

Lawrence DM, Slingo JM (2004a) An annual cycle of vegetation in a GCM. Part I: Implementation and impact on evaporation. Clim Dyn, 22, 87–105

Lawrence DM, Slingo JM (2004b) An annual cycle of vegetation in a GCM. Part II: Global impacts on climate and hydrology. Clim Dyn, 22, 107–122

Levis S, Foley JA, Pollard D (2000) Large-Scale Vegetation Feedbacks on a Doubled CO_2 Climate. J Clim, 13, 1313–1325

Levis S, Foley JA, Pollard D (1999) Potential high-latitude vegetation feedbacks on CO2-induced climate change. Geophys Res Let, 26, 747-750

Liang S, Fang H, Chen M, Shuey CJ, Walthall C, Daughtry C, Morisette J, Schaaf C, Strahler A (2002) Validating MODIS land surface reflectance and albedo products: Methods and preliminary results. Remote Sens Environ, 83, 149-162

Liang X-Z, Xu M, Gao W, Kunkel K, Slusser J, Dai Y, Min Q, Houser PR, Rodell M, Schaaf CB, Gao F (2005) Development of land surface albedo parameterization based on Moderate Resolution Imaging Spectroradiometer (MODIS) data. J Geophys Res, 110, D11107, doi:10.1029/2004JD005579

Lieth H (1974) Phenology and Seasonality Modeling, Springer, Berlin, Heidelberg, New York

Lin ZH, Zeng QC, Ouyang B (1996) Sensitivity of the IAP two level AGCM to surface albedo variations. Theor Appl Climatol, 55, 157-162.

Lofgren BM (1995) Surface albdo-climate feedback simulated using two-way coupling. J Clim, 8, 2543-2562

Louis JF (1979) A parametric model of vertical eddy fluxes in the atmosphere. Boundary-Layer Meteorol, 17, 187-202

Loustau D, Berbigier P, Roumagnac P, Arruda-Pacheco C, David SA, Ferreira MI, Perreira JS, Tavares R (1996) Transpiration of a 64-year-old maritime pine. Oecologia, 107, 33-42

Loustau D, Berbigier P, Granier A, El Hadj Moussa F (1992) Interception loss, through fall and stem flow beneath the pine canopy. J Hydrol, 138, 449-467

Lu L, Shuttleworth WJ (2002) Incorporating NDVI derived LAI into the climate version of RAMS and its impact on regional climate. J Hydrometeor, 3, 347–362

Lucht W, Schaaf CB, Strahler AH (2000) An algorithm for the retrieval of albedo from space using semiempircal BRDF models. IEEE Trans Geosci Remote Sens, 38, 977-998

Majewski D (1991) The Europa-Modell of the Deutscher Wetterdienst. ECMWF Seminar on Numerical Methods in Atmospheric Models, 2, 147-191

Maynard K, Royer JF (2004) Effects of ''realistic'' land-cover change on a greehouse-warmed African climate. Clim Dyn, 22, 343–358

Menzel A, Sparks TH, Estrella N, Koch E, Aasa A, Ahas R, Alm-Kübler K, Bissolli P, Braslavská O, Briede A, Chmielewski F-M, Crepinsek Z, Curnel Y, Dahl Å, Defila C, Donnelly A, Filella Y, Jatczak K, Mage F, Mestre A, Nordli Ø, Peñuelas J, Pirinen P, Remisová V , Scheifinger H, Striz M, Susnik A, Van Vliet AJH, Wielgolaski F-E, Zach S, Zust A (2006) European phenological response to climate change matches the warming pattern. Glob Chang Biol, 12 , 1969–1976

Menzel A, Jakobi G, Ahas R, Scheifinger H, Estrella N (2003) Variations of the climatological growing season (1951-2000) in Germany compared with other countries. Int J Climatol, 23, 793-812

Menzel A (2003) Plant phenological anomalies in Germany and their relation to air temperature and NAO. Clim Chang, 57, 243-263

Menzel A (2002) Phenology: Its importance to the global change community. Clim Chang, 54, 379-385

Menzel A, Estrella N, Fabian P (2001) Spatial and temporal variability of the phenological seasons in Germany from 1951-1996. Glob Chang Biol, 7, 657-666

Menzel A (2000) Trends in phenological phases in Europe between 1951 and 1996. Int J Biometeorol, 44, 76-81

Menzel A, Fabian P (1999) Growing season extended in Europe. Nature, 397, 659

Mintz Y (1984) The sensitivity of numerically simulated climates to land-surface boundary conditions. In: Houghton JT (Ed.) The Global Climate. Cambridge. Uni. Press, 79–105

Mitchell TD, Carter TR, Jones PD, Hulme M, New M (2004) A comprehensive set of high-resolution grids of monthly climate for Europe and the globe: The observed record (1901–2000) and 16 scenarios (2001–2100). Working Pap. 55, Tyndall Cent, Norwich, UK

Murray MB, Cannel MGR, Smith RI (1989) Date of bud burst of fifteen tree species in Britain following climatic warming. J Appl Ecol, 26, 693-700

Myhre G, Myhre A (2003) Uncertainties in radiative forcing to surface albedo changes caused by land use changes. J Clim, 16, 1511-1524

Myneni RB, Hoffman S, Knyazikhin Y, Privette JL, Glassy J, Tian Y, Wang Y, Song X, Zhang Y, Smith GR, Lotsch A, Friedl M, Morisette JT, Votava P, Nemani RR, Running SW (2002) Global products of vegetation leaf area and fraction absorbed PAR from year one of MODIS data. Remote Sens Environ, 83, 214-231

Myneni RB, Keeling CD, Tucker CJ, Asrar G, Nemani RR (1997) Increased plant growth in the northern high latitudes from 1981-1991. Nature, 386, 698-702

Nakicenovic N, Alcamo J, Davis G, de Vries B, Fenhann J, Gaffin S, Gregory K, Grübler A, Jung TY, Kram T, La Rovere EL, Michaelis L, Mori S, Morita T, Pepper W, Pitcher H, Price L, Raihi K, Roehrl A, Rogner H-H, Sankovski A, Schlesinger M, Shukla P, Smith S, Swart R, van Rooijen S, Victor N, Dadi Z (2000) IPCC Special Report on Emissions Scenarios, Cambridge University Press, Cambridge, UK and New York, USA

Neilson, RP Marks D (1994) A global perspective of regional vegetation and hydrological sensitivities and risks from climatic change. J Veg Sci, 5, 715-730

New M, Hulme M, Jones PD (2000) Representing twentieth-century space-time climate variability. Part II: Development of 1901–96 monthly grids of terrestrial surface climate. J Clim, 13, 2217–2238

Niu GY, Yang ZL (2004) Effects of vegetation canopy processes on snow surface energy and mass balances, J Geophys Res, 109, D23111, doi:10.1029/2004JD004884

Oleson KW, Niu GY, Yang ZL, Lawrence DM, Thornton PE, Lawrence PJ, Stockli R, Dickinson RE, Bonan GB, Levis S, Dai A, Qian T (2008) Improvements to the Community Land Model and their impact on the hydrological cycle. J Geophys Res, 113, G01021, doi:10.1029/2007JG000563.

Olson, JS (1994a) Global ecosystem framework: definitions. USGS EROS Data Center Internal Report, Sioux Falls, SD, 37 pp.

Olson, JS (1994b) Global ecosystem framework: translation strategy. USGS EROS Data Center Internal Report, Sioux Falls, SD, 39 pp.

Osborne TM, Lawrence DM, Slingo JM, Challinor AJ, Wheeler TR (2004) Influence of vegetation on the local climate and hydrology in the tropics: sensitivity to soil parameters. Clim Dyn, 23, 45-61

Pan Z, Arritt RW, Gutowski WJ, Takle ES (2001) Soil moisture in a regional climate model: simulation and projection. Geophys Res Lett, 28, 2947–2950

Pfeifer S (2006) Modeling cold cloud processes with the regional climate model REMO. Dissertation, Reports on Earth System Science 23, Max-Planck-Institute for Meteorology Hamburg

Pielke RA, Walko RL, Steyaert L, Vidale P, Liston G, Lyons W, Chase T (1999) The influence of anthropogenic landscape changes on weather in South Florida. Mon Weather Rev, 127,1663–1673

Pielke RA, Avissar R, Raupach M, Dolman AJ, Zeng X, Denning AS (1998) Interactions between the atmosphere and terrestrial ecosystems: influence on weather and climate. Glob Chang Biol, 4, 461–475

Pielke RA, Lee TJ, Copeland JH, Eastman JL, Ziegler CL, Finley CA (1997) Use of USGS-provided data to improve weather and climate simulations. Ecol Appl, 7, 3-21

Pitman A, McAvaney B (2004) Impact of varying the complexity of the land surface energy balance on the sensitivity of the Australian climate to increasing carbon dioxide. Clim Res, 25, 191–203

Pitman AJ, Henderson-Sellers A, Desborough CE, Yang ZL, Abramopoulos F, Boone A, Dickinson RE, Gedney N, Koster R, Kowalczyk E, Lettenmaier D, Liang X, Mahfouf JF, Noilhan J, Polcher J, Qu W, Robock A, Rosenzweig C, Schlosser CA, Shmakin AB, Smith J, Suarez M, Verseghy D, Wetzel P, Wood E, Xue Y, (1999) Key results and implications from phase 1(c) of the Project for Intercomparison of Land-surface Parametrization Schemes, Clim Dyn, 15 (9), 673-684

Privette JL, Myneni RB, Knyazikhin Y, Mukelabai M, Roberts G, Tian Y, Wang Y, Leblanc SG (2002) Early spatial and temporal validation of MODIS LAI product in the Southern Africa Kalahari. Remote Sens Environ, 83, 232–243

Rechid D, Raddatz TJ, Jacob D (2008a) Parameterization of snow-free land surface albedo as a function of vegetation phenology based on MODIS data and applied in climate modelling. Theor Appl Climatol, DOI 10.1007/s00704-008-0003-y

Rechid D, Hagemann S, Jacob D (2008b) Sensitivity of climate models to seasonal variability of snow-free land surface albedo.Theor Appl Climatol, DOI 10.1007/s00704-007-0371-8

Rechid D, Jacob D (2006) Influence of monthly varying vegetation on the simulated climate in Europe. Meteorol Z, 15, 99-116

Rechid D (2001) Untersuchung zur Parameterisierung von Landoberflächen im regionalen Klimamodell REMO. Diploma Thesis, Max-Planck-Institute for Meteorology, Hamburg

Rodriguez-Camino E, Avissar R (1998) Comparison of three land surface schemes with the Fourier Amplitude Sensitivity Test (FAST). Tellus, 50A, 313-332

Roeckner E, Bäuml G, Bonaventura L, Brokopf R, Esch M, Giorgetta M, Hagemann S, Kirchner I, Kornblueh L, Manzini E, Rhodin A, Schlese U, Schulzweida U, Tompkins A (2003) The atmospheric general circulation model ECHAM-5: Part I. Model description. Report 349, Max-Planck-Institute for Meteorology, Hamburg

Roesch A, Wild M, Gilgen H, Ohmura A (2001) A new snow cover fraction parameterization for the ECHAM4 GCM. Clim Dyn, 17, 933-946S

Rötzer T, Grote R, Pretzsch H (2004) The timing of bud burst and its effect on tree growth. Int J Biometeorol 48, 109-118

Rötzer T, Chmielewski FM (2001) Phenological maps of Europe. Clim Res, 18, 249-257

Rötzer T, Wittenzeller M, Haeckel H, Nekovar J (2000) Phenology in central Europe – differences and trends of spring phenophases in urban and rural areas. Int J Biometeorol, 44, 60-66

Rowntree PR (1991) Atmospheric parameterization schemes for evaporation over land: basic concepts and climate modelling aspects. In: Schmugge, T J; Andre, J (Eds), 1991: Land Surface Evaporation - Measurement and Parameterization. Springer Verlag, 5-29

Rowntree PR, Sangster AB (1986) Modelling the impact of land surface changes on Sahel rainfall. Rep. 9, World Climate Research Programme, Geneva

Saha SK, Rinke A, Dethloff K, Kuhry P (2006) Influence of a complex land surface scheme on Arctic climate simulations. J Geophys Res, 111, D22104, doi:10.1029/2006JD007188

Sánchez E, Gaertner M, Gallardo C, Padorno E, Arribas A, Castro M (2007) Impacts of a change in vegetation description on simulated European summer present-day and future climates. Clim Dyn, 29, 319-332

Schaaf CB, Gao F, Strahler AH, Lucht W, Li X, Tsang T, Strugnee N, Zhang XY, Jin Y, Muller JP, Lewis P, Barnsley M, Hobson P, Disney M, Roberts G, Dunderdale M, Doll C, d'Entremont RP, Hu B, Liang S, Privette JL (2002) First operational BRDF, albedo and nadir reflectance products from MODIS. Remote Sens Environ, 83, 135-148

Schaber J, Badeck FW (2003) Physiology-based phenology models for forest tree species in Germany. Int J Biometeorol. 47, 193-201

Sardeshmukh PD, Hoskins BJ (1987) The generation of global rotational flow by steady idealized tropical divergence. J. Atmos. Sci., 45, 1228-1251

Scheifinger H, Menzel A, Koch E, Peter C, Ahas R (2002) Atmospheric mechanisms governing the spatial and temporal variability of phenological phases in central Europe. Int J Climatol, 22, 1739-1755

Schnelle F (1955) Pflanzen-Phänologie. Akademische Verlagsgesellschaft Geest und Portig. Leipzig

Schurgers G, Mikolajewicz U, Gröger M, Maier-Reime E, Vizcaíno M, Winguth A (2007) The effect of land surface changes on Eemian climate. Clim Dyn, 29, 357-373

Schwartz MD, Reed BC, White MA (2002) Assessing satellite-derived start-of-season measures in the conterminous USA. Int J Climatol, 22, 1793-1805

Schwartz MD, Reiter BE (2000) Changes in North American spring. Int J Climatol, 20, 929-932

Sellers PJ, Randall DA, Collatz GJ, Berry JA, Field CB, Dazlich DA, Zhang C, Collelo GD, Bounoua L (1996a) A revised land surface parameterization (SIB2) for atmospheric GCMs, part. I. Model formulation. J Clim, 9, 676-705

Sellers PJ, Los SO, Tucker CJ, Justice CO, Dazlich DA, Collatz GJ, Randall DA (1996b) A revised land surface parameterization (SIB2) for atmospheric GCMs, part. II. The gerneration of global fields of terrestrial biophysical parameters from satellite data. J Clim, 9, 706-737

Sellers PJ (1991) Modelling and observing land-surface-atmosphere interactions on large scales. Sur Geophys, 12, 85-114

Sellers PJ, Mintz Y, Sud YC, Dalcher A (1986) A simple biosphere (SiB) for use within general circulation models. J Atmos Sci, 43, 505-531

Semmler T, Jacob D, Schlünzen KH, Podzun R (2004) Influence of sea ice treatment in a regional climate model on boundary layer values in the Fram Strait region. Mon Weather Rev, 132, 985-999

Seneviratne S, Luethi D, Litschi M, Schaer C (2006) Land-atmosphere coupling and climate change in Europe. Nature, 443, 205-209

Seneviratne S, Pal J, Eltahir E, Schar C (2002) Summer dryness in a warmer climate: a process study with a regional climate model. Clim Dyn, 20, 69–85

Shukla J, Mintz Y (1982) Influence of land surface evapotranspiration on the earth's climate. Science, 215, 1498–1501

Simmons AJ, Burridge DM (1981) An energy and angular-momentum conserving vertical finite-difference scheme and hybrid vertical coordinate. Mon Weather Rev, 109, 758-766

Sitch S, Smith B, Prentice IC, Arneth A, Bondeau A, Cramer W, Kaplan J, Levis S, Lucht, W, Sykes M, Thonicke K, Venevsky S (2003) Evaluation of ecosystem dynamics, plant geography and terrestrial carbon cycling in the LPJ Dynamic Vegetation Model. Glob Chang Biol, 9, 161–185

Snyder P, Delire C, Foley JA (2004) Evaluating the influence of different vegetation biomes on the global climate. Clim Dyn, 23, 279-302

Song J (1999) Phenological influences on the albedo of prairie grassland and crop fields. Int J Biometeorol, 42, 153-157

Sparks TH, Menzel A (2002) Observed changes in seasons: An overview. Int J Climatol, 22, 1715-1725

Stohlgreen TJ, Chase TN, Pielke RA, Timothy S, Kittel GF, Baron JS (1998) Evidence that local land use practices influence regional climate, vegetation, and stream flow patterns in adjacent natural areas. Glob Chang Biol, 4, 495-504

Strahler AH, Lucht W, Schaaf CB, Tsang T, Gao F, Li X, Muller JP, Lewis P, Barnsley MJ (1999) MODIS BRDF/albedo product: Algorithm theoretical basis document. NASA EOS-MODIS document, v5.0, NASA Goddard Space Flight Cent, Greenbelt, Md, 53 pp

Studer S, Appenzeller C, Defila C (2005) Interannual variability and decadal trends in alpine spring phenology: A multivariate analysis approach. Clim chang, 73, 395-414

Sud YC, Sellers PJ, Mintz Y, Chou MD, Waker GK, Smith WE (1990) Influence of the biosphere on the global circulation and hydrologic cycle – a GCM simulation experiment. Agric Forest Meteor, 52, 133–180

Sud YC, Shukla J, Mintz Y (1988) Influence of land surface roughness on atmospheric circulation and precipitation: A sensitivity study with a general circulation model. J Appl Meteor, 27, 1036–1054

Suh MS, Lee DK (2004) Impacts of land use/cover changes on surface climate over east Asia for extreme climate cases using RegCM2. J Geophys Res 109. doi:10.1029/2002JD002670

Tan B, Hu J, Zhang P, Huang D, Shabanov N, Weiss M, Knyazikhin Y, and Myneni RB (2005) Validation of Moderate Resolution Imaging Spectroradiometer leaf area index product in croplands of Alpilles, France. J Geophys Res, 110, D01107, doi:10.1029/2004JD004860.0.

Tanaka HL, Ishizaki N, Nohara D (2005) Intercomparison of the Intensities and Trends of Hadley, Walker and Monsoon Circulations in the Global Warming Projections. SOLA, 1, 77-80

Tucker CJ, Slayback DA, Pinzon JE, Los SO, Myneni RB, Taylor MG (2001) Higher northern latitude normalized difference vegetation index and growing season trends from 1982 to 1999. Int J Biometeorol, 45, 184-190

Turner DP, Ritts WD, Cohen WB, Maeirsperger TK, Gower ST, Kirschbaum AA, Running SW, Zhao M, Wofsy SC, Dunn AL, Law BE, Campbell JL, Oechel WC, Kwon HJ, Meyers TP, Small EE, Kurc SA, Gamon JA (2005) Site-level evaluation of satellite-based global terrestrial gross primary production and net primary production monitoring. Glob Chang Biol, 11, 666-684

Uppala SM, Kallberg PW, Simmons AJ, Andrae U, Bechtold VD, Fiorino M, Gibson JK, Haseler J, Hernandez A, Kelly GA, Li X, Onogi K, Saarinen S, Sokka N, Allan RP, Andersson E, Arpe K, Balmaseda MA, Beljaars ACM, Van De Berg L, Bidlot J, Bormann N, Caires S, Chevallier F, Dethof A, Dragosavac M, Fisher M, Fuentes M, Hagemann S, Holm E, Hoskins BJ, Isaksen L, Janssen PAEM, Jenne R, McNally AP, Mahfouf JF, Morcrette JJ, Rayner NA, Saunders RW, Simon P, Sterl A, Trenberth KE, Untch A, Vasiljevic D, Viterbo P, Woollen J (2005) The ERA-40 Re-analysis. Q J R Meteorol Soc, 131, 2961-3012

US Geological Survey (2002) Global land cover characteristics data base version 2.0. http://edcdaac.usgs.gov/glcc/globedoc2_0.html

US Geological Survey (1997) Global land cover characteristics data base. http://edcwww.cr.usgs.gov/landdaac/glcc/globe_int.html

Vidale P, Luthi D, Frei C, Seneviratne S, Schar C (2003) Predictability and uncertainty in a regional climate model. J Geophys Res, 108, doi:10.1029/2002JD002810

Voldoire A, Royer JF (2004) Tropical deforestation and climate variability. Clim Dyn, 22, 857-874

Wang K, Liu J, Zhou X, Sparrow M, Ma M, Sun Z, and Jiang W (2004) Validation of the MODIS global land surface albedo product using ground measurements in a semidesert region on the Tibetan Plateau J Geophys Res, 109, D05107, doi:10.1029/2003JD004229229

White MA, Thornthon PE, Running SW (1997) A continental phenology model for monitoring vegetation responses to interannual climatic variability. Glob Biogeochem Cycles, 11, 217-234

Warrilow DA, Sangster AB, Slingo A (1986) Modelling of land surface processes and their influence on European climate. Meteorological Office, Met O 20 Technical Note DCTN 38, Backnell, UK

Woodward FI, McKee IF (1991) Vegetation and climate. Environ Int, 17 535-546

Woodward FI (1987) Climate and plant distribution. Cambridge University Press, London.

Yang ZL (2004) Modeling land surface processes in short-term weather and climate studies. In: Zhu X, Observations, theory, and modeling of atmospheric variability. World Scientific Series on Meteorology of East Asia, Vol. 3, World Scientific Publishing Corporation, Singapore, 288-313

Yang ZL, Dai Y, Dickinson RE, Shuttleworth WJ (1999) Sensitivity of ground heat flux to vegetation cover fraction and leaf area index. J Geophys Res, 104, 19505-19514

Zhang X, Friedl MA, Schaaf CB, Strahler AH, Hodges JCF, Gao F, Reed BC, Huete A (2003) Remote Sens Environ 84, 471-475

Zeng X, Shaikh M, Dai Y, Dickinson RE, and Myneni R (2002) Coupling of the Common Land Model to the NCAR Community Climate Model J Clim, 15, 1832– 1854

Zheng Y, Yu G, Qian Y, Miao M, Zeng X, Liu H (2002) Simulations of regional climatic effects of vegetation change in China. Q J R Meteorol Soc, 128, 2089–2114

Zhou L, Dickinson RE, Tian Y, Zeng X, Dai Y, Yang ZL, Schaaf CB, Gao F, Jin Y, Strahler A, Myneni RB, Yu H, Wu W, Shaikh M, (2003) Comparison of seasonal and spatial variations of albedos from Moderate-Resolution Imaging Spectroradiometer (MODIS) and Common Land Model J Geophys Res, 108, D15, 4488, doi:10.1029/2002JD003326

Zhou L, Tucker CJ, Kaufmann RK, Slayback D, Shabanov NV, Myneni RB (2001) Variations in northern vegetation activity inferred from satellite data of vegetation index during 1981 to 1999. J Geophys Res, 106, 20069-20083

Danksagung

Zu allerest möchte ich von Herzen meiner Familie danken: meinem geliebten Juan, für dein Verständnis und deine Geduld, für dein Vertrauen in meine Arbeit und deine Aufmunterung in Phasen der Mutlosigkeit, für deine ewige Liebe; und meiner geliebten Roshin, dass du immer Verständnis dafür hattest, dass Mami wieder das ganze Wochenende arbeiten musste; und meinem geliebten Ramon, der schon unzählige Stunden mit Mama vorm Computer verbracht hat - ich liebe euch so sehr!

Mein ganz besonderer Dank gilt Frau Dr. Daniela Jacob für die wissenschaftliche Betreuung, für die Möglichkeit, an dem spannenden Thema meiner Dissertation selbständig und eigenverantwortlich arbeiten zu können, und für das immer vorhandene Verständnis, wenn ich wegen Fieber der Kinder die Arbeit plötzlich stehen und liegen lassen musste sowie für die Möglichkeit, die Arbeitszeit dementsprechend flexibel zu gestalten. Ich möchte mich auch ganz herzlich bei Herrn Professor Dr. Hartmut Graßl für die wissenschaftliche Betreuung meiner Arbeit bedanken. Weiterhin danke ich Herrn Dr. Stefan Hagemann für die vielen guten Ratschläge und für das Interesse am Voranschreiten meiner Arbeit.

Ich möchte mich bei der gesamten Gruppe der Regionalmodellierung für die gute Arbeitsatmosphäre bedanken, es hat immer Spaß gemacht, ins Büro zu kommen. Ich bedanke mich bei unserem wissenschaftlichen Programmierer Ralf Podzun für die vielen technischen Hilfestellungen und besonders für die Hilfe bei der technischen Kopplung des Phänologieschemas mit REMO. Ganz besonders danke ich Holger Göttel für die vielen Antworten auf meine unzähligen Fragen, für die besonders nette Arbeitsatmosphäre in unserem gemeinsamen Büro und das Verständnis, wenn mal wieder ein Baby mit an Bord war. Auch bedanken möchte ich mich bei Katharina Bülow, die mir in unzähligen Gesprächen immer wieder Mut zum Weitermachen gegeben und es immer verstanden hat, mich mit Worten, Blumen und Farben am Arbeitsplatz aufzumuntern. Für die vielen netten Gespräche und fruchtbaren Diskussionen während gemeinsamer Kaffee- und Teepausen und während der Gruppentreffen danke ich euch allen.

Für die MPI-internen Begutachtungen meiner Veröffentlichungen bedanke ich mich bei Ute Karstens, Susanne Pfeifer, Christian Reick, Thomas Raddatz, Philip Lorenz und Stefan Hagemann. Ich danke auch allen anonymen Reviewern der Manuskripte, deren wissenschaftliche Argumentation und inhaltliche Abrundung sehr von den zahlreichen Anmerkungen profitierten.

Weiterhin bedanke ich mich für die interessante Arbeit und gute Koordination innerhalb des Projektes QUIRCS. Besonders möchte ich mich bei Sven Kotlarski bedanken für die gute Zusammenarbeit in diesem Projekt und die alleinige Übernahme der Projektarbeit während meiner Erziehungsurlaubszeit. Auch für die interessante Aufgabe in dem MPI-internen Projekt, die Sensitivität des Globalmodells ECHAM5 auf die saisonal variable Hintergrundalbedo zu testen, bedanke ich mich bei Stefan Hagemann und Erich Roeckner sowie für die technische Hilfestellung bei der Einarbeitung in die Globalmodellierung bei Monika Esch und Uwe Schulzweida.

Bei der täglichen Aufgabe, die Promotion, die wissenschaftliche Projektarbeit sowie die Kinderbetreung und -erziehung parallel zu bewältigen, bin ich sehr dankbar für die Hilfe von Mariana und Philip, und ganz besonders von Marion und Farid, die den Kindern im Flohzirkus mit ihrer Fürsorge und Liebe ein zweites zu Hause schenken. Außerdem danke ich von Herzen meiner lieben Freundin Helga, die mir einfach immer zugehört hat, die mich immer verstanden hat.

Und nun möchte ich meine tiefe Dankbarkeit für die bedingungslose Hilfe meiner lieben Großfamilie ausdrücken. Ich danke besonders meinen lieben Schwiegereltern Ursula und Djamil, für die unzähligen Male, an denen ihr meine Kinder, mich und meinen Laptop bei euch aufgenommen habt, damit ich mal wieder ein Stück in meiner Arbeit vorankomme. Vielen Dank, dass wir immer bei euch willkommen sind, vielen Dank, dass ihr immer für uns da seid! Mein ganz besonderer Dank gilt meiner lieben Schwägerin Avin, ich danke dir für deine Freundschaft, für deine Aufmunterung und ganz besonders für die vielen Montage in diesem Jahr, an denen du dich so liebevoll um meine Kinder gekümmert hast. Ich danke auch Marco und Nils für die vielen schönen gemeinsamen Stunden. Für die Hilfe bei der sprachlichen Überarbeitung bedanke ich mich ganz besonders bei meiner Schwägerin Katja. Ich danke Seyran, Alfonso, Miriam, Yasmin und Sarah, dass ihr Roshin immer so herzlich bei euch aufgenommen habt. Mein Dank geht auch an Margitta, Jürgen und Jeanette. Meinem Bruder Danny danke ich für seine Hilfe in den letzten Wochen. Ich danke auch Gulperi, Renas, Galina und Robin, ich danke euch allen, dass wir immer so gut zusammenhalten!

Die gesamten Veröffentlichungen in der Publikationsreihe des MPI-M
„Berichte zur Erdsystemforschung“,
„Reports on Earth System Science“,
ISSN 1614-1199

sind über die Internetseiten des Max-Planck-Instituts für Meteorologie erhältlich:

http://www.mpimet.mpg.de/wissenschaft/publikationen.html



ISSN 1614-1199